

Summary of the lecture



Faculty of Physics UW

Jacek.Szczytko@fuw.edu.pl

Summary of the lecture

1. Introduction – semiconductor heterostructures

Revision of solid state physics: Born-Oppenheimer approximation, Hartree-Fock method and one electron Hamiltonian, periodic potential, Bloch states, band structure, effective mass.

2. Nanotechnology

Revision of solid state physics: tight-binding approximation, Linear Combination of Atomic Orbitals (LCAO).

Nanotechnology. Semiconductor heterostructures. Technology of low dimensional structures. Bandgap engineering: straddling, staggered and broken gap. Valence band offset.

3. Quantum wells (1)

Infinite square quantum well. Finite square quantum well. Quantum well in heterostructures: finite square well with different effective masses in the well and barriers.

4. Quantum wells (2)

Harmonic potential (parabolic well). Triangular potential. Wentzel – Krammers – Brillouin (WKB) method.

Band structure in 3D, 2D. Coulomb potential in 2D

Summary of the lecture

5. Quantum dots, Quantum wells in 1D, 2D and 3D

Quantum wells in 1D, 2D and 3D. Quantum wires and quantum dots. Bottom-up approach for low-dimensional systems and nanostructures. Energy gap as a function of the well width.

6. Optical transitions in nanostructures

Time-dependent perturbation theory, Fermi golden rule, interband and intraband transitions in semiconductor heterostructures

7. Work on the article about quantum dots

Students have to read the article (Phys. Rev. Lett., Nature, Science, etc.) and answer questions. Discussion.

8. Carriers in heterostructures

Density of states of low dimensional systems. Doping of semiconductors. Heterojunction, p-n junction, metal-semiconductor junction, Schotky barrier

Summary of the lecture

9. Tunneling transport

Continuity equation. Potential step. Tunneling through the barrier. Transfer matrix approach. Resonant tunneling. Quantum unit of conductance.

10. Quantized conductance

Quantized conductance. Coulomb blockade, one-electron transistor.

11. Work on the article about the tunneling or conductance

Students have to read the article (Phys. Rev. Lett., Nature, Science, etc.) and answer questions. Discussion.

12. Electric field in low-dimensional systems

Scalar and vector potentials. Carriers in electric field: scalar and vector potential in Schrodinger equation. Schrodinger equation with uniform electric field. Local density of states. Franz-Kieldysh effect.

Summary of the lecture

13. Magnetic field in low-dimensional systems

Carriers in magnetic field. Schrodinger equation with uniform magnetic field – symmetric gauge, Landau gauge. Landau levels, degeneracy of Landau levels.

14. Electric and magnetic fields in low-dimensional systems

Schrodinger equation with uniform electric and magnetic field. Hall effect. Shubnikov-de Haas effect. Quantum Hall effect. Fractional Quantum Hall Effect. Hofstadter butterfly. Fock-Darwin spectra

15. Revision

Revision and preparing for the exam.

Summary of the exercises

1. Introduction – semiconductor heterostructures

Schrodinger equation. Wave packet, Gaussian wavepacket .

2. Nanotechnology

Tight-binding approximation: graphene bandstructure.

3. Quantum wells (1)

Infinite square quantum well. Finite square quantum well. Finite square well with different effective masses in the well and barriers.

4. Quantum wells (2)

Harmonic potential (parabolic well). Triangular potential. Wentzel – Krammers – Brillouin (WKB) method.

5. Double quantum wells. Quantum dots.

Double quantum wells. Quantum dots (2D and 3D harmonic potential)

Summary of the exercises

6. Optical transitions in nanostructures

Interband and intraband transitions in semiconductor heterostructures. Continuity equation.

7. Carriers in heterostructures (1)

Transfer matrix approach. Potential step.

8. Carriers in heterostructures (2)

Tunneling through the barrier.

9. Resonant tunneling

Resonant tunneling.

10. Quantized conductance

Quantized conductance. Coulomb blockade.

11. Local density of states

Local density of states.

Summary of the exercises

12. Electric field in low-dimensional systems

Carriers in electric field: scalar and vector potential in Schrodinger equation.

13. Magnetic field in low-dimensional systems

Schrodinger equation with uniform magnetic field – symmetric gauge, Landau gauge. Landau levels, degeneracy of Landau levels.

14. Electric and magnetic fields in low-dimensional systems

Schrodinger equation with uniform electric and magnetic field. Conductivity and resistivity tensors

15. Hall effect. Fock-Darvin spectrum

Hall effect. Fock-Darvin spectrum.

Assessment criteria:

Homeworks

Discussion of scientific papers

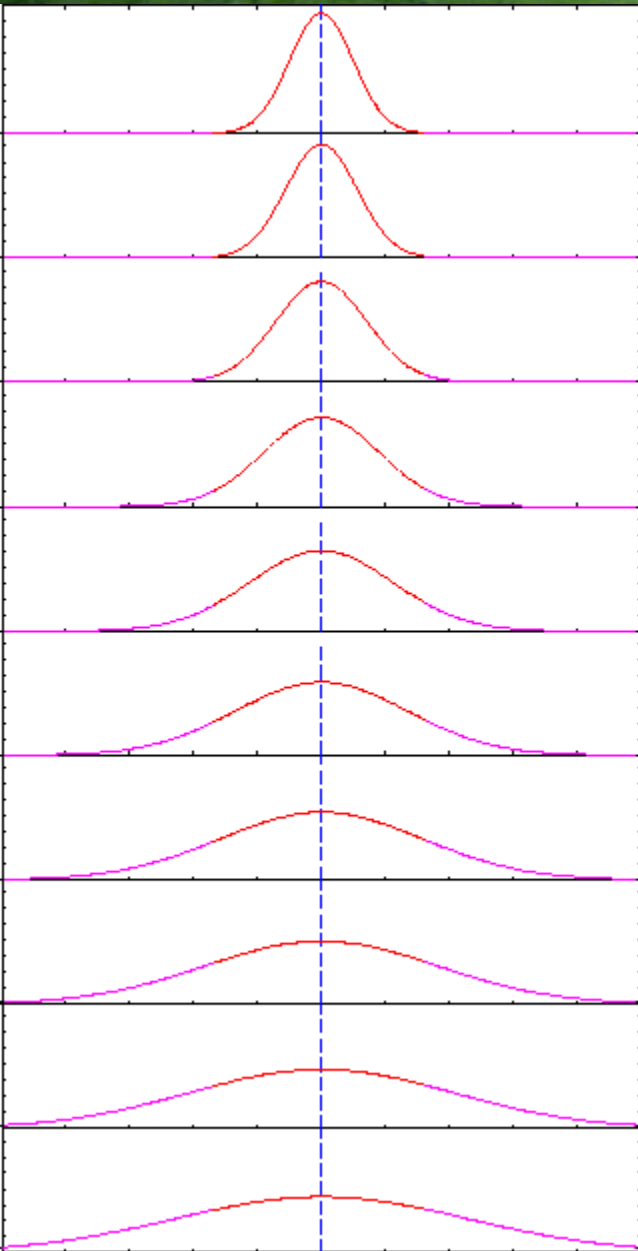
Tests to check the effective use of the skills acquired during the lecture

Exam: final test and oral exam



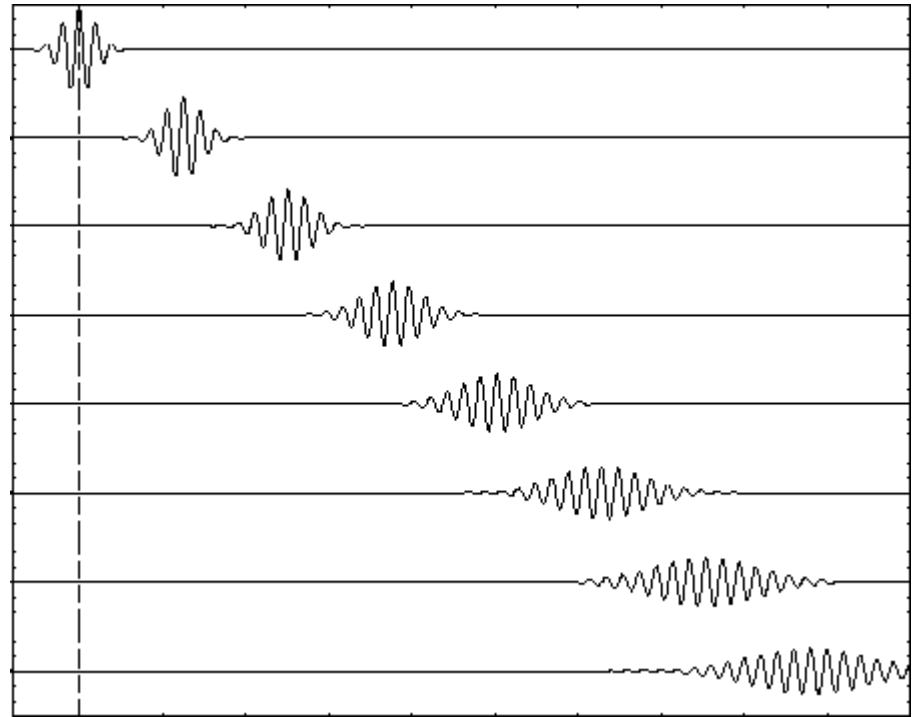
"THE SMALLER IT ALL GETS, THE
BIGGER WE GET."

Pakiet falowy



$$\psi(x, 0) = A \exp\left(-\frac{x^2}{2a^2} + ik_0x\right) \quad \sigma = \frac{\hbar}{ma^2}$$

$$\psi(x, t) = \frac{A}{\sqrt{1+i\sigma t}} e^{ik_0x - i\omega_0 t} \exp\left[-\frac{(x - v_0 t)^2}{2a^2(1+i\sigma t)}\right]$$



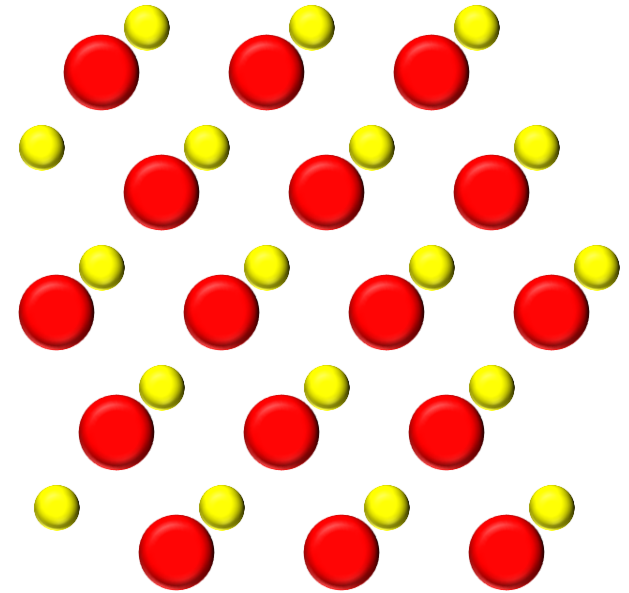
Periodic potential

Bloch theorem

$$\varphi_{n,\vec{k}}(\vec{r}) = u_{n,\vec{k}}(\vec{r}) e^{i\vec{k}\vec{r}}$$

Bloch wave,
Bloch function

Bloch amplitude,
Bloch envelope



The solution of the one-electron Schrödinger equation for a periodic potential has a form of modulated plane wave:

$$u_{n,\vec{k}}(\vec{r}) = u_{n,\vec{k}}(\vec{r} + \vec{R})$$

We introduced coefficient n for different solutions corresponding to the same \vec{k} (*index*). \vec{k} -vector is an element of the *first Brillouin zone*.

$$u_{n,\vec{k}}(\vec{r}) = \sum_{\vec{G}} C_{\vec{k}-\vec{G}} e^{i\vec{G}\vec{r}}$$

Tight-Binding Approximation

$$E(\vec{k}) \approx \frac{1}{N} \left\langle \Phi_{j,\vec{k}}(\vec{r}) \left| H \right| \Phi_{j,\vec{k}}(\vec{r}) \right\rangle =$$
$$= \sum_{n,m} \exp[i\vec{k}(\vec{R}_n - \vec{R}_m)] \int \varphi_j^*(\vec{r} - \vec{R}_m) [E_j + V'(\vec{r} - \vec{R}_n)] \varphi_j(\vec{r} - \vec{R}_n) dV$$

Only the vicinity of \vec{R}_n

Only diagonal terms $\vec{R}_n = \vec{R}_m$ in E_j

When the atomic states $\varphi_j(\vec{r} - \vec{R}_n)$ are spherically symmetric (*s*-states), then overlap integrals depend only on the distance between atoms:

$$E_n(\vec{k}) \approx E_j - A_j - B_j \sum_m \exp[i\vec{k}(\vec{R}_n - \vec{R}_m)]$$

$$A_j = - \int \varphi_j^*(\vec{r} - \vec{R}_n) [V'(\vec{r} - \vec{R}_n)] \varphi_j(\vec{r} - \vec{R}_n) dV$$

$$B_j = - \int \varphi_j^*(\vec{r} - \vec{R}_m) [V'(\vec{r} - \vec{R}_n)] \varphi_j(\vec{r} - \vec{R}_n) dV$$

Restricted to only the nearest neighbours of \vec{R}_n

Tight-Binding Approximation

For sc structure: $\vec{R}_n - \vec{R}_m = (\pm a, 0, 0); (0, \pm a, 0); (0, 0, \pm a);$

$$E_n(\vec{k}) \approx E_j - A_j - 2B_j[\cos k_x a + \cos k_y a + \cos k_z a]$$

$$B_j = - \int \varphi_j^*(\vec{r} - \vec{R}_m) [V'(\vec{r} - \vec{R}_n)] \varphi_j(\vec{r} - \vec{R}_n) dV$$

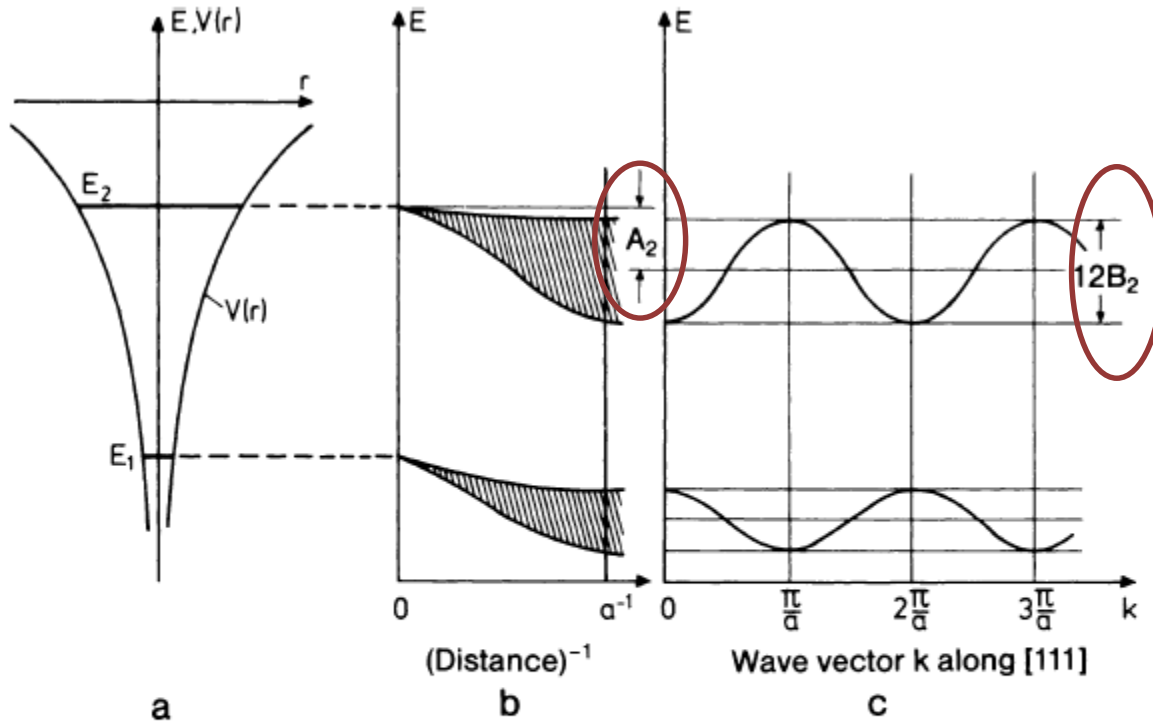


Fig. 7.8 a-c. Qualitative illustration of the result of a tight-binding calculation for a primitive cubic lattice with lattice constant a . (a) Position of the energy levels E_1 and E_2 in the potential $V(r)$ of the free atom. (b) Reduction and broadening of the levels E_1 and E_2 as a function of the reciprocal atomic separation r^{-1} . At the equilibrium separation a the mean energy decrease is A and the width of the band is $12B$. (c) Dependence of the one-electron energy E on the wave vector $k(1, 1, 1)$ in the direction of the main diagonal [111]

Tight-Binding Approximation

For sc structure: $\vec{R}_n - \vec{R}_m = (\pm a, 0, 0); (0, \pm a, 0); (0, 0, \pm a);$

$$E_n(\vec{k}) \approx E_j - A_j - 2B_j[\cos k_x a + \cos k_y a + \cos k_z a]$$

$$B_j = - \int \varphi_j^*(\vec{r} - \vec{R}_m) [V'(\vec{r} - \vec{R}_n)] \varphi_j(\vec{r} - \vec{R}_n) dV$$

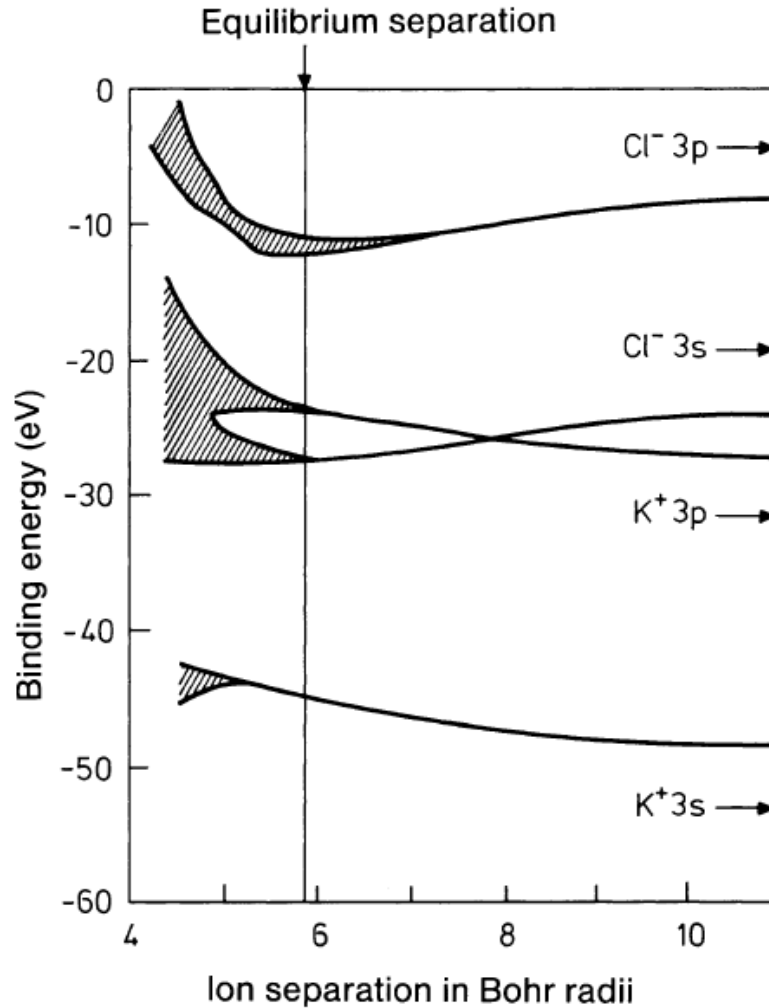


Fig. 7.10. The four highest occupied energy bands of KCl calculated as a function of the ionic separation in Bohr radii ($a_0 = 5.29 \times 10^{-9}$ cm). The energy levels in the free ions are indicated by arrows. (After [7.2])

Tight-Binding Approximation

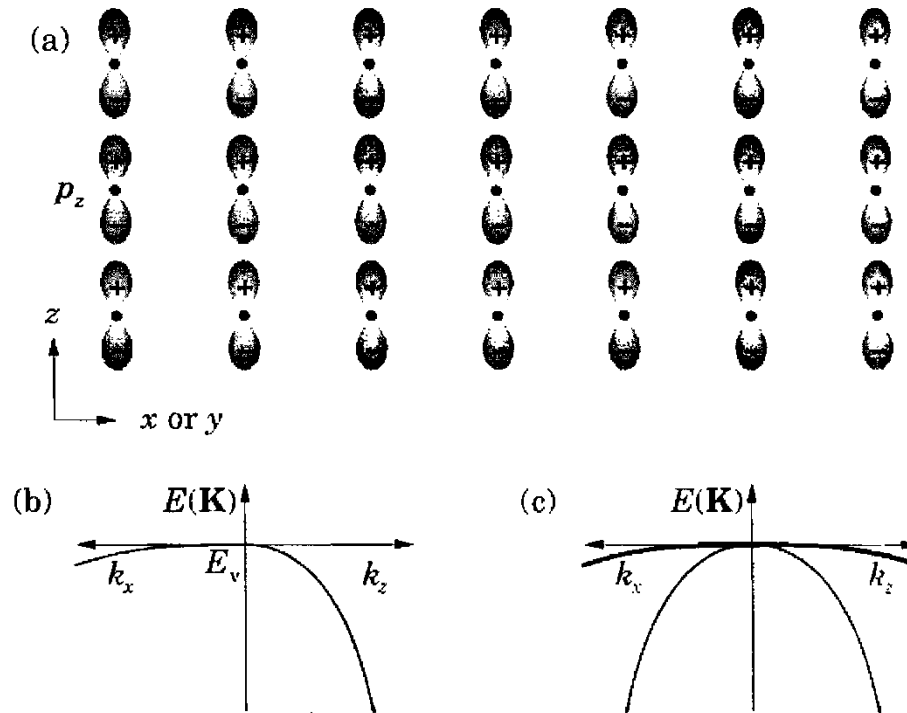
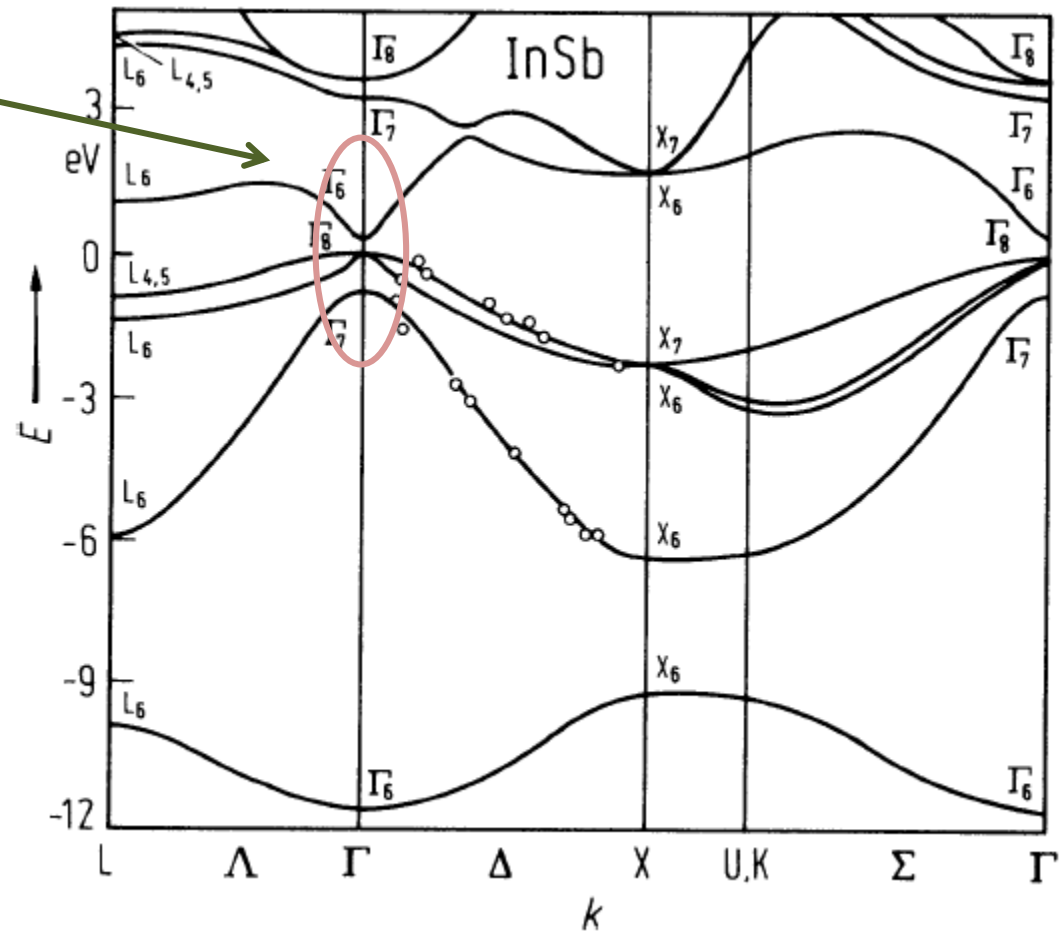


FIGURE 2.17. Valence bands constructed from p orbitals. (a) Lattice of p_z orbitals. (b) Band structure of the p_z orbitals only; the band is 'light' along k_z to the right and 'heavy' along k_x (or k_y) to the left. (c) Total bands from all three p orbitals, showing a doubly degenerate 'heavy' band and a single 'light' band.

k·p perturbation theory – effective mass

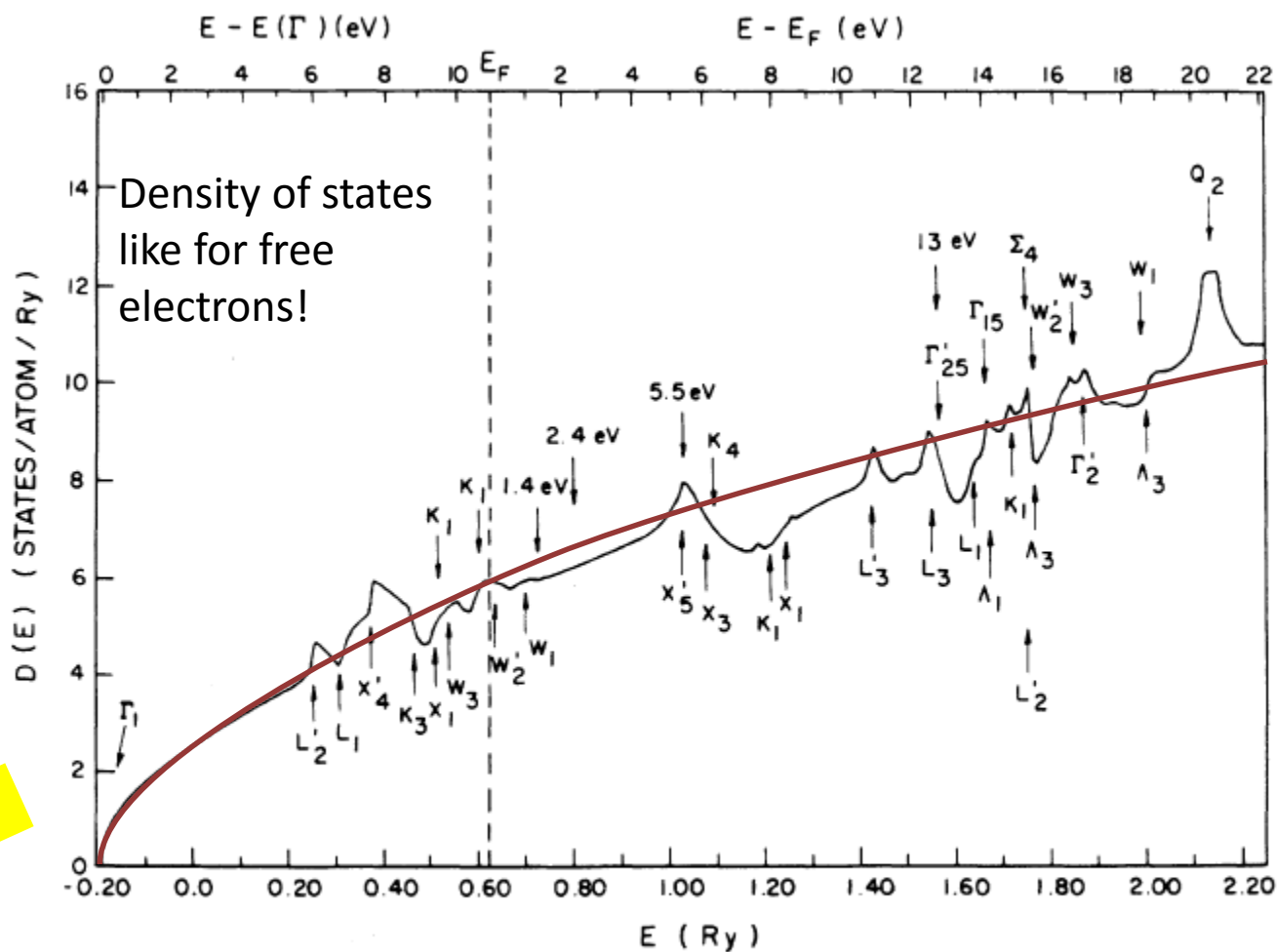
close bands



Expanding $E_n(\vec{k}) = \left(E_n - \frac{\hbar^2 \vec{k}^2}{2m} \right)$ around an extreme point, e.g. $k = 0$:

Landolt-Boernstein

Tight-Binding Approximation



Szmulowicz, F., Segall, B.: Phys. Rev. B21, 5628 (1980).

Tutaj 08.10.2014

Michał Baj

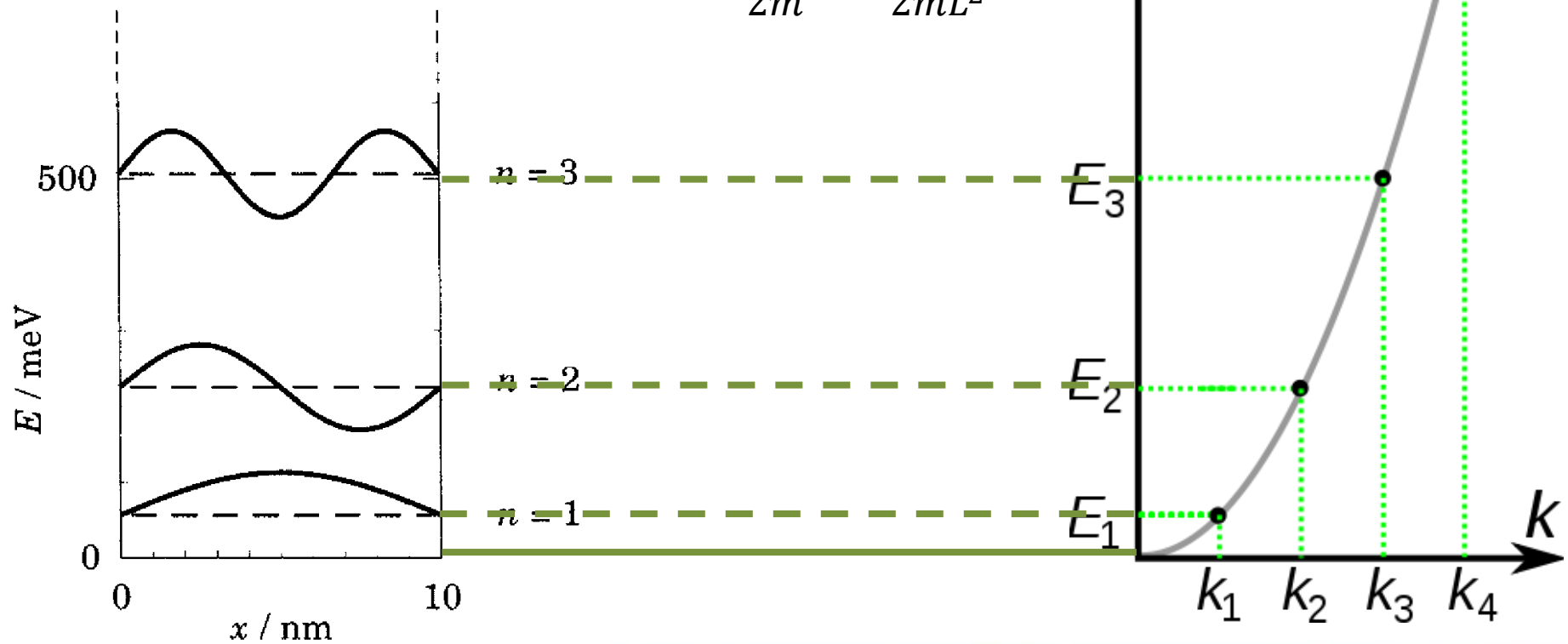
Infinite square quantum well

Inside the quantum well:

$$\psi(x, t) = \sqrt{\frac{2}{L}} \sin(k_n x) e^{-i\omega t}$$

$$k_n = \frac{n\pi}{L}$$

$$\varepsilon_n = \frac{\hbar^2 k_n^2}{2m} = \frac{\hbar^2 n^2 \pi^2}{2mL^2}$$

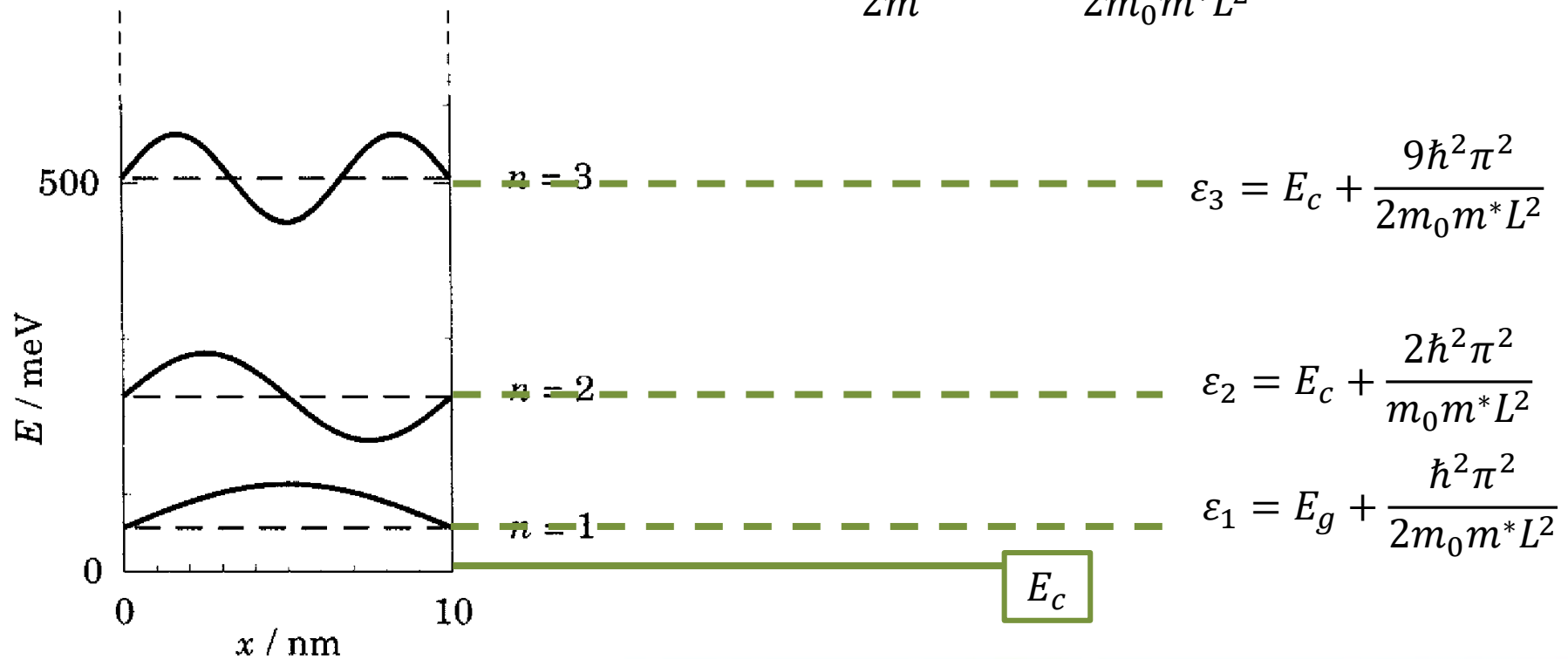


Infinite square quantum well

Inside the quantum well:

$$\psi(x, t) = \sqrt{\frac{2}{L}} \sin(k_n x) e^{-i\omega t} \quad k_n = \frac{n\pi}{L}$$

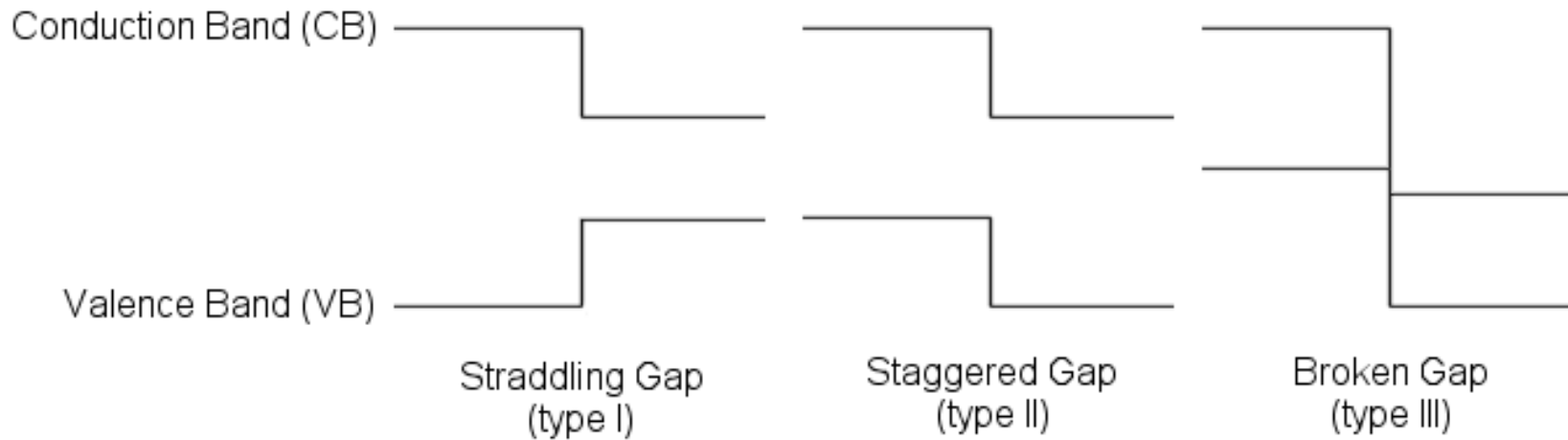
$$\varepsilon_n = E_c + \frac{\hbar^2 k_n^2}{2m} = E_c + \frac{\hbar^2 n^2 \pi^2}{2m_0 m^* L^2}$$



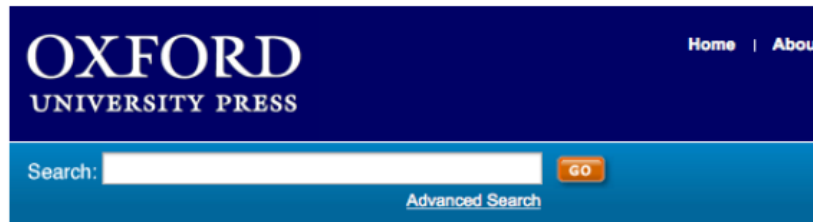
Bandgap engineering

W jaki sposób możemy zmieniać strukturę pasmową heterostruktury:

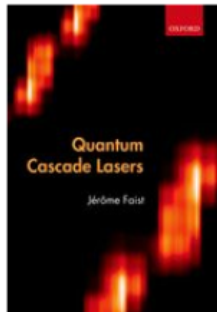
- wybierając materiał
- kontrolując skład
- kontrolując naprężenie



Quantum Cascade Lasers
Giacomo Scalari
scalari@phys.ethz.ch
ETH Zürich



You are here: [Home](#) > [Academic, Professional, & General](#) > [Physics](#) > Quantum Cascade Lasers



Quantum Cascade Lasers

Jérôme Faist

320 pages | 225 b/w line illustrations | 246x171mm

978-0-19-852824-1 | Hardback | 14 March 2013

Also available as: [eBook](#)

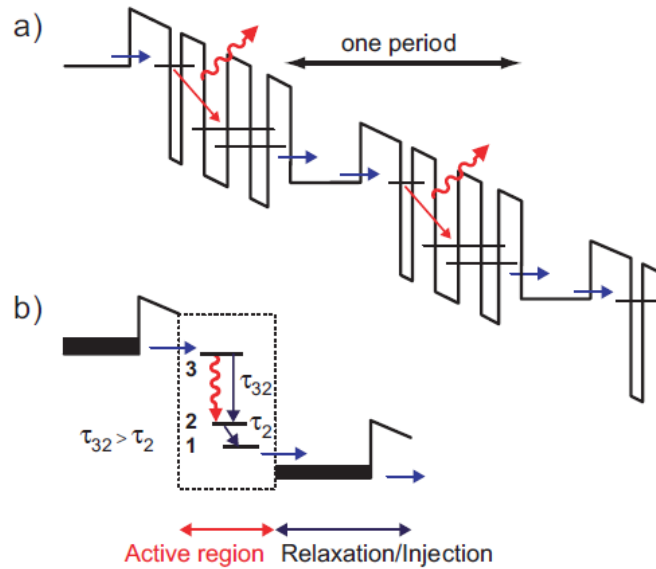
[About
this Book](#)

[Author
Information](#)

[Reviews](#)

[Table of
Contents](#)

Basic design concept

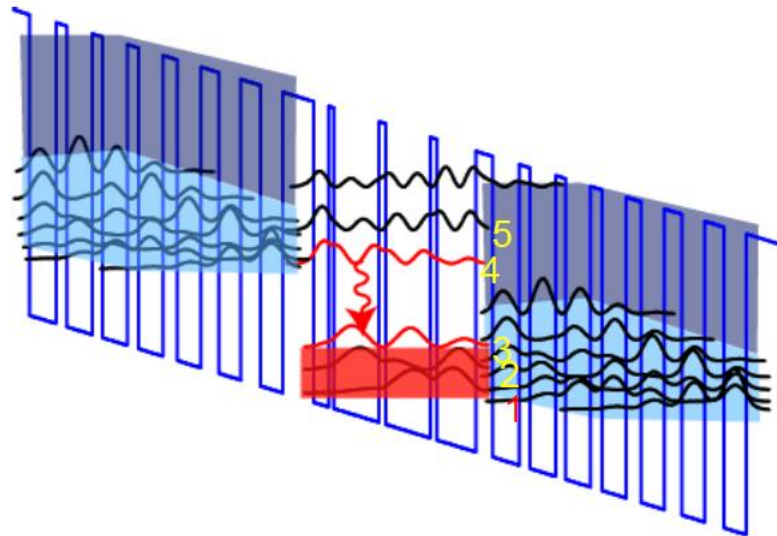
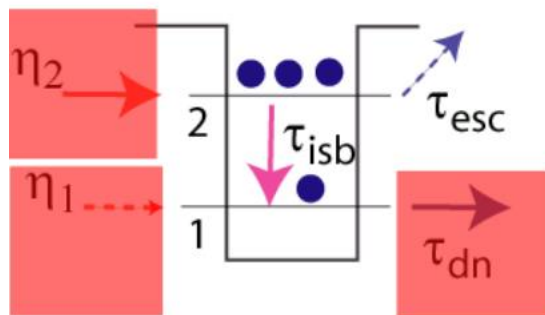


Requirements:

- establish population inversion → Active region
- prevent domain formation → Injection region
- cool electron distribution

J. Faist, F. Capasso, C. Sirtori, D. L. Sivco, A.L. Hutchinson, A.Y. Cho, Science **264**, 477 (1994)

Two phonons

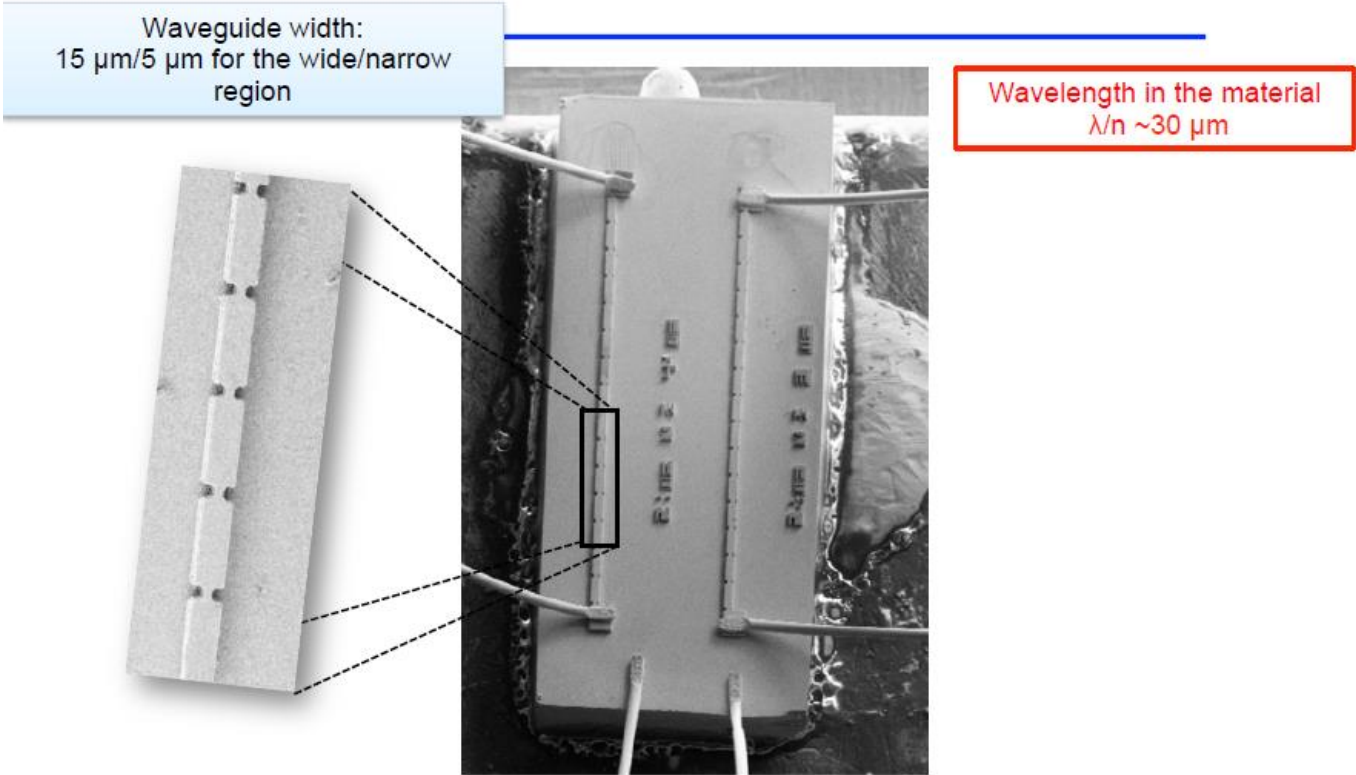


Two phonon resonance

Double resonant phonon extraction and high injection efficiency

(D. Hofstetter et al., APL 2001)

THz photonic wire laser



Amanti et al. Optics Express, **18**, 6390 (2010)

Finite potential well – square well

Inside the well:

$$-\frac{a}{2} < z < \frac{a}{2}$$

$$-\frac{\hbar^2}{2m_0m_W} \frac{d^2}{dz^2} \psi(z) = (E_n - E_W) \psi(z)$$

$$k_n = \frac{1}{\hbar} \sqrt{2mm_W(E_n - E_W)}$$

$$\psi(z, t) = C \begin{cases} \cos(k_n z) \\ \sin(k_n z) \end{cases} e^{-i\omega_n t}$$

$$\kappa_n = \frac{1}{\hbar} \sqrt{2mm_B(E_B - E_n)}$$

The barrier:

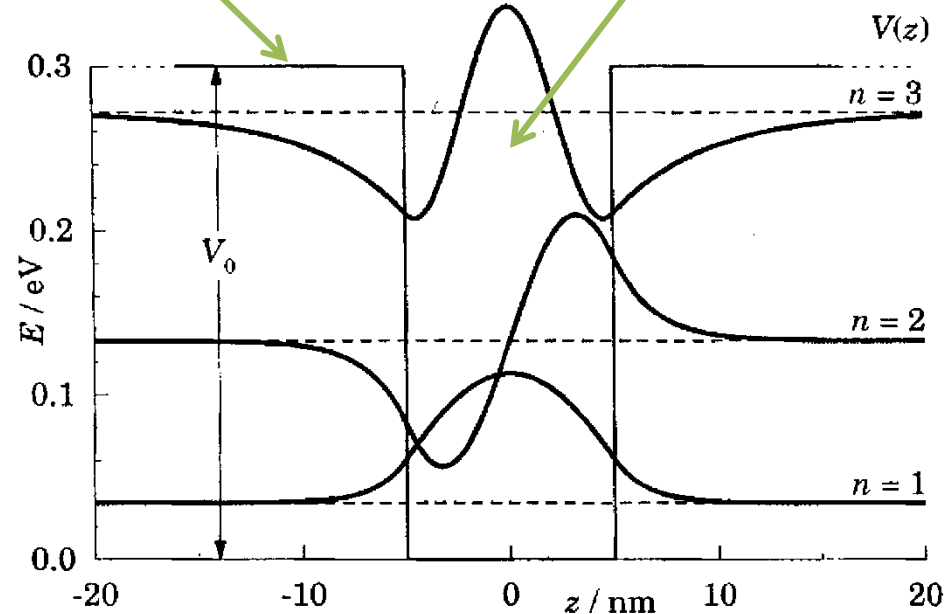
$$\frac{\hbar^2 \kappa^2}{2m m_B} = E_B - E_n = B$$

$$\psi(z) = D \exp(\pm \kappa_n z)$$

Matching conditions:

$$\frac{1}{m_B} \frac{d\psi}{dz} \Big|_{z=\frac{a}{2}} = \frac{1}{m_W} \frac{d\psi}{dz} \Big|_{z=\frac{a}{2}}$$

$$\frac{Ck}{m_W} \begin{cases} -\sin\left(k_n \frac{a}{2}\right) \\ \cos\left(k_n \frac{a}{2}\right) \end{cases} = -\frac{D\kappa}{m_B} \exp\left(k_n \frac{a}{2}\right)$$



Finite potential well – square well

THE DIFFERENT mass in the well and in the barrier:

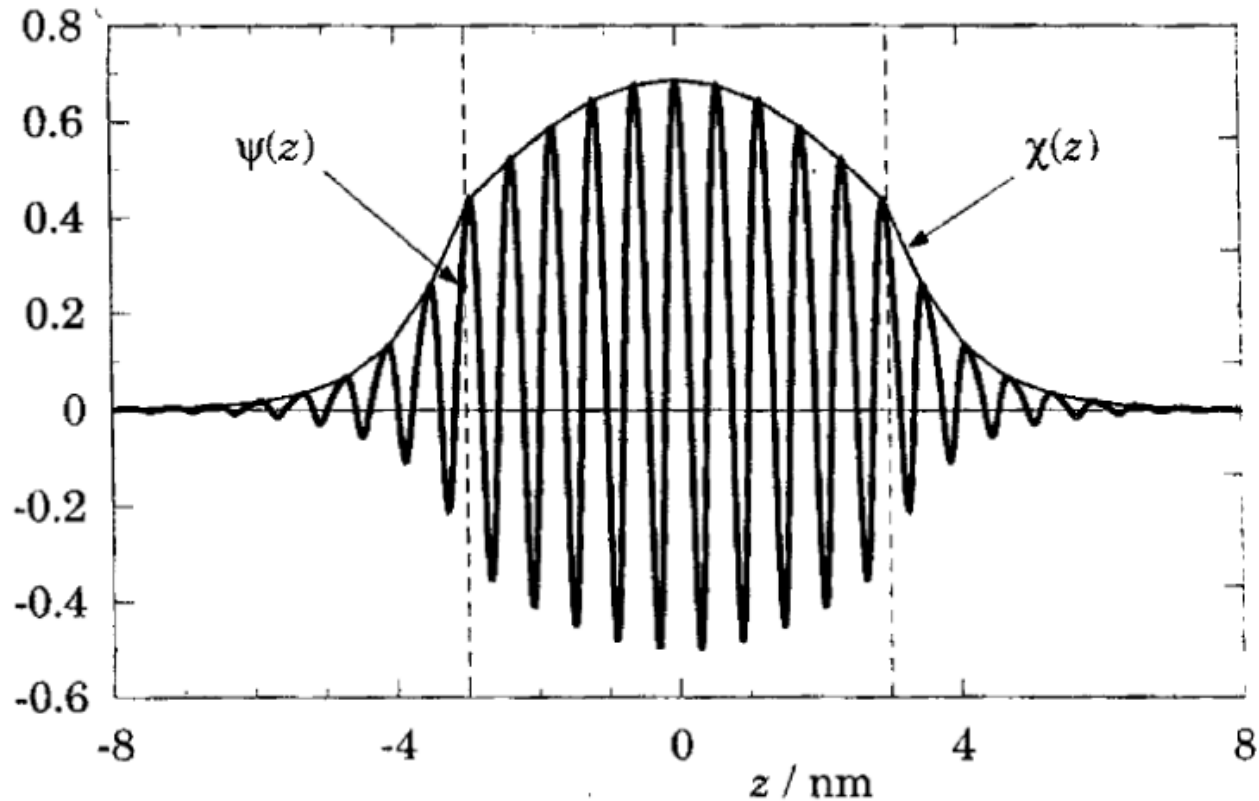


FIGURE 3.22. Wave function for the lowest state in a 6 nm quantum well in a heterostructure, including the Bloch functions. The thin curve is an approximate envelope function joining the peaks of the full wave function. [Redrawn from Burt (1994).]

Harmonic potential

$$\left[-\frac{\hbar^2}{2m} \frac{d^2}{dz^2} + V(z) \right] \psi(z) = \varepsilon \psi(z) \quad V(z) = \frac{1}{2} K z^2 = \frac{1}{2} m \omega_0^2 z^2 \quad \varepsilon_n = \left(n - \frac{1}{2} \right) \hbar \omega_0$$

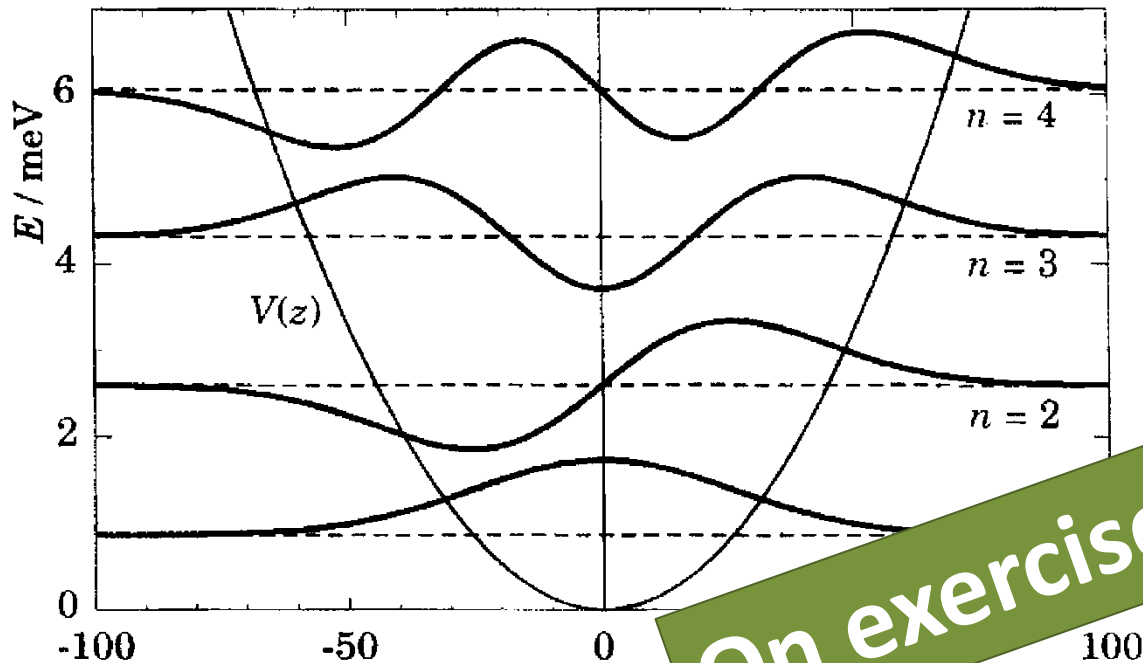


FIGURE 4.4. Potential well $V(z)$, energy levels, and wave functions of a harmonic oscillator. The potential is generated by a magnetic field of 1 T acting on electrons in GaAs.

Quantum harmonic oscillator

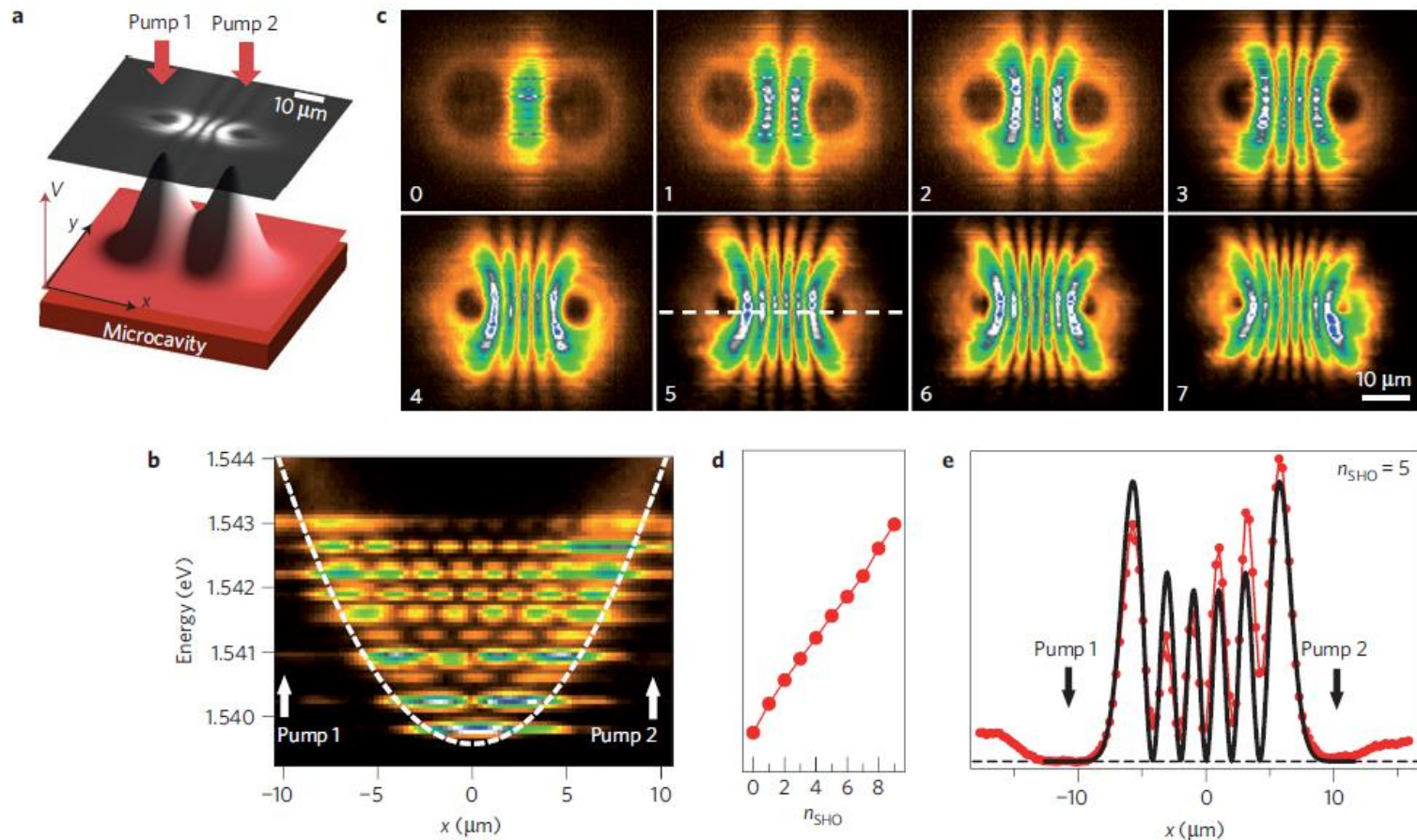


Figure 1 | Spatially mapped polariton-condensate wavefunctions. **a**, Experimental scheme with two $1\ \mu\text{m}$ -diameter pump spots separated by $20\ \mu\text{m}$ focused on the planar microcavity. The effective potential V (red) produces multiple condensates (grey image shows $n_{\text{SHO}} = 3$ mode). **b**, Real-space spectra along line between pump spots. **c**, Tomographic images of polariton emission (repulsive potential seen as dark circles around pump spots). Labelled according to n_{SHO} assigned from **d**. **d**, Extracted mode energies versus quantum number. **e**, Hermite-Gaussian fit of $\psi_{\text{SHO}}^{n=5}(x)$ to image cross-section, dashed in **c**.

Nat. Phys. 8, 190, (2012)

Triangular well

$$\left[-\frac{\hbar^2}{2m} \frac{d^2}{dz^2} + eFz \right] \psi(z) = \varepsilon \psi(z)$$

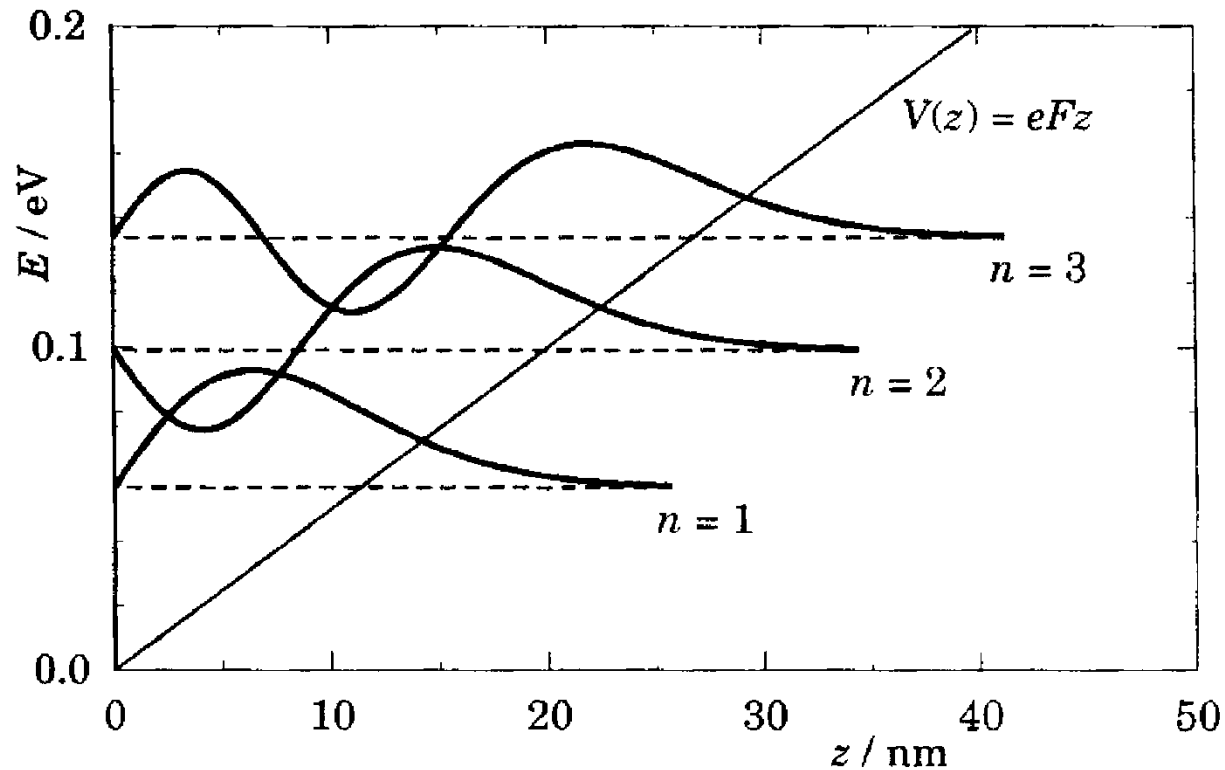
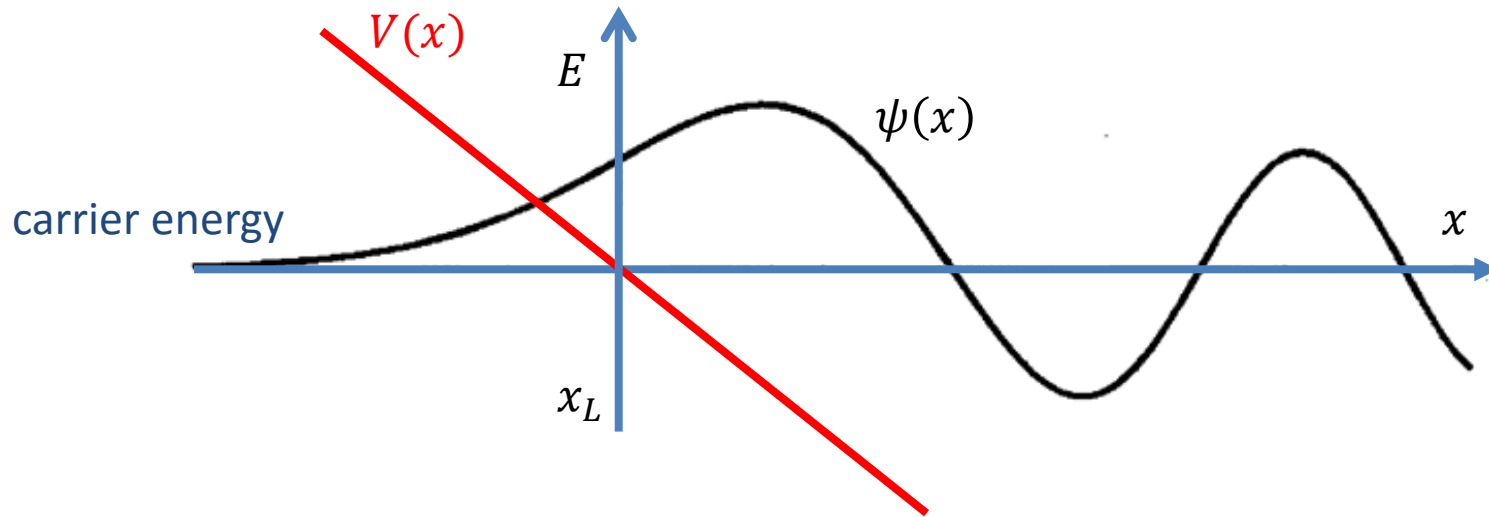


FIGURE 4.6. Triangular potential well $V(z) = eFz$, showing the energy levels and wave functions. The scales are for electrons in GaAs and a field of 5 MV m^{-1} .

WKB approximation

WKB approximation (Wentzel – Krammers – Brillouin) – for slowly varying potential



$$\psi(x) \sim \frac{2}{\sqrt{k(x)}} \cos \left[\int_{x_L}^x k(x') dx' - \frac{\pi}{4} \right], \quad x \gg x_L$$

$$\psi(x) \sim \frac{1}{\sqrt{\kappa(x)}} \exp \left[- \int_{x_L}^x \kappa(x') dx' \right], \quad x \ll x_L$$

Coulomb potential in 2D

$$\Psi(\mathbf{r}) = R(r)\Phi(\phi)$$

Radial therm:

$$-\frac{1}{2} \left(\frac{d^2}{dr^2} + \frac{1}{r} \frac{d}{dr} - \frac{m^2}{r^2} + \frac{2}{r} \right) R(r) = ER(r)$$

O! joj-joj-joj! (some substitutions, derivations nad equations):

$$R_{n,m}(\rho) = e^{-\frac{\rho}{2}} \sum_{j=0}^{N(n)} a_0 \frac{|m| + j - n}{j(2|m| + j)} \rho^{|m|+j}$$

Finally:

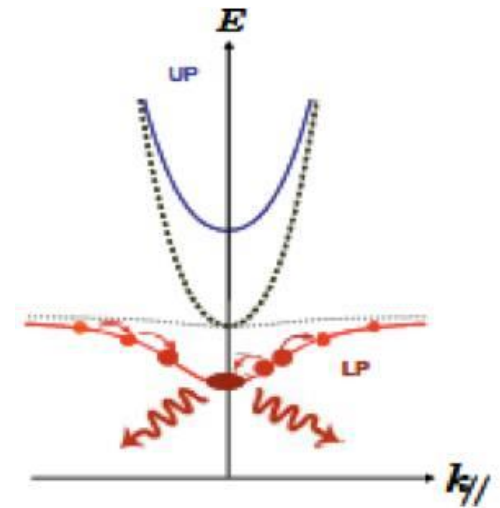
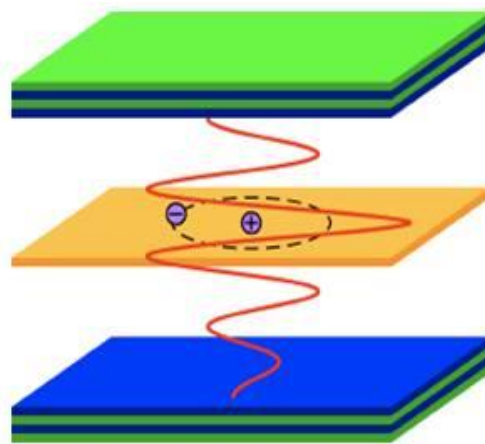
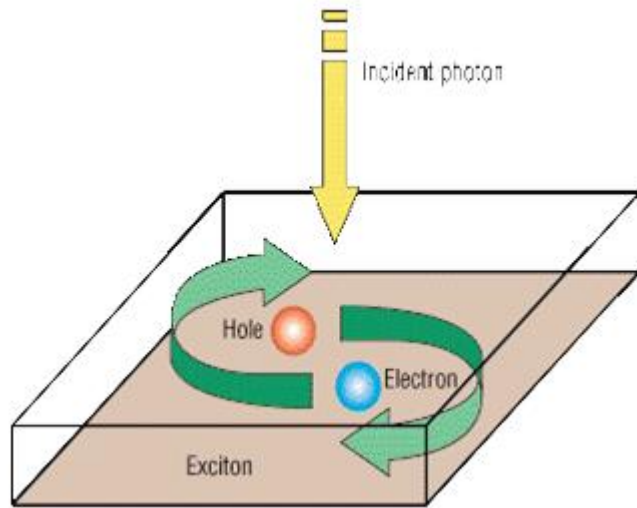
$$Ry^* = \left(\frac{e^2}{4\pi\epsilon_r\epsilon_0} \right)^2 \frac{m^*}{2\hbar^2} = \frac{1}{2} \frac{e^2}{4\pi\epsilon_0\epsilon_r a_B^*} = \left(\frac{m^*}{m_0} \right) \frac{Ry}{\epsilon_r^2} \quad a_B^* = \epsilon_r \left(\frac{m_0}{m^*} \right)$$

$$E_n = - \frac{Ry^*}{\left(n - \frac{1}{2} \right)^2}$$

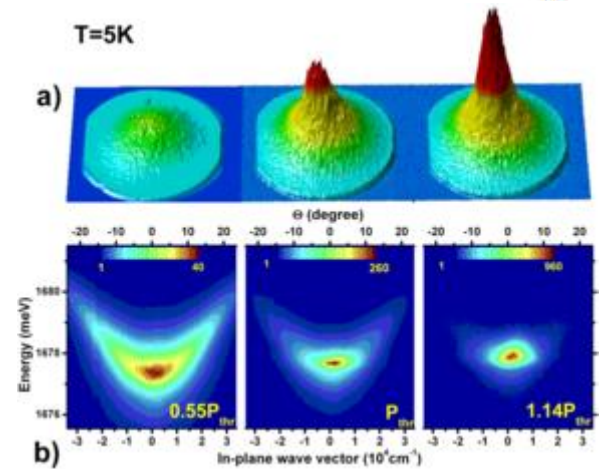
For Hydrogen $Ry = 13.6$ eV and $a_B = 0.053$ nm

For GaAs semiconductor $Ry^* \approx 5$ meV and $a_B^* \approx 10$ nm

Polaritons



Dr Nataliya Bobrovskaya



http://www.stanford.edu/group/yamamotogroup/research/EP/EP_main.html

Time-dependent perturbation theory

Time-dependent Schrödinger equation:

$$i\hbar \frac{\partial}{\partial t} \psi = H_0 + V(t)$$

$$\psi(x, t) = \sum_n A_n(t) \varphi_n(x) e^{-iE_n t / \hbar}$$

By analogy

Time-independent potential

$$H_0 = -\frac{\hbar^2}{2m} \frac{\partial^2}{\partial x^2} + U(x)$$

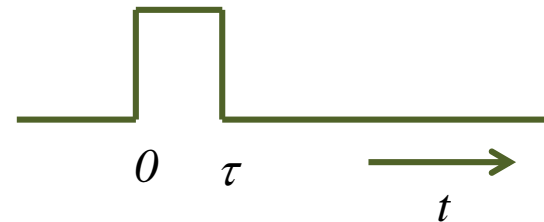
$$\psi(x, t) = A \varphi(x) e^{-iEt / \hbar}$$

Time-independent potential

$$H = H_0 + V(t)$$

The simplest case:

$$V(t) = \begin{cases} W(t) & \text{dla } 0 \leq t \leq \tau \\ 0 & \text{dla } t < 0 \text{ i } t > \tau \end{cases}$$



Summary – Fermi golden rule

The probability of transition per unit time:

$$W(t) = W \\ 0 \leq t \leq \tau$$

$$P_{mn} = \frac{w_{mn}}{\tau} = \frac{2\pi}{\hbar} |\langle m|W|n\rangle|^2 \delta(E_m - E_n)$$

Transitions are possible only for states, for which $E_m = E_n$

$$W(t) = w^\pm e^{\pm i\omega t} \\ 0 \leq t \leq \tau$$

$$P_{nm} = \frac{w_{nm}}{\tau} = \frac{2\pi}{\hbar} |\langle n|w^\pm|m\rangle|^2 \delta(E_n - E_m \pm \hbar\omega)$$

Transitions are possible only for states, for which $E_m = E_n \pm \hbar\omega$

The perturbation in a form of an electromagnetic wave:

$$A_{nm} = \frac{\omega_{nm}^3 e^2}{3\pi\epsilon_0 \hbar c^3} |\langle m|\vec{r}|n\rangle|^2 = \frac{4\alpha}{3} \frac{\omega_{nm}^3}{c^2} |\langle m|\vec{r}|n\rangle|^2$$

$$P_{nm} = A_{nm} \delta(E_n - E_m \pm \hbar\omega)$$

Selection rules in condensed matter

Proof sketch

Bloch function of a carrier in the crystal:

$$\Psi(\vec{r}) = \sum_{n,k} c_{n,k} u_{n,k}(\vec{r}) e^{i\vec{k}\vec{r}}$$

For the electron:

$$\Psi_c(\vec{r}) \approx \sum_k c_{1,k} u_{\Gamma_6,0}(\vec{r}) e^{i\vec{k}\vec{r}} = u_{\Gamma_6,0}(\vec{r}) F_e(\vec{r})$$

For the hole:

$$\Psi_v(\vec{r}) \approx \sum_{J_z = \pm 3/2, \pm 1/2, k} c_{J_z,k} u_{\Gamma_8,J_z}(\vec{r}) e^{i\vec{k}\vec{r}} = \sum_{J_z = \pm 3/2, \pm 1/2, k} u_{\Gamma_8,J_z}(\vec{r}) F_{J_z}(\vec{r})$$

Intersubband dipole optical transitions:

$$\langle \Psi_c(\vec{r}) | \vec{p} | \Psi_{v,J_z}(\vec{r}) \rangle = \langle u_{\Gamma_6,0}(\vec{r}) | u_{\Gamma_8,J_z}(\vec{r}) \rangle \langle F_e(\vec{r}) | \vec{p} | F_{J_z}(\vec{r}) \rangle + \langle u_{\Gamma_6,0}(\vec{r}) | \vec{p} | u_{\Gamma_8,J_z}(\vec{r}) \rangle \langle F_e(\vec{r}) | F_{J_z}(\vec{r}) \rangle \\ = 0$$

Optical transitions

E_f final energy

E_i initial energy

$E_f = E_i + \hbar c Q$ energy conservation rule

$K_f = K_i + Q$ momentum conservation rule

Photon momentum $\hbar\omega = \hbar c Q$. For $\hbar\omega = 1 \text{ eV}$ we got $Q \approx 10^7 \text{ m}^{-1}$. The size of the Brillouin zone is about $\frac{\pi}{a} \approx \frac{\pi}{0.5 \text{ nm}} = 10^{10} \text{ m}^{-1}$. Therefore $K_f = K_i + Q \approx K_i$

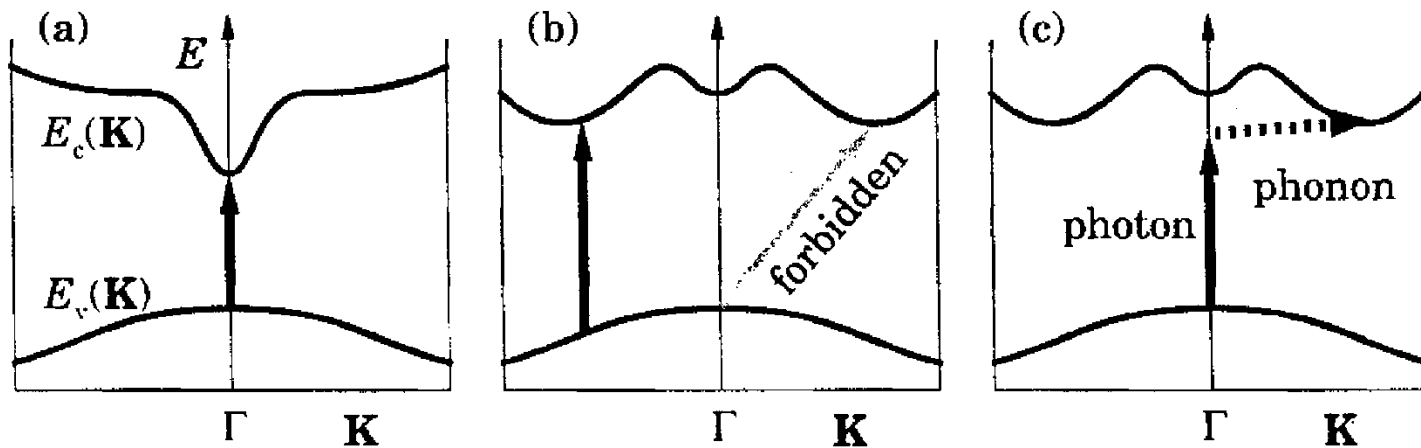


FIGURE 2.20. Optical absorption across the band gap in different types of semiconductor. (a) Absorption across a direct band gap at Γ . (b) Absorption across an indirect band gap is forbidden but vertical transitions occur for all \mathbf{K} . (c) Transition across an indirect band gap with absorption of both a phonon and a photon.

Optical transitions

$$\varepsilon_{e,n_e} = E_c^{GaAs} + \frac{\hbar^2 \pi^2 n_e^2}{2m_0 m_e a^2}$$

$$\varepsilon_{h,n_h} = E_v^{GaAs} - \frac{\hbar^2 \pi^2 n_h^2}{2m_0 m_h a^2}$$

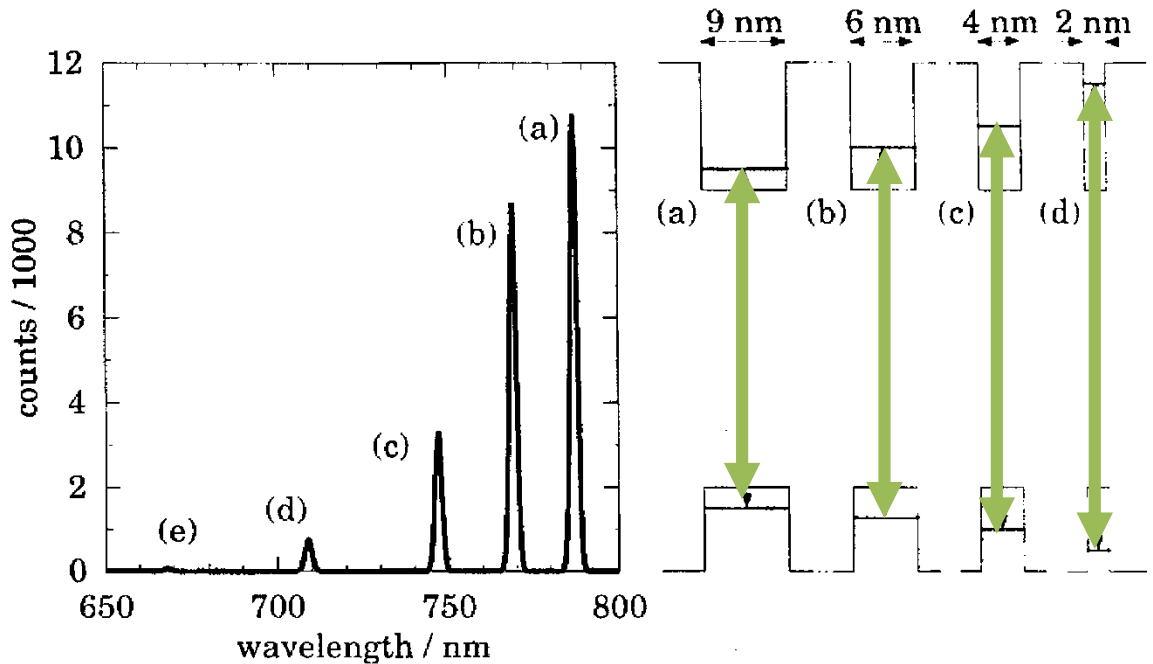


FIGURE 1.4. Photoluminescence as a function of wavelength for a sample with four quantum wells of different widths, whose conduction and valence bands are shown on the right. The barriers between the wells are much thicker than drawn. [Data kindly supplied by Prof. E. L. Hu, University of California at Santa Barbara.]

$$\hbar\omega_n = \varepsilon_{e,n_e} - \varepsilon_{h,n_h} = E_g^{GaAs} + \frac{\hbar^2 \pi^2 n^2}{2m_0 a^2} \left(\frac{1}{m_e} + \frac{1}{m_h} \right) = E_g^{GaAs} + \frac{\hbar^2 \pi^2 n^2}{2m_0 m_{eh} a^2}$$

Optical effective mass

$$\frac{1}{m_{eh}} = \frac{1}{m_e} + \frac{1}{m_h}$$

PHYSICAL REVIEW B **84**, 165319 (2011)

Magnetophotoluminescence study of intershell exchange interaction in CdTe/ZnTe quantum dots

T. Kazimierzuk,^{1,*} T. Smoleński,¹ M. Goryca,^{1,2} Ł. Kłopotowski,³ P. Wojnar,³ K. Fronc,³ A. Golnik,¹ M. Nawrocki,¹
J. A. Gaj,^{1,†} and P. Kossacki^{1,2}

¹*Institute of Experimental Physics, Faculty of Physics, University of Warsaw, Hoża 69, PL-00-681 Warsaw, Poland*

²*Laboratoire National des Champs Magnétiques Intenses, CNRS-UJF-UPS-INSA, BP 166, F-38042 Grenoble cedex 9, France*

³*Institute of Physics, Polish Academy of Sciences, Al. Lotników 32/64, PL-02-688 Warsaw, Poland*

(Received 25 May 2011; revised manuscript received 2 August 2011; published 21 October 2011)

VOLUME 93, NUMBER 20

PHYSICAL REVIEW LETTERS

week ending
12 NOVEMBER 2004

Probing the Spin State of a Single Magnetic Ion in an Individual Quantum Dot

L. Besombes,^{*} Y. Léger, L. Maingault, D. Ferrand, and H. Mariette

*CEA-CNRS group “Nanophysique et Semiconducteurs”, Laboratoire de Spectrométrie Physique, CNRS,
and Université Joseph Fourier, BP87, F-38402 St Martin d’Heres, France*

J. Cibert

Laboratoire Louis Néel, CNRS, BP 166X, F-38042 Grenoble, France

(Received 29 June 2004; published 11 November 2004)

Low dimensional structures

The particle moves in the well which potential depends on \mathbf{k} , in fact $k = |\mathbf{k}|$

$$\left[-\frac{\hbar^2}{2m_0 m_W} \frac{d^2}{dz^2} + \frac{\hbar^2 \mathbf{k}^2}{2m_0 m_W} + E_W \right] u_n(z) = \varepsilon u_n(z)$$

$$\left[-\frac{\hbar^2}{2m_0 m_B} \frac{d^2}{dz^2} + \frac{\hbar^2 \mathbf{k}^2}{2m_0 m_B} + E_B \right] u_n(z) = \varepsilon u_n(z)$$

$$V_0(k) = (E_B - E_W) + \frac{\hbar^2 k^2}{2m_0} \left(\frac{1}{m_B} - \frac{1}{m_W} \right)$$

The particle gains partially the effective mass of the barrier:

E.g. in GaAs-AlGaAs heterostructure $m_B > m_W$ thus the well gets „shallow“

$$E_n(k) = \varepsilon_n(k) + \frac{\hbar^2 k^2}{2m_0 m_W} \approx \varepsilon_n(k=0) + \frac{\hbar^2 k^2}{2m_0 m_{eff}}$$

energy of the bound state depends on k

$$m_{eff} \approx m_W P_W + m_B P_B$$

the probability of finding a particle

Low dimensional structures

The particle moves in the well which potential depends on \mathbf{k} , in fact $k = |\mathbf{k}|$

$$\left[-\frac{\hbar^2}{2m_0 m_W} \frac{d^2}{dz^2} + \frac{\hbar^2 \mathbf{k}^2}{2m_0 m_W} + E_W \right] u_n(z) = \varepsilon u_n(z)$$

$$\left[-\frac{\hbar^2}{2m_0 m_B} \frac{d^2}{dz^2} + \frac{\hbar^2 \mathbf{k}^2}{2m_0 m_B} + E_B \right] u_n(z) = \varepsilon u_n(z)$$

$$V_0(k) = (E_B - E_W) + \frac{\hbar^2 k^2}{2m_0} \left(\frac{1}{m_B} - \frac{1}{m_W} \right)$$

The particle gains partially the effective mass of the barrier:

E.g. in GaAs-AlGaAs heterostructure $m_B > m_W$ thus the well gets „shallow”

$$E_n(k) = \varepsilon_n(k) + \frac{\hbar^2 k^2}{2m_0 m_W} \approx \varepsilon_n(k=0) + \frac{\hbar^2 k^2}{2m_0 m_{eff}}$$

energy of the bound state depends on k

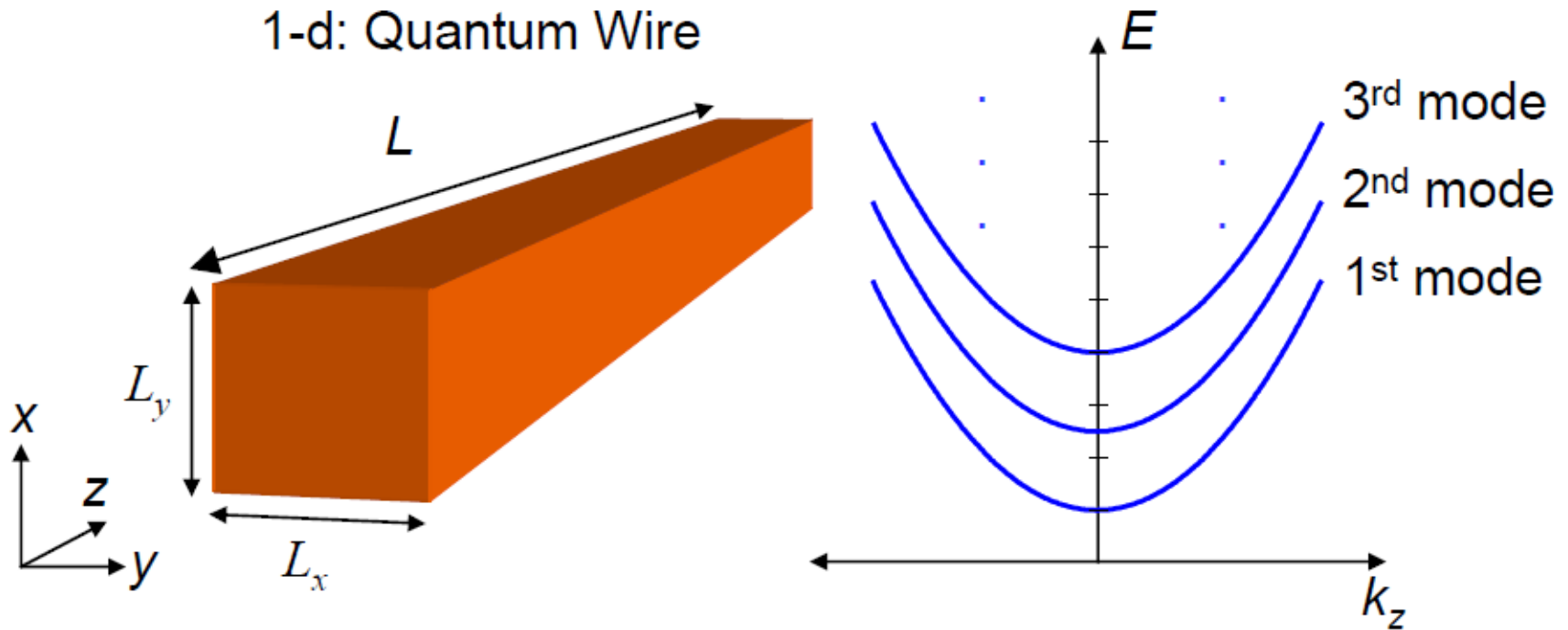
$$m_{eff} \approx m_W P_W + m_B P_B$$

the probability of finding a particle

Quantum wire

$$\psi_{k_x, m, n}(x, y, z) = u_{m, n}(x, y) \exp(ik_z z) = \text{albo np.} = u_{n, l}(r, \theta) \exp(ik_z z)$$

$$E_n(k_x, k_y) = \varepsilon_{m, n} + \frac{\hbar^2 k_z^2}{2m}$$



Marc Baldo MIT OpenCourseWare Publication May 2011

Quantum wire

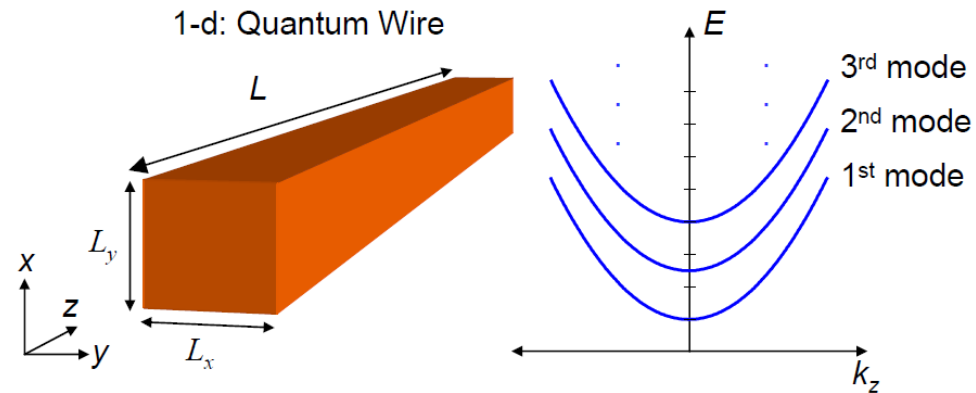
$$\psi_{k_x, m, n}(x, y, z) = u_{m, n}(x, y) \exp(ik_z z) = \text{also np.} = u_{n, l}(r, \theta) \exp(ik_z z)$$

$$E_n(k_x, k_y) = \varepsilon_{m, n} + \frac{\hbar^2 k_z^2}{2m}$$

Square quantum well 2D $L_x L_y$, infinite potential:

$$\psi_{k_x, m, n}(x, y, z) = u_{m, n}(x, y) \exp(ik_z z) = \exp(ik_m x) \exp(ik_n y) \exp(ik_z z)$$

With boundary conditions $L_x k_m = n_x \pi$ and $L_y k_n = n_y \pi$ (discrete spectrum)

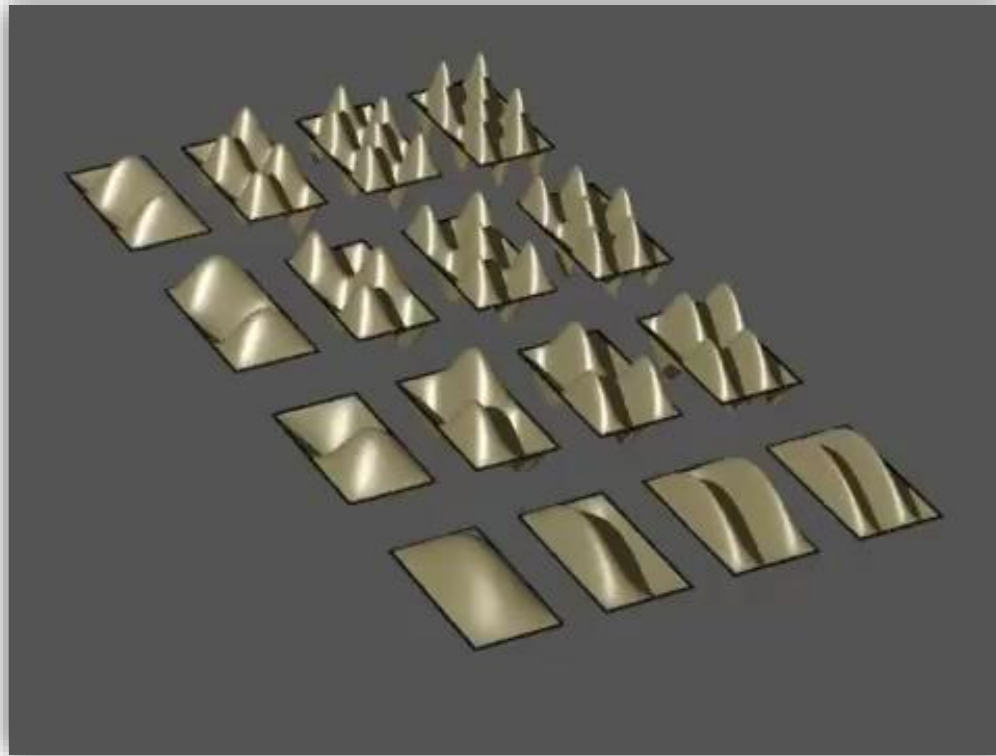


Marc Baldo MIT OpenCourseWare Publication May 2011

Quantum wire

Rectangular wire ($a \times b$) – solutions like:

$$\epsilon_{n_x, n_y} = \frac{\hbar^2 \pi^2}{2m} \left(\frac{n_x^2}{L_x^2} + \frac{n_y^2}{L_y^2} \right)$$

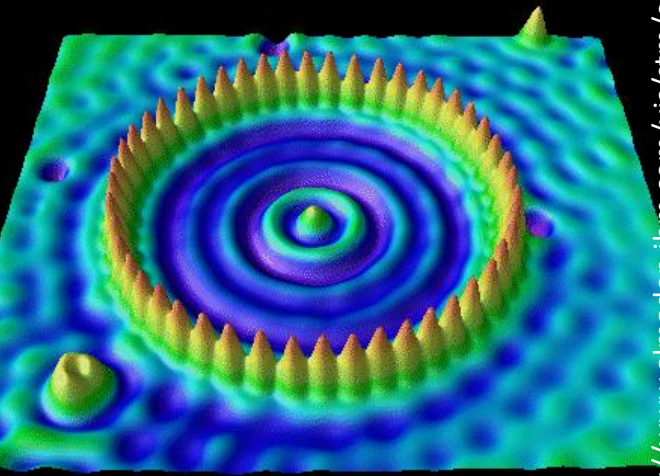


http://wn.com/2d_and_3d_standing_wave

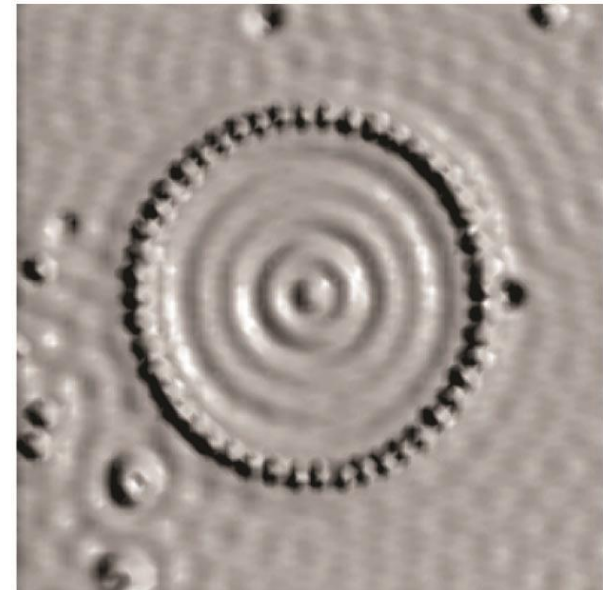
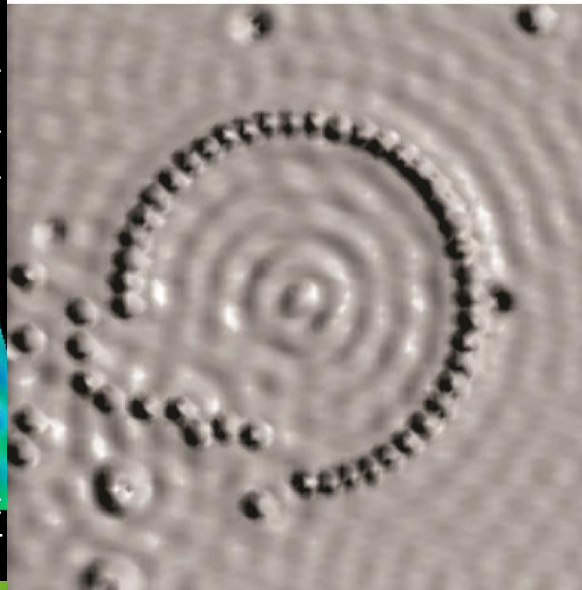
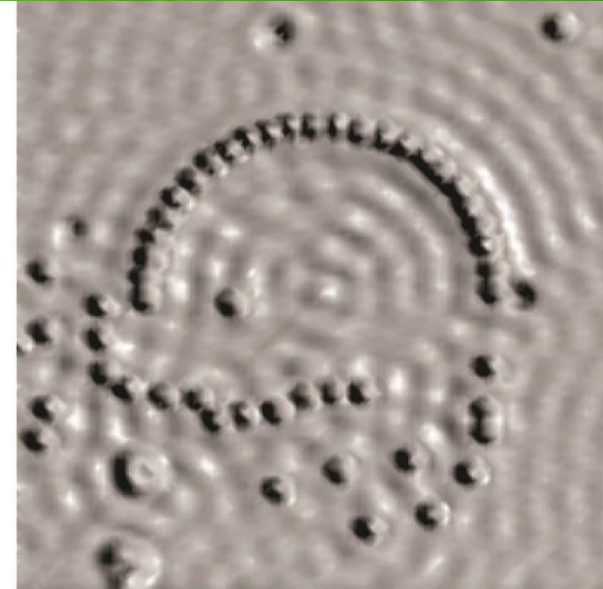
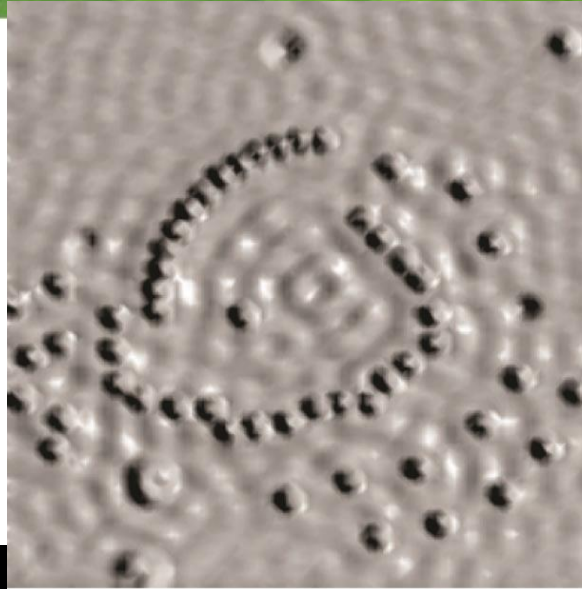
Quantum wells 2D and 3D

Cylindrical well

low temperature scanning tunneling microscope (STM)



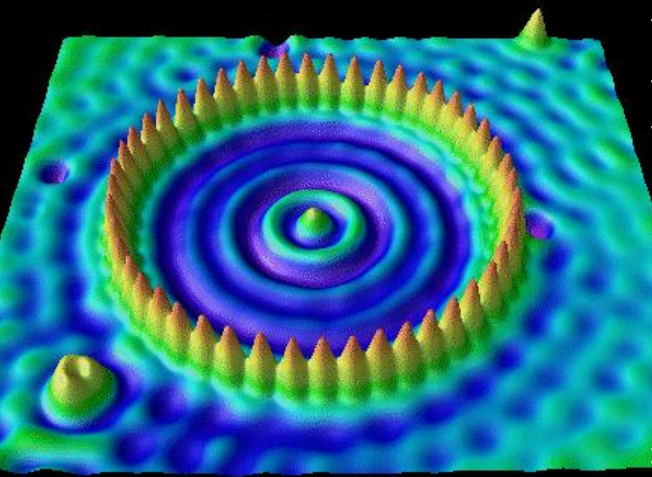
<http://www.almaden.ibm.com/vis/stm/corral.htm> #stm16



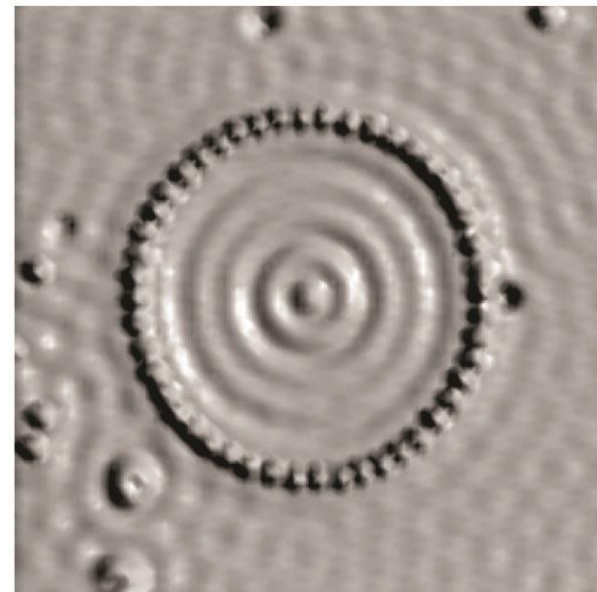
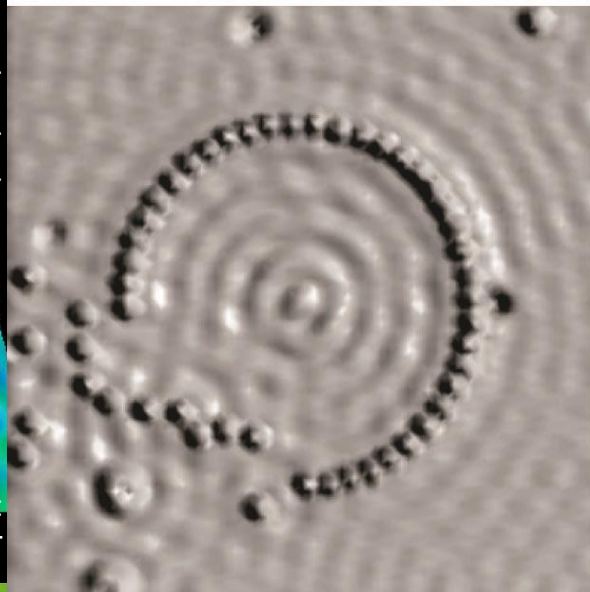
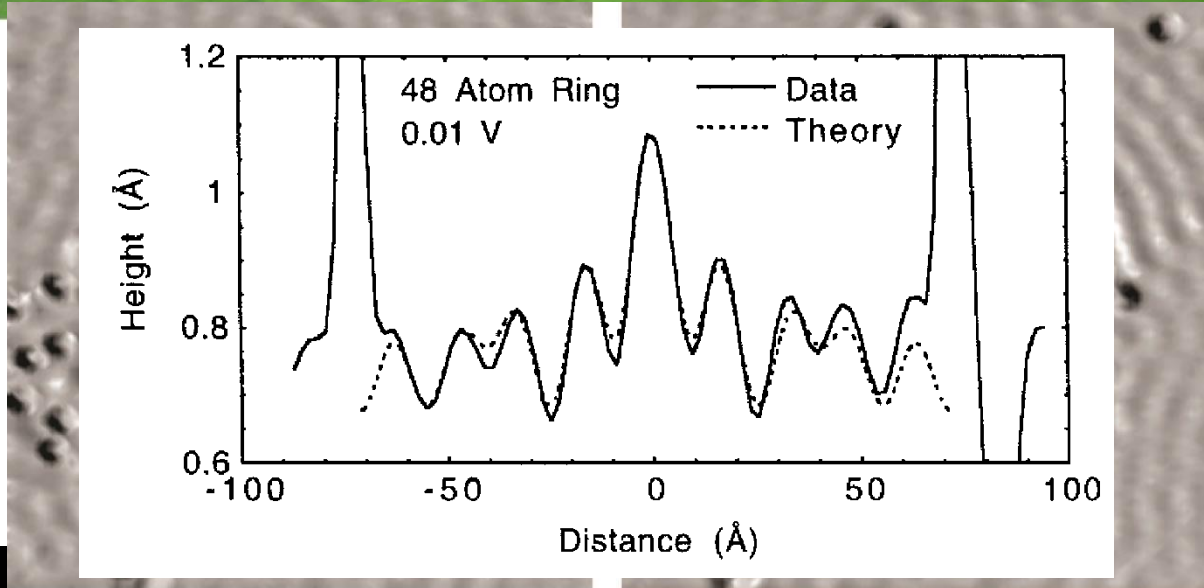
Quantum wells 2D and 3D

Cylindrical well

low temperature scanning tunneling microscope (STM)



<http://www.almaden.ibm.com/vis/stm/corral.htm> #stm16



Harmonic potential 2D

$$E_n^x = \hbar\omega_0 \left(n_x + \frac{1}{2} \right) \text{ in the } x\text{-direction and the same in } y$$

$$E_n^y = \hbar\omega_0 \left(n_y + \frac{1}{2} \right)$$

$$E_n = E_n^x + E_n^y = \hbar\omega_0(N + 1)$$

Degeneracy?

$$N = n_x + n_y$$

2D disk shaped dot

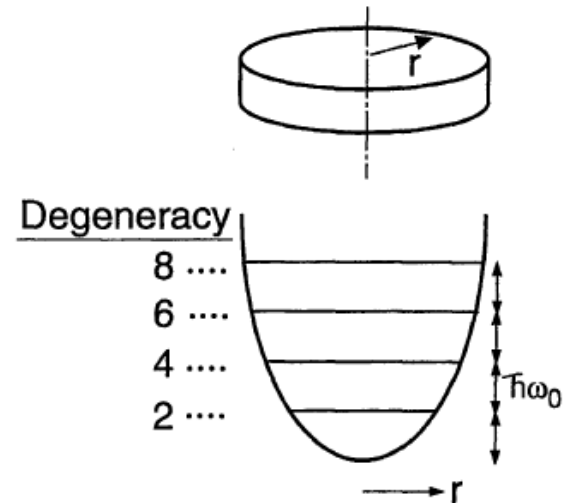


Fig. 5. Schematic model for the vertical dot with a harmonic lateral potential. The single-particle states are laterally confined into discrete equidistant 0D levels whose degeneracies are 2, 4, 6, 8, ... including spin degeneracy from the lowest level.

Jpn. J. Appl. Phys. Vol. 36 (1997) pp. 3917-3923
Part 1, No. 6B, June 1997

Harmonic potential 2D

$$E_n^x = \hbar\omega_0 \left(n_x + \frac{1}{2} \right) \text{ in the } x\text{-direction and the same in } y$$

$$E_n^y = \hbar\omega_0 \left(n_y + \frac{1}{2} \right)$$

$$E_n = E_n^x + E_n^y = \hbar\omega_0(N + 1)$$

Degeneracy?

$$N = n_x + n_y$$

$$g_N = N + 1$$

N	(n_x, n_y)
0	(0,0)
1	(1,0) (0,1)
2	(2,0) (1,1) (0,2)
3	(3,0) (2,1) (1,2) (0,3)

2D disk shaped dot

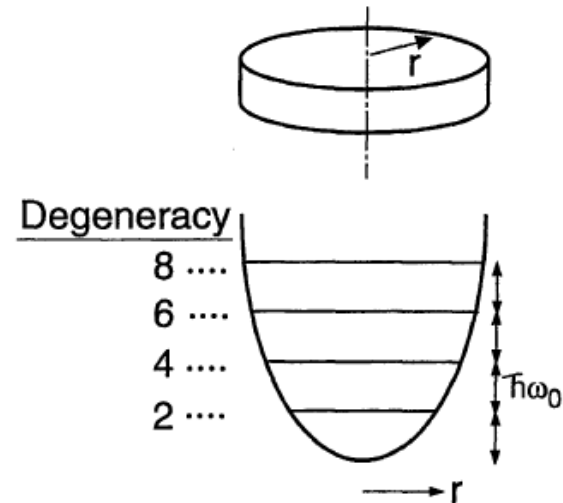


Fig. 5. Schematic model for the vertical dot with a harmonic lateral potential. The single-particle states are laterally confined into discrete equidistant 0D levels whose degeneracies are 2, 4, 6, 8, ... including spin degeneracy from the lowest level.

Jpn. J. Appl. Phys. Vol. 36 (1997) pp. 3917-3923
Part 1, No. 6B, June 1997

Density of states

Density of states Number of states per unit energy $\rho^{nD}(E)$ depends on the dimension

The density of states in k -space of n dimension (and the unite volume) $\rho_k^{nD} = 2 \left(\frac{1}{2\pi} \right)^n$

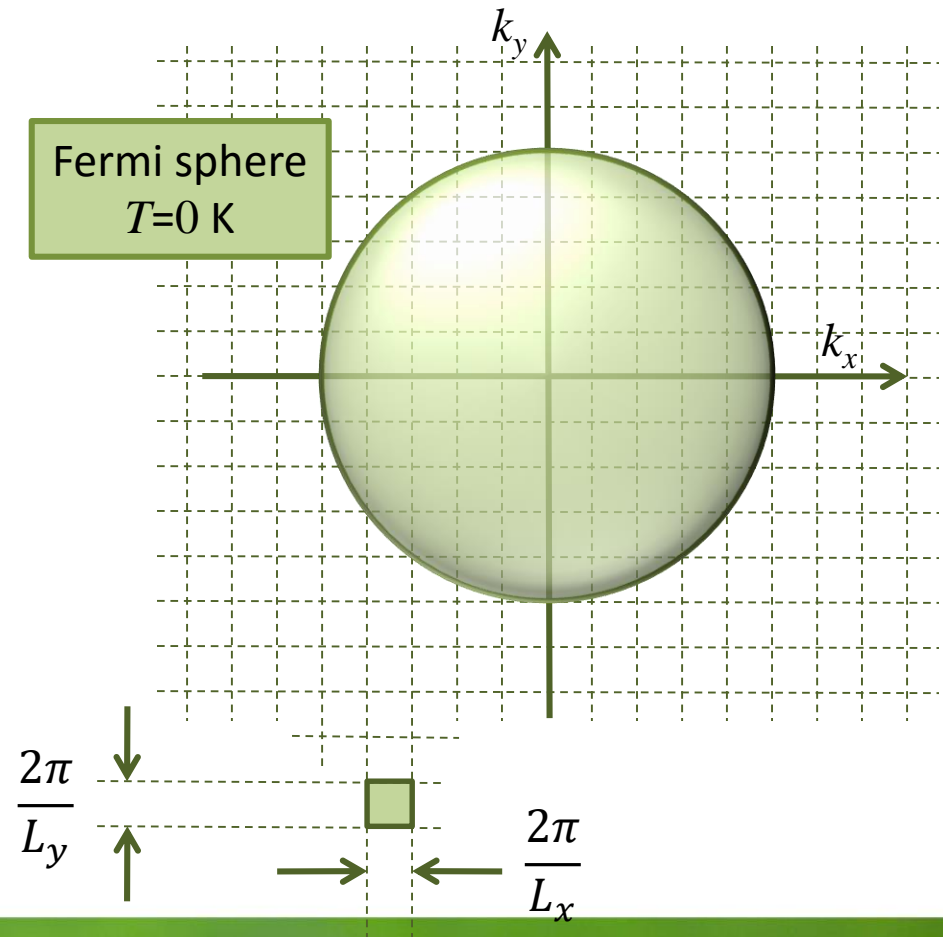
3D case

$$\rho^{3D}(E)dE = \rho_k^{3D} d\vec{k} = 2 \left(\frac{1}{2\pi} \right)^3 4\pi k^2 dk$$

For a spherical and parabolic band:

$$\rho_c^{3D}(E) = \frac{1}{2\pi^2} \left(\frac{2m_0 m_c^*}{\hbar^2} \right)^{3/2} \sqrt{E - E_c}$$

$$\rho_v^{3D}(E) = \frac{1}{2\pi^2} \left(\frac{2m_0 m_h^*}{\hbar^2} \right)^{3/2} \sqrt{E_v - E}$$



Density of states – 2D

$$\psi_{k_x, k_y, n}(x, y, z) = \exp(ik_x x) \exp(ik_y y) u_n(z) = \psi_{\mathbf{k}, n}(\mathbf{r}, z) = \exp(i\mathbf{k} \cdot \mathbf{r}) u_n(z)$$

$$E_n(k_x, k_y) = \varepsilon_n + \frac{\hbar^2 k_x^2}{2m} + \frac{\hbar^2 k_y^2}{2m} \quad E_n(\mathbf{k}) = \varepsilon_n + \frac{\hbar^2 \mathbf{k}^2}{2m}$$

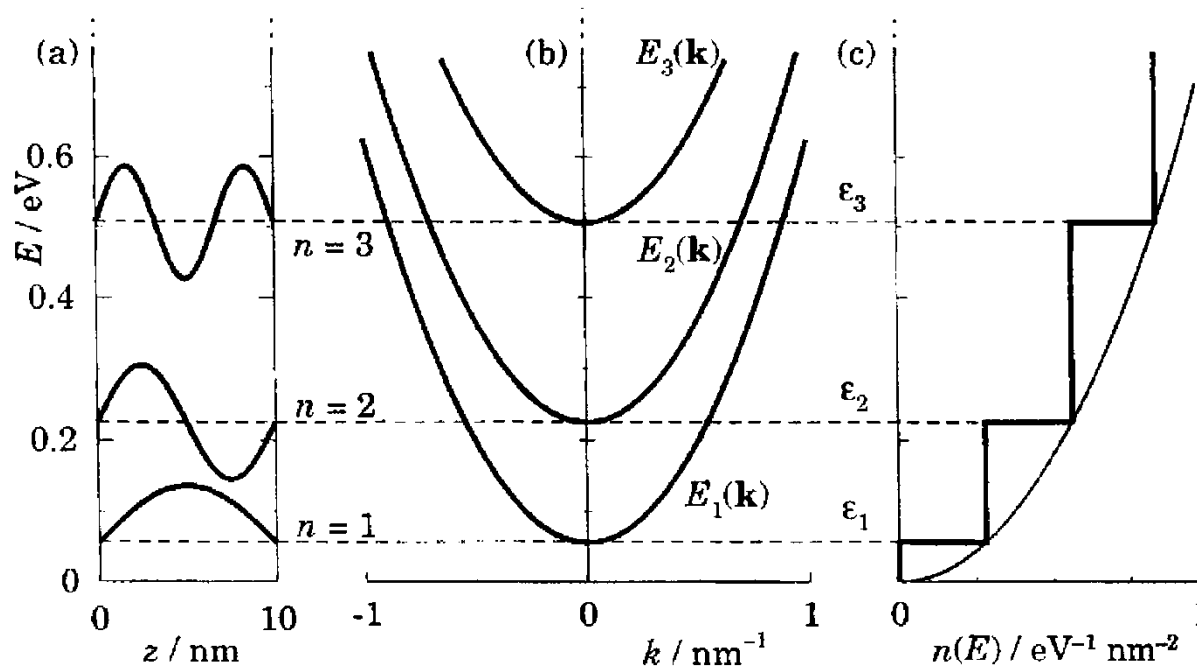


FIGURE 4.7. (a) Potential well with energy levels, (b) total energy including the transverse kinetic energy for each subband, and (c) steplike density of states of a quasi-two-dimensional system. The example is an infinitely deep square well in GaAs of width 10 nm. The thin curve in (c) is the parabolic density of states for unconfined three-dimensional electrons.

Density of states – 1D

1D density of states for a spherical and parabolic band:

$$\rho^{1D}(E)dE = \rho_k^{1D} d\vec{k} = 2 \left(\frac{1}{2\pi} \right)^1 2 dk$$

$$\rho^{1D}(E)dE = \frac{2}{\pi} \sqrt{\frac{m_0 m^*}{2\hbar^2}} \sum_{a_x, a_y} \frac{\theta(E - E_{a_x, a_y})}{\sqrt{E - E_{a_x, a_y}}} dE$$

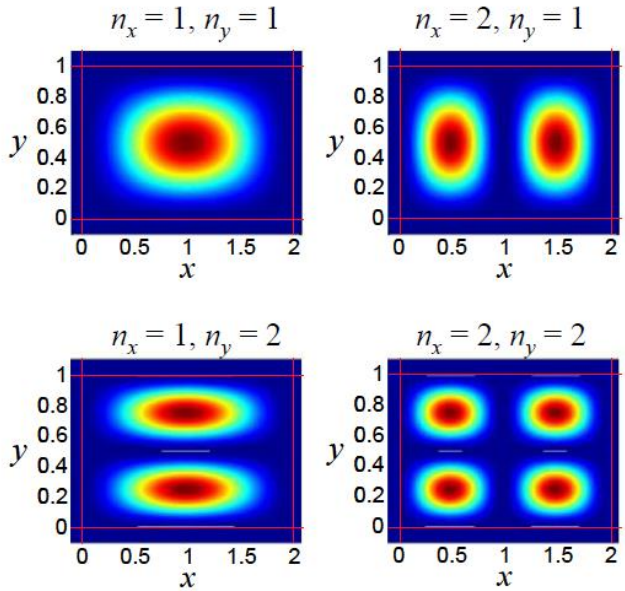
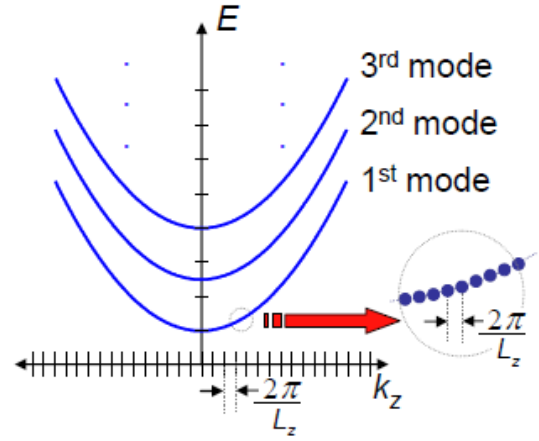
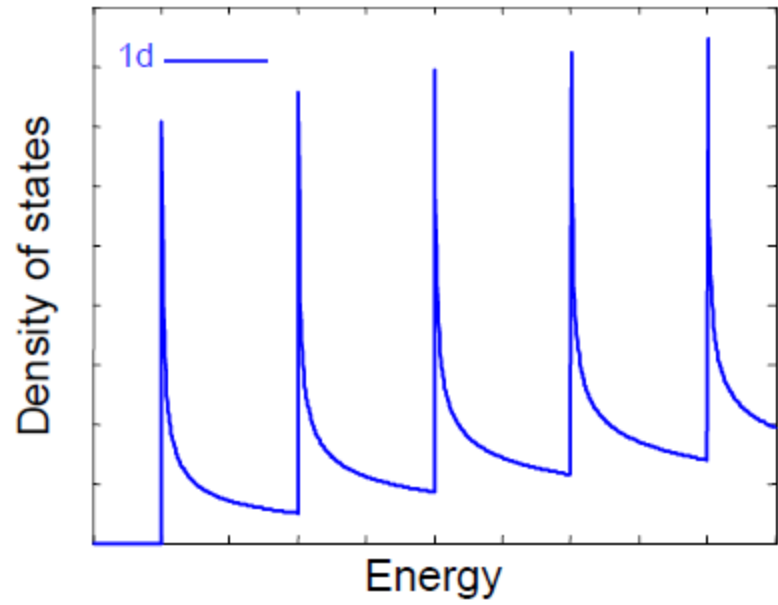


Fig. 2.13. The first four modes of the quantum wire. Since in this example, $L_x > L_y$ the $n_x = 2, n_y = 1$ mode has lower energy than the $n_x = 1, n_y = 2$ mode.

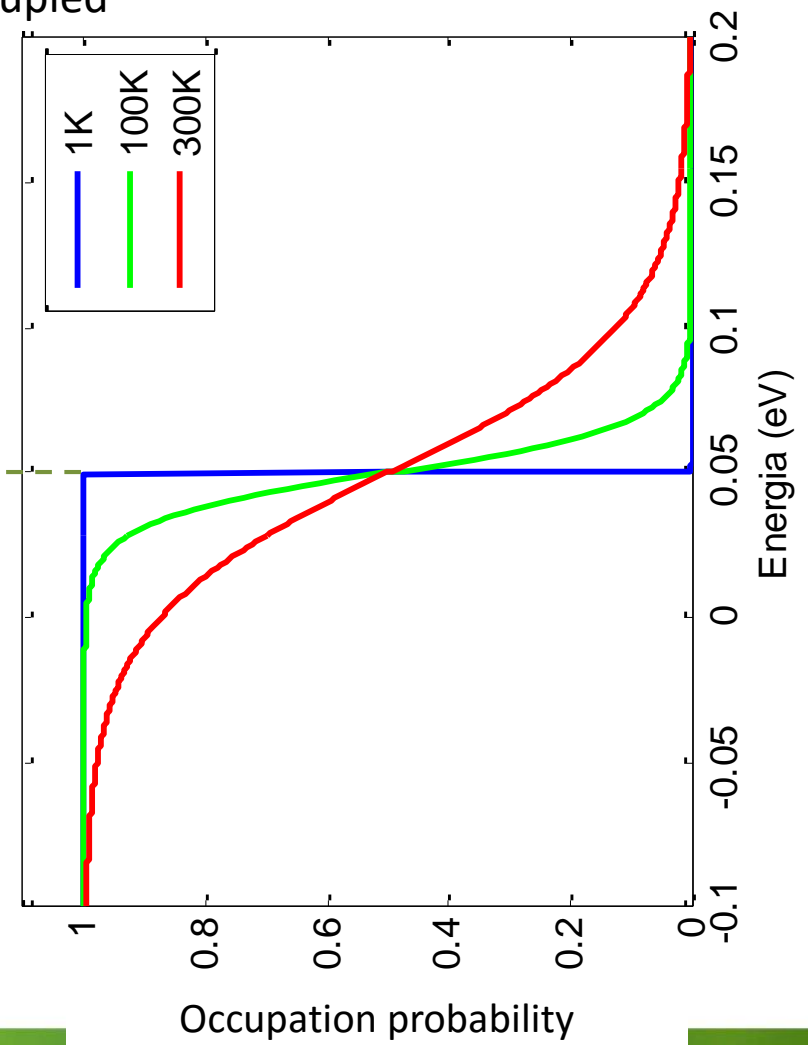
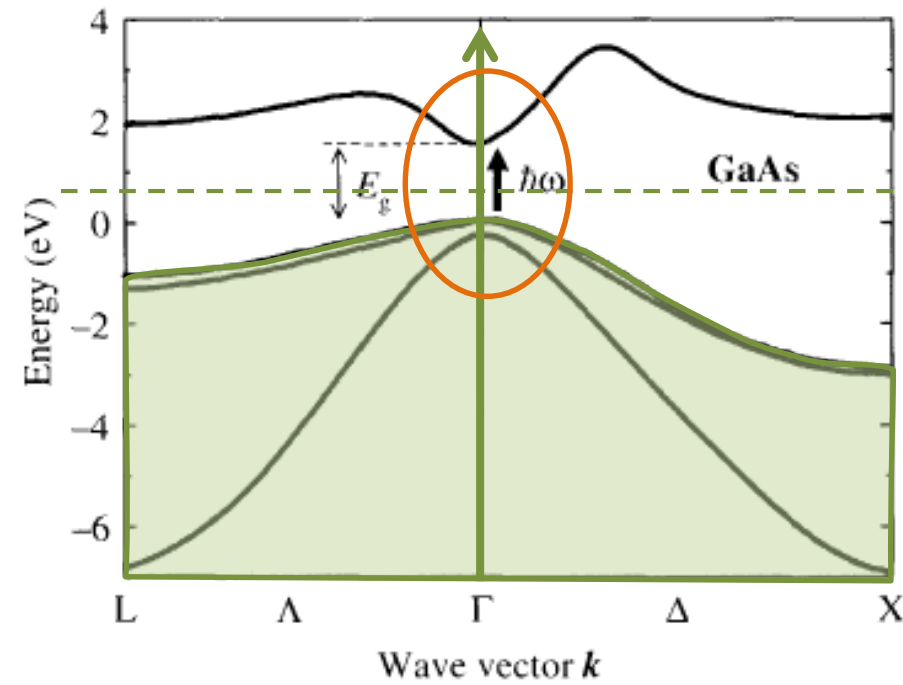


Marc Baldo MIT OpenCourseWare Publication May 2011

The Fermi-Dirac distribution

The probability that a state of the energy E will be occupied
 E_F – chemical potential

$$f_0 = \frac{1}{e^{\frac{E-E_F}{k_B T}} + 1}$$



Electrons statistics in crystals

The case of a semiconductor, in which both the electron gas and hole gas are far from the degeneracy:

the probability of filling of the electronic states:

$$f_e \approx e^{-\frac{E_G}{2k_B T} - \frac{E_e}{k_B T} + \frac{\xi}{k_B T}}$$

and of holes $f_h = 1 - f_e$

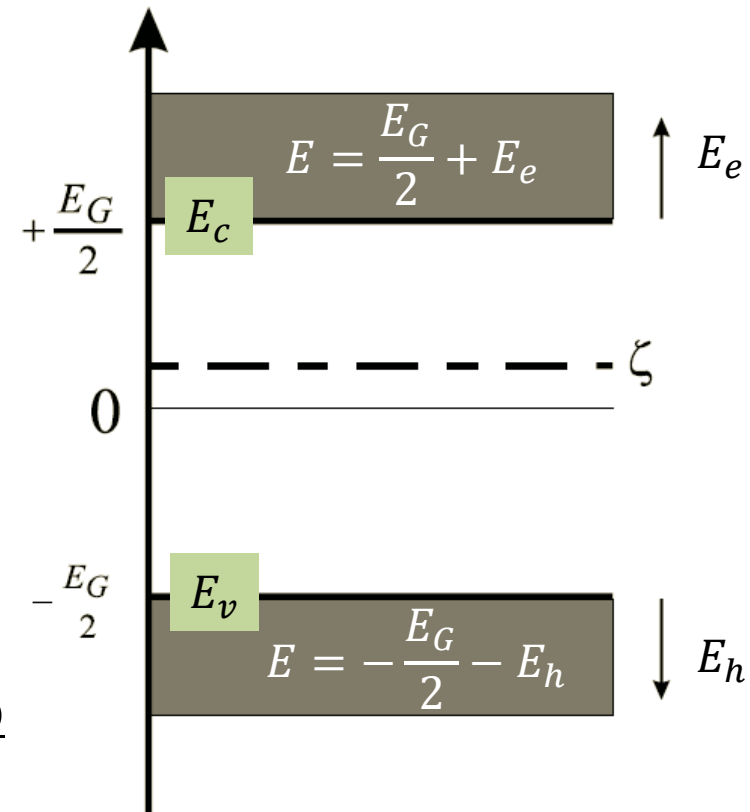
$$f_h \approx e^{-\frac{E_G}{2k_B T} - \frac{E_h}{k_B T} - \frac{\xi}{k_B T}}$$

$$\int_0^{\infty} \sqrt{x} e^{-x} dx = \frac{\sqrt{\pi}}{2}$$

Thus:

$$n(\xi) = 2 \left(\frac{m_e^* k_B T}{2\pi \hbar^2} \right)^{3/2} e^{-\frac{E_G}{2k_B T}} \cdot e^{\frac{\xi}{k_B T}} = N_c(T) e^{-\frac{(E_c - \xi)}{k_B T}}$$

$$p(\xi) = 2 \left(\frac{m_h^* k_B T}{2\pi \hbar^2} \right)^{3/2} e^{-\frac{E_G}{2k_B T}} \cdot e^{-\frac{\xi}{k_B T}} = N_v(T) e^{-\frac{(\xi - E_v)}{k_B T}}$$



The occupation of impurity levels

The ratio of the probability of finding dopant / defect of $n + 1$ electrons and of n electrons:

$$\frac{p_{n+1}}{p_n} = \frac{N_{n+1}/N_{total}}{N_n/N_{total}} = \frac{\sum_{j;n_j=n+1} e^{-\beta[E_j-(n+1)\xi]}}{\sum_{k;n_k=n} e^{-\beta[E_k-n\xi]}} = \frac{g_{n+1}}{g_n} \cdot e^{-\beta[(E_{n+1}-E_n)-\xi]}$$

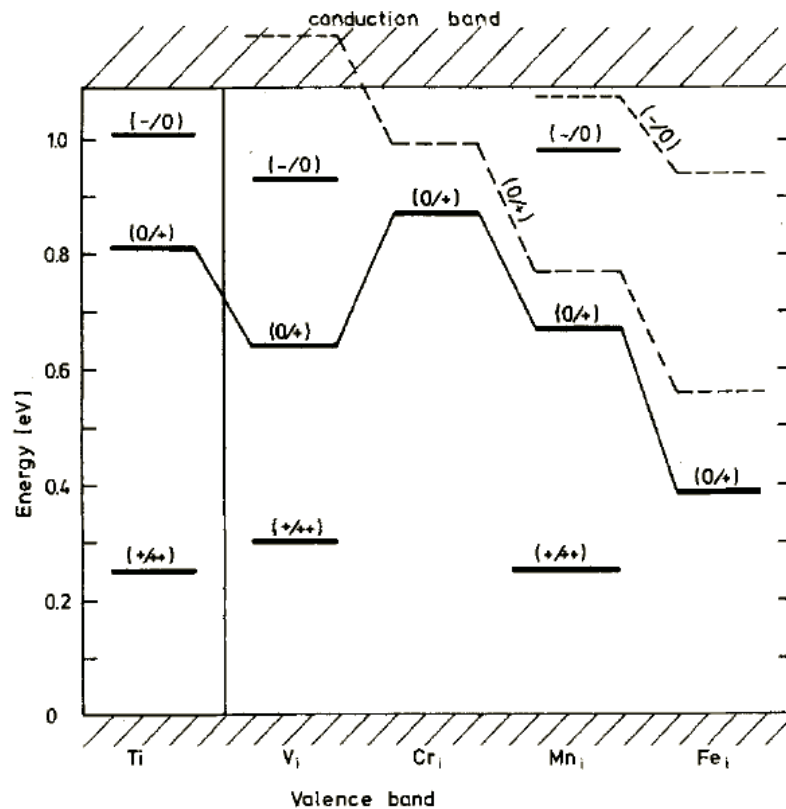


Fig. 15. Energy levels of interstitial 3d metals in silicon (full lines), see Table 3, compared with the results of X_α calculations of DeLeo et al. [15] (broken lines)

$\sum_n N_n = N$ – impurity (dopants) concentration

E_{n+1} i E_n – the lowest of all subsystem energies E_j with $n + 1$ and n electrons respectively

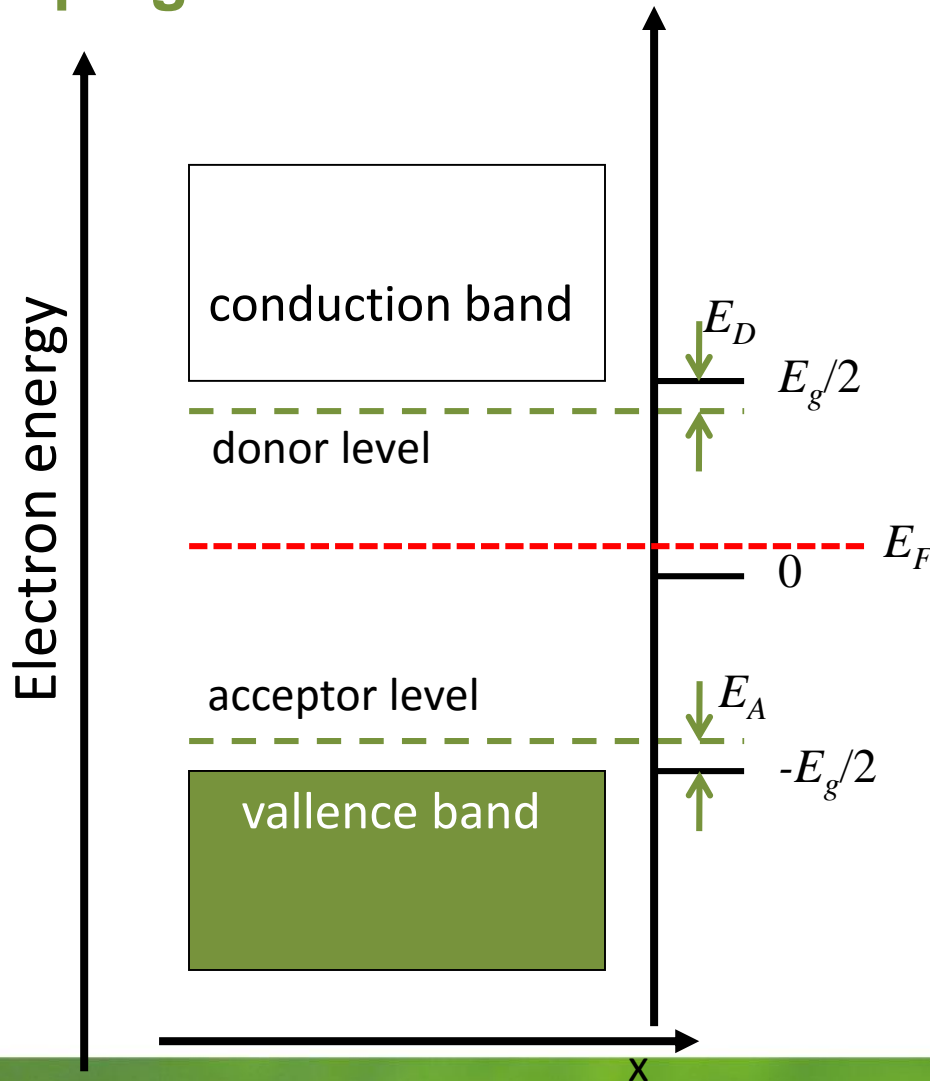
Successive impurity energy levels are filled with the increase of the Fermi level.

$E^{n+1/n}$ – so-called *energy level* of the impurity/defect „numbered” by charge states $n + 1$ and n

g_{n+1} , g_n – so-called degeneracy of states of subsystem of $n + 1$ and n electrons

Dopants, impurities and defects

Doping



The carrier concentration in extrinsic semiconductor (*niesamoistny*)

Consider a semiconductor, in which:

N_A – concentration of acceptors

N_D – concentration of donors

p_A – concentration of neutral acceptors

n_D – concentration of neutral donors

n_c – concentration of electrons in conduction band

p_v – concentration of holes in valence band

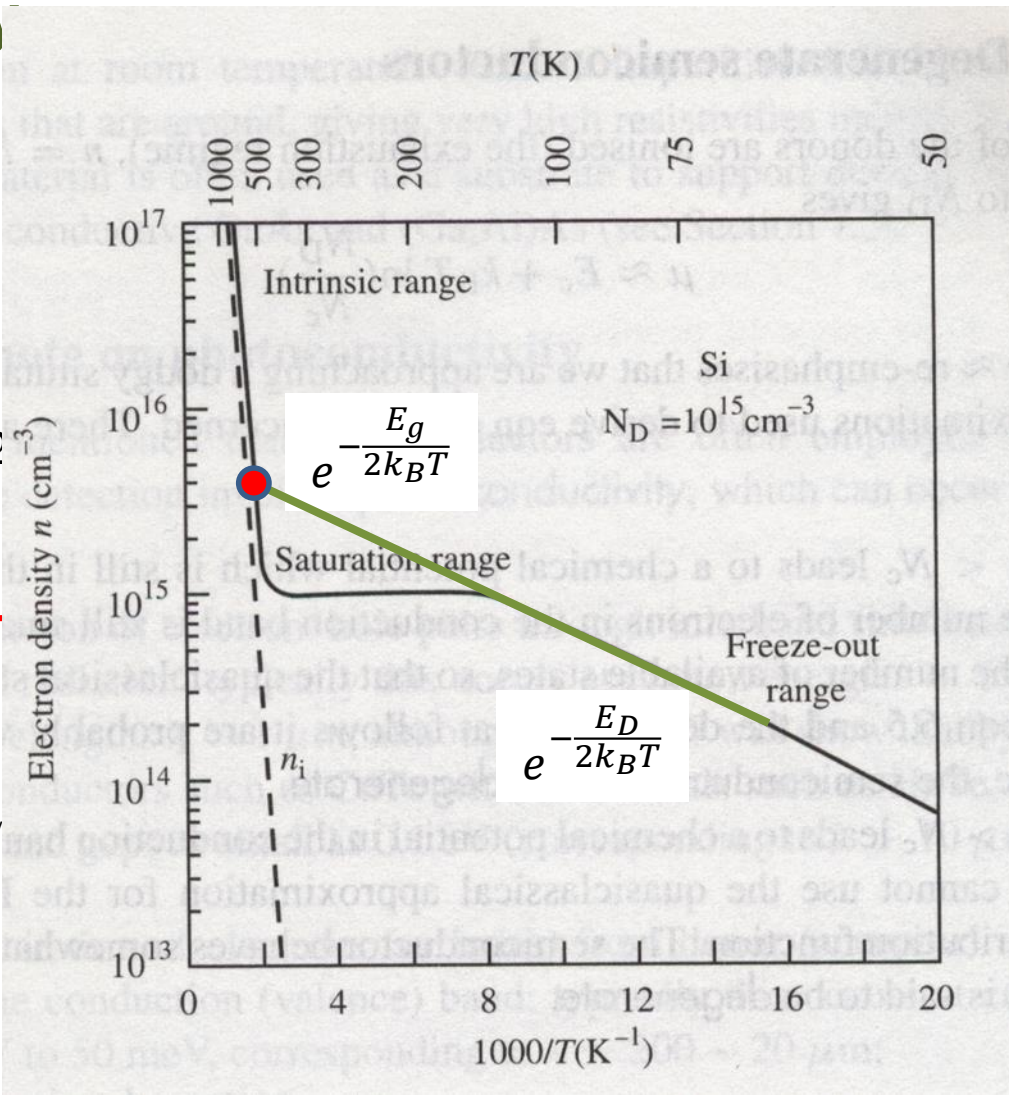
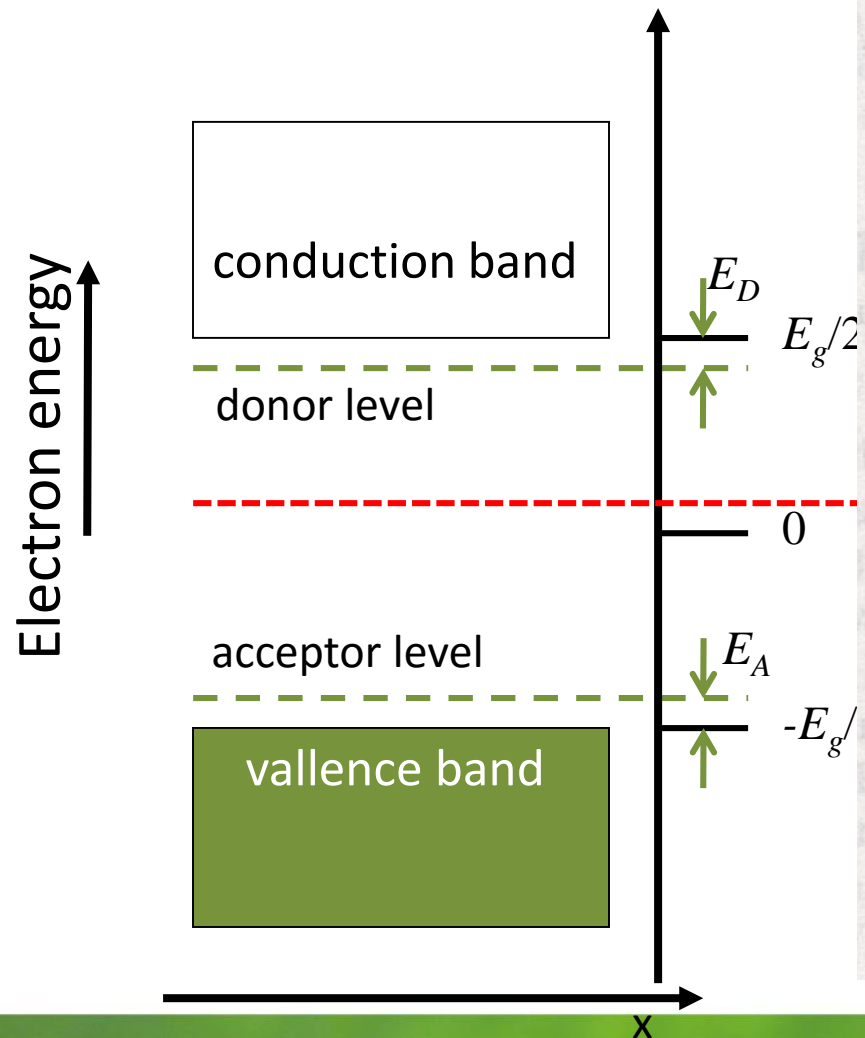
From the charge neutrality of the crystal:

$$n_c + (N_A - p_A) = p_v + (N_D - n_D)$$

$$n_c + n_D = (N_D - N_A) + p_v + p_A$$

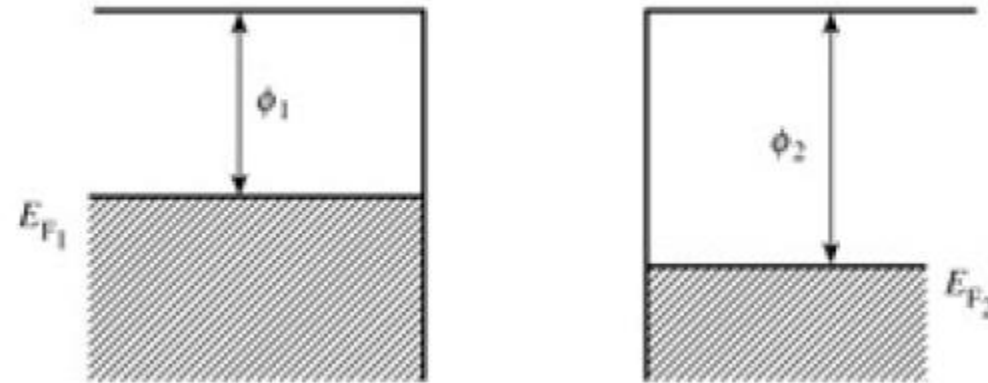
Dopants, impurities and defects

Equation of Charge Neutrality

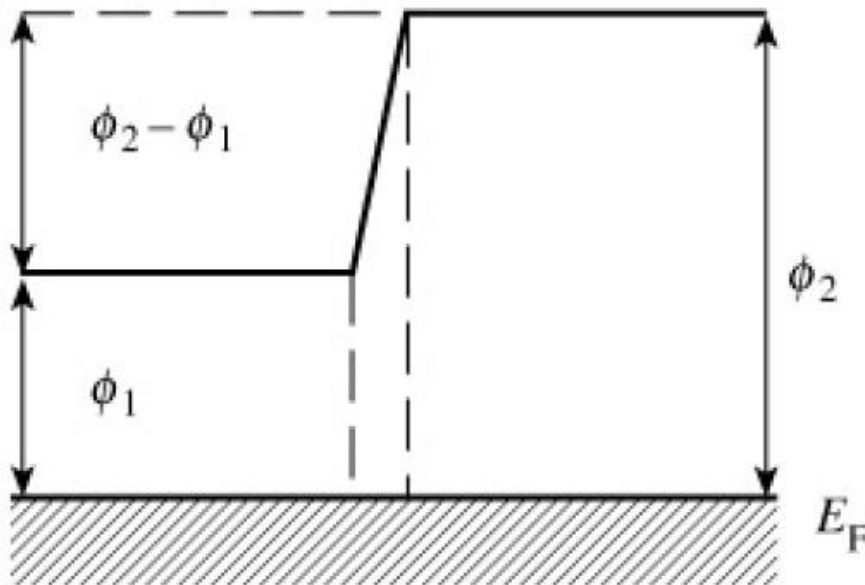


The construction of energy band diagrams

Złącze metal-metal



Suppose, that $\phi_2 - \phi_1 \approx 1 \text{ eV}$
 Estimate the number of electrons that pass from one metal to another to create equilibrium potential difference.
 Assume that the distance between the metals is $5 \times 10^{-10} \text{ m}$.



Electric field: $E = \frac{\Delta\phi}{d} = 2 \times 10^9 \frac{\text{V}}{\text{m}}$

The surface charge: $\sigma = \epsilon_0 E$

The concentration: $n^{2D} = \frac{\sigma}{e} = 1.12 \times 10^{13} \text{ cm}^{-2}$

The concentration in metal

$$n^{3D} = 5 \times 10^{22} \text{ cm}^{-3}$$

$$n^{2D} = 1.5 \times 10^{15} \text{ cm}^{-2}$$

Within the width of 1 lattice parameter ~1% of charge

Electrical properties of materials Solymar, Walsh (6.11)

Pg. 143

The doping of semiconductors

From the Maxwell equations:

$$\nabla \vec{D} = \rho_s - \text{net charge density}$$

$$\vec{E} = -\nabla \phi = -\nabla U$$

$$\nabla \vec{D} = \epsilon_0 \epsilon \nabla \vec{E} = -\epsilon_0 \epsilon \nabla^2 \phi \stackrel{\text{def}}{=} -\epsilon \Delta U = \rho_s$$

Charge conservation

$$eN_A x_p = eN_D x_n = Q$$

Poisson equation:

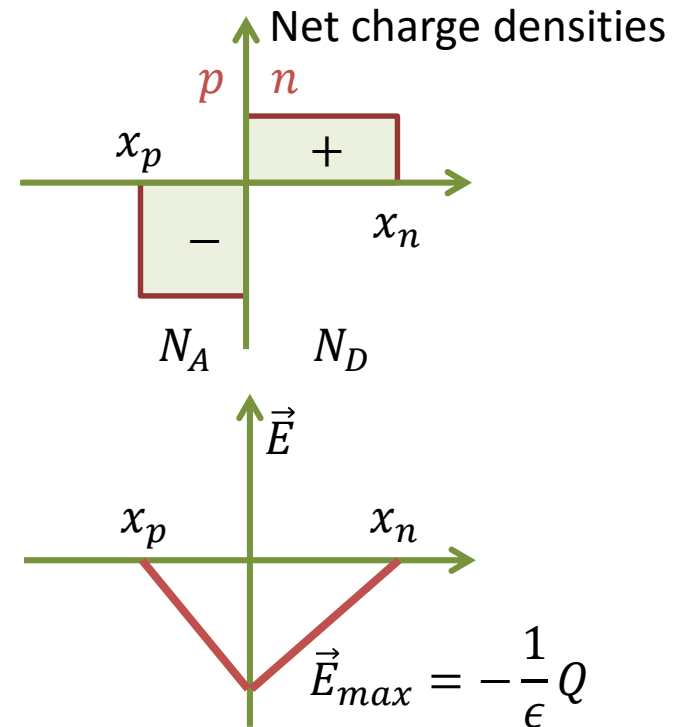
$$\frac{d^2 U}{dx^2} = -\frac{1}{\epsilon} \rho_s = \frac{1}{\epsilon} eN_A$$

Thus the electric field in the range $(x_p, 0)$:

$$\vec{E} = -\frac{dU}{dx} = \frac{1}{\epsilon} eN_A (x + C) = \frac{1}{\epsilon} eN_A (x - x_p)$$

Similarly for $(0, x_n)$:

$$\vec{E} = -\frac{dU}{dx} = \frac{1}{\epsilon} eN_D (x + C) = \frac{1}{\epsilon} eN_D (x - x_n)$$



The doping of semiconductors

Charge conservation

$$eN_A x_p = eN_D x_n = Q$$

The total width of the depletion region w

$$w = x_n - x_p = \sqrt{\frac{2\epsilon U_0}{e(N_A + N_D)}} \left(\sqrt{\frac{N_A}{N_D}} + \sqrt{\frac{N_D}{N_A}} \right)$$

If, say, $N_A \gg N_D$ (p -type doping)

then:

$$w = \sqrt{\frac{2\epsilon U_0}{eN_D}} \quad \text{i} \quad |x_n| > |x_p|$$

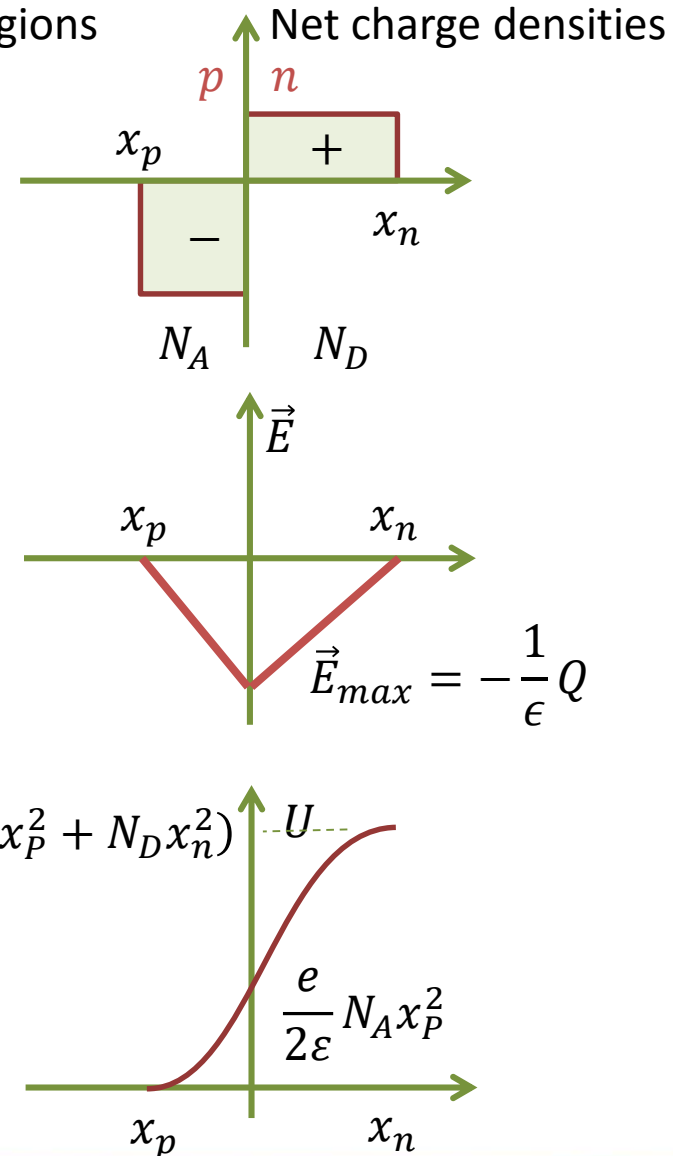
if the p -region is more highly doped, practically all of the potential drop is in the n -region. The less donors are the wider this region is.

(for $N_A \ll N_D$ is vice-versa!)

E.g. $N_D = 10^{15} \text{ cm}^{-3}$ for typical $U_0 = 0.3 \text{ V}$

We have $w \approx 180 \text{ nm}$. If the change from acceptor impurities to donor impurities is gradual, then $w \approx 1 \text{ }\mu\text{m}$

Depletion regions



$$U_0 = \frac{e}{2\epsilon} (N_A x_p^2 + N_D x_n^2)$$

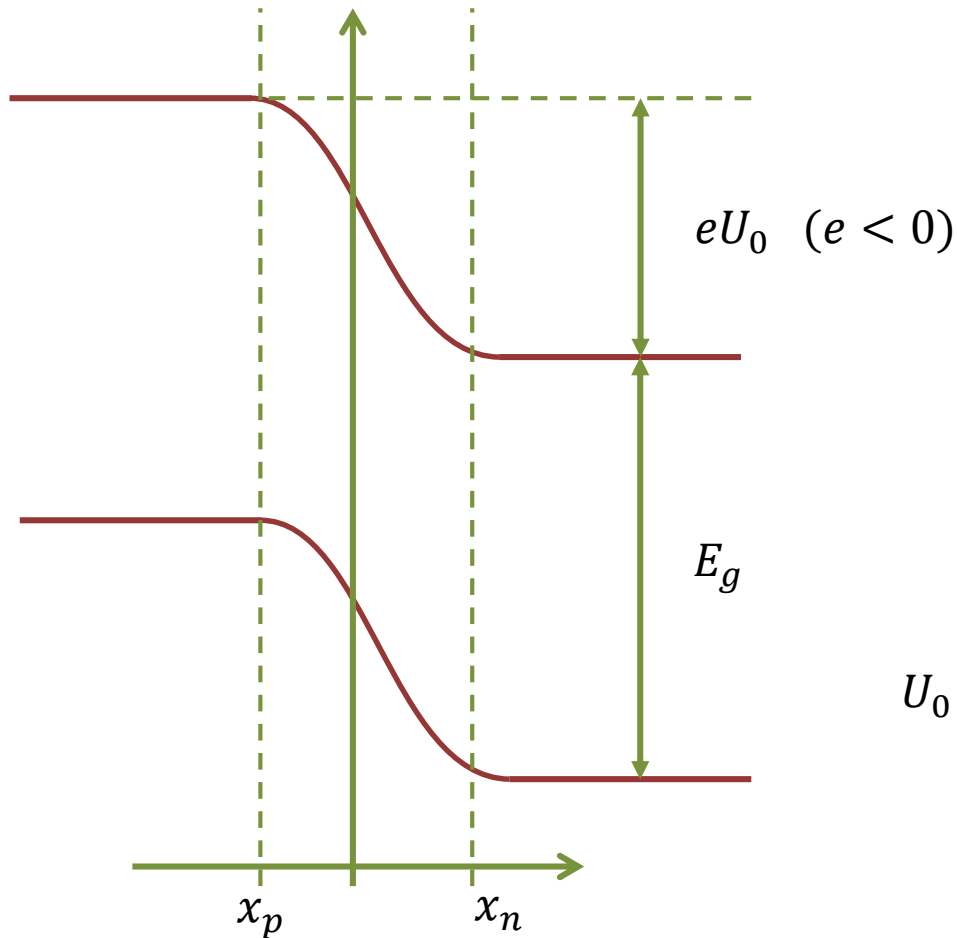
$$\frac{e}{2\epsilon} N_A x_p^2$$

Heterojunction

Charge conservation

$$eN_A x_p = eN_D x_n = Q$$

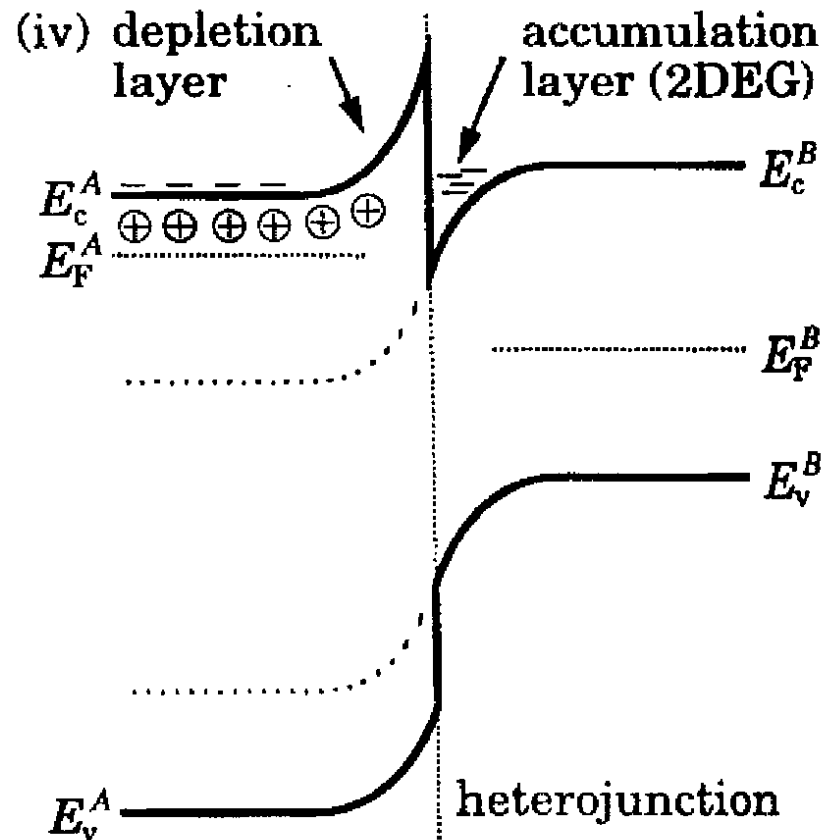
TUTAJ 20151126



$$U_0 = \frac{e}{2\epsilon} (N_A x_p^2 + N_D x_n^2)$$

The graph shows the potential U versus position x . The potential is zero for $x < x_p$ and increases parabolically in the depletion region between x_p and x_n . The maximum potential at the junction is U . The slope of the potential at the junction is $\frac{e}{2\epsilon} N_A x_p^2$.

The construction of energy band diagrams



Restore \bar{E}_c^A on side E_c^A and \bar{E}_v^A on side E_v^A , including discontinuities at the junction.

The current and charge density

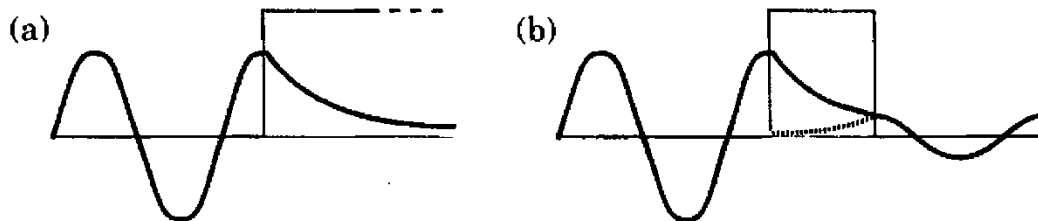
Current density:
$$J(\vec{r}, t) = J(\vec{r}) = \frac{\hbar q}{2 i m} (\Psi^* \nabla \Psi - \Psi \nabla \Psi^*)$$

In the case of de Broigle wave:
$$\Psi(x, t) = [A_+ e^{ikx} + A_- e^{-ikx}] e^{-i\omega t}$$

$$J(\vec{r}) = \frac{\hbar q k}{m} (|A_+|^2 - |A_-|^2) \quad \text{each wave carry current}$$

In the case of the evanescent (decaying) wave:
$$\Psi(x, t) = [B_+ e^{\kappa x} + B_- e^{-\kappa x}] e^{-i\omega t}$$

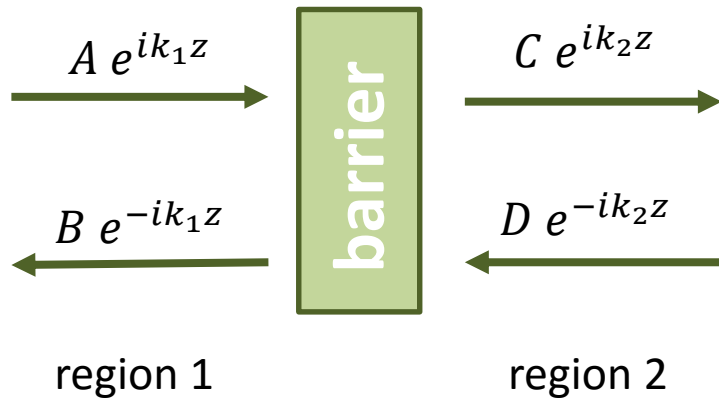
$$J(\vec{r}) = \frac{\hbar q \kappa}{i m} (B_+ B_-^* - B_+^* B_-) = \frac{2 \hbar q \kappa}{m} \text{Im} (B_+ B_-^*)$$



Only the superposition of + i – amplitudes gives real current!

FIGURE 1.5. Current carried by counter-propagating decaying waves. (a) An infinitely thick barrier contains a single decaying exponential that carries no current. (b) A finite barrier contains both growing and decaying exponentials and passes current. (The wave function is complex, so the figure is only a rough guide.)

Tunnelling



$$\begin{pmatrix} C \\ D \end{pmatrix} = T^{(21)} \begin{pmatrix} A \\ B \end{pmatrix} = \begin{pmatrix} T_{11} & T_{12} \\ T_{12}^* & T_{11}^* \end{pmatrix} \begin{pmatrix} A \\ B \end{pmatrix}$$

$$r = -\frac{T_{12}^*}{T_{11}^*} \quad t = -\frac{1}{T_{11}^*}$$

$$T^{(21)}(0) = \begin{pmatrix} 1/t^* & -r^*/t^* \\ -r/t & 1/t \end{pmatrix}$$

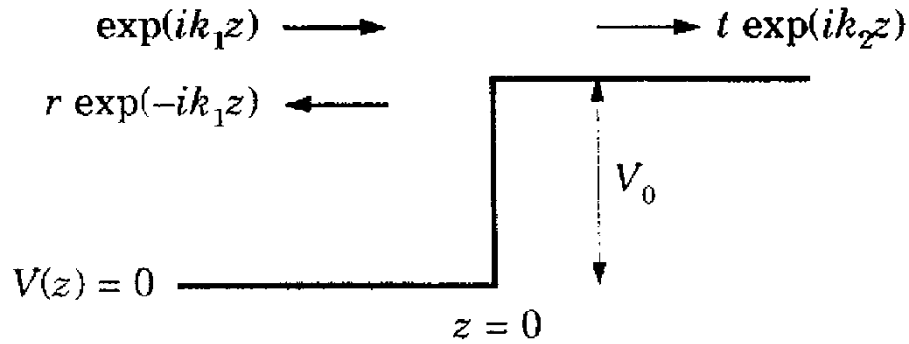
$$T^{(21)}(d) = \begin{pmatrix} e^{-ik_2 d} & 0 \\ 0 & e^{ik_2 d} \end{pmatrix} T^{(21)}(0) \begin{pmatrix} e^{ik_1 d} & 0 \\ 0 & e^{ik_1 d} \end{pmatrix} = A_2^{-1}(d) T(0) A_1(d)$$

The other direction: $\begin{pmatrix} B \\ A \end{pmatrix} = T^{(12)} \begin{pmatrix} D \\ C \end{pmatrix}$

$$T^{(12)}(0) = \begin{pmatrix} 1/t^* & r/t \\ r^*/t^* & 1/t \end{pmatrix}$$

Tunnelling

Examples:



$$T + R = 1$$

$$T = \frac{4k_1 k_2}{(k_1 + k_2)^2}$$

$$R = \left(\frac{k_1 - k_2}{k_1 + k_2} \right)^2$$

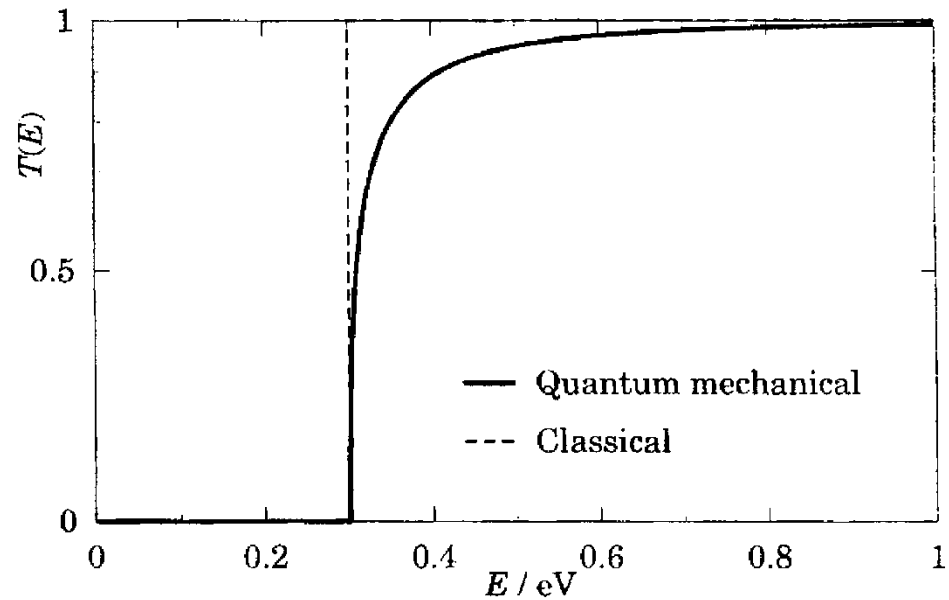


FIGURE 5.3. Transmission coefficient $T(E)$ as a function of the energy E of the incident electron for a step 0.3 eV high in GaAs. The broken line is the classical result.

Tunnelling

Przykłady:

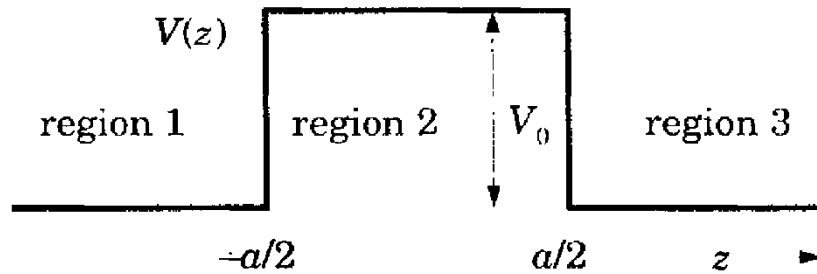


FIGURE 5.5. Potential barrier with $V(z) = V_0$ for $|z| < a/2$ and $V(z) = 0$ elsewhere.

$E > V_0$

$$T = \frac{4k_1^2 k_2^2}{4k_1^2 k_2^2 + (k_1^2 - k_2^2)^2 \sin^2 k_2 a} = \left[1 + \frac{V_0^2}{4E(E - V_0)} \sin^2 k_2 a \right]^{-1}$$

$E < V_0$

$$T = \frac{4k_1^2 \kappa_2^2}{4k_1^2 \kappa_2^2 + (k_1^2 + \kappa_2^2)^2 \sinh^2 \kappa_2 a} = \left[1 + \frac{V_0^2}{4E(V_0 - E)} \sinh^2 \kappa_2 a \right]^{-1}$$

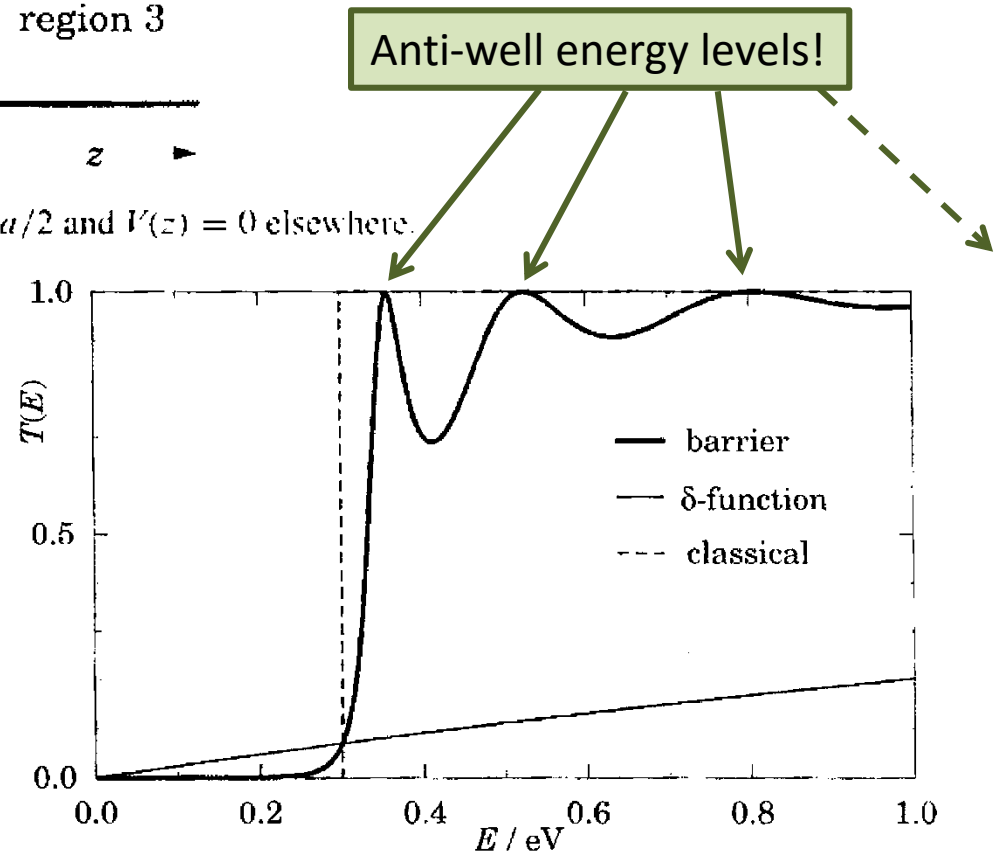


FIGURE 5.6. Transmission coefficient $T(E)$ as a function of energy E for a square potential barrier of height $V_0 = 0.3$ eV and thickness $a = 10$ nm in GaAs. The thin curve is for a δ -function barrier of the same strength $S = V_0 a$, and the broken curve is the classical result for a barrier of the same height.

Tunnelling

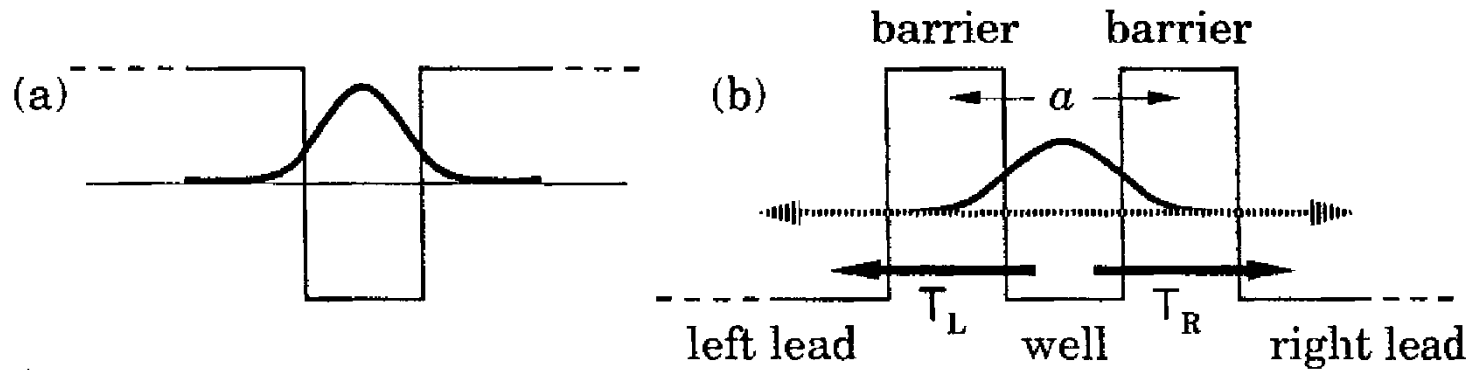


FIGURE 5.10. (a) A finite square potential well with a true bound state. (b) The same well but with barriers of finite thickness, where the bound state becomes resonant or quasi-bound.

$$t = \frac{t_L t_R}{1 - r_L r_R \exp 2ika}$$

$$\phi = 2ka + \rho_L + \rho_R$$

$$T = |t|^2 = \frac{T_L T_R}{(1 - \sqrt{R_L R_R})^2 + 4\sqrt{R_L R_R} \sin^2 \frac{1}{2} \phi}$$

$$T_{pk} = \frac{T_L T_R}{(1 - \sqrt{R_L R_R})^2} \approx \frac{4T_L T_R}{(T_L + T_R)^2}$$

Tunnelling

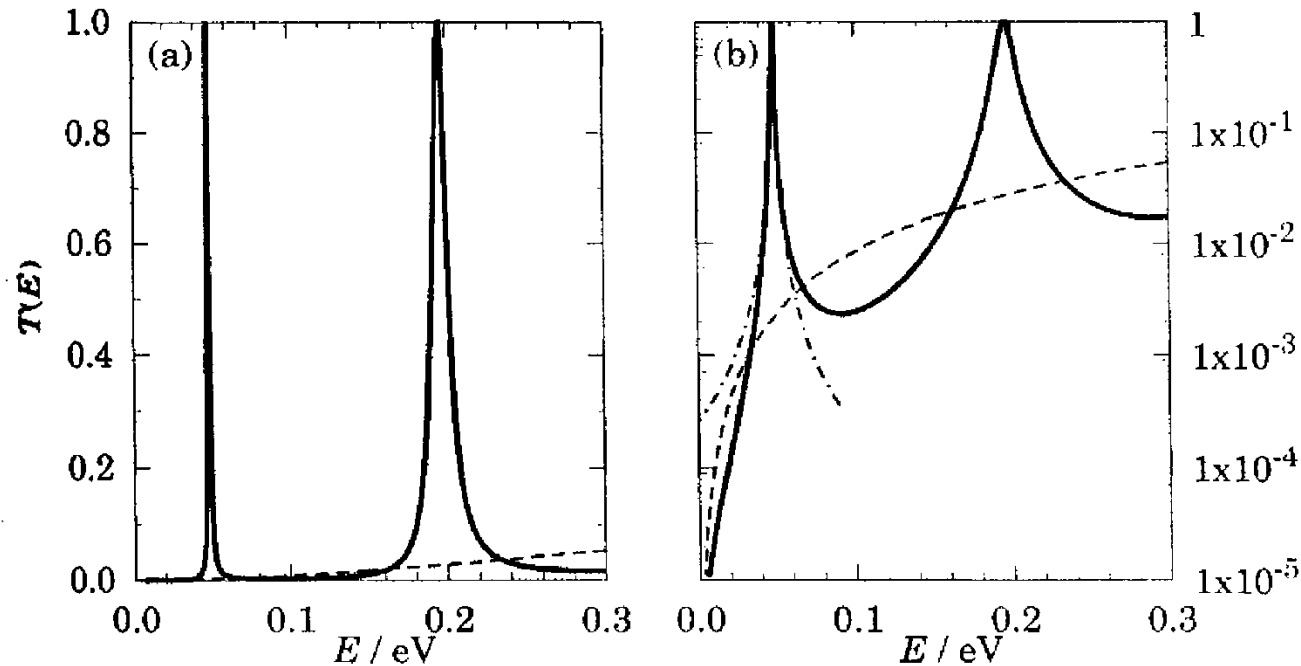


FIGURE 5.11. Transmission coefficient of a resonant-tunnelling structure on (a) linear and (b) logarithmic scales. The barriers are δ -functions of strength $0.3 \text{ eV} \times 5 \text{ nm}$ separated by 10 nm . The solid curve is $T(E)$ for the whole structure, the dashed curve shows the square of $T(E)$ for a single barrier and would apply to the double-barrier structure if there were no resonance, and the chain curve is the Lorentzian approximation to the lowest resonance.

$$T = |t|^2 = \frac{T_L T_R}{(1 - \sqrt{R_L R_R})^2 + 4\sqrt{R_L R_R} \sin^2 \frac{1}{2} \phi}$$

$$T_{pk} = \frac{T_L T_R}{(1 - \sqrt{R_L R_R})^2} \approx \frac{4T_L T_R}{(T_L + T_R)^2}$$

Tunnelling

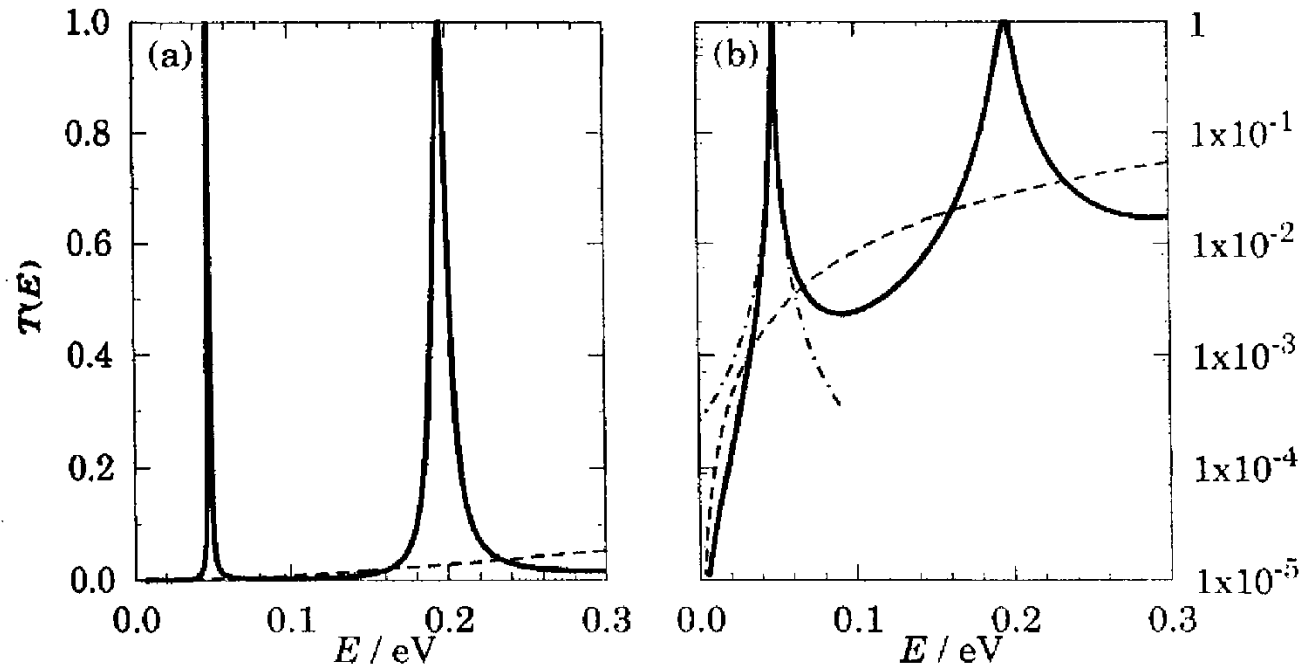


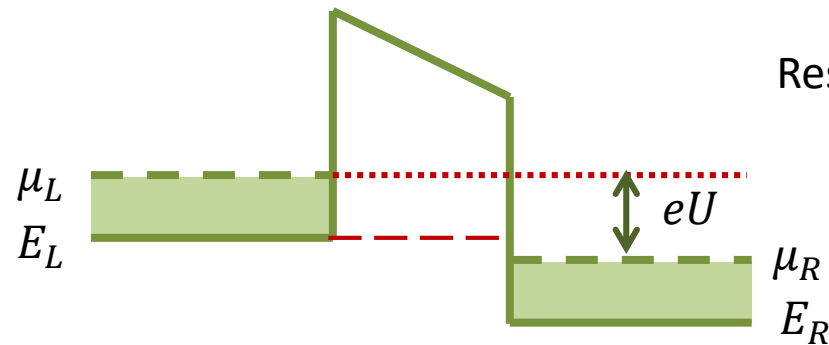
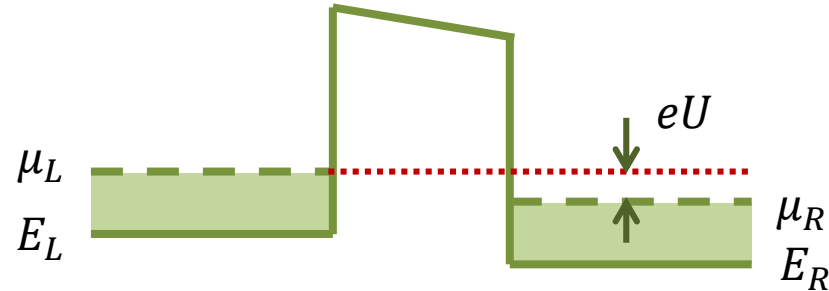
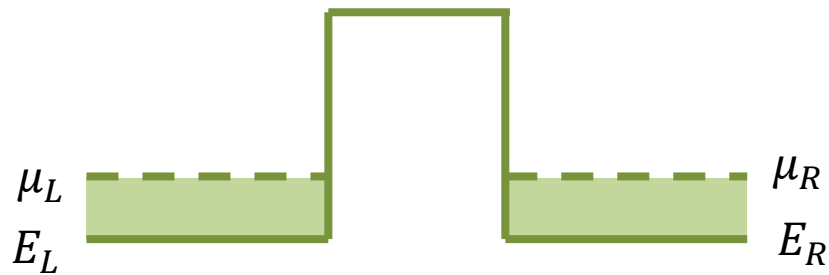
FIGURE 5.11. Transmission coefficient of a resonant-tunnelling structure on (a) linear and (b) logarithmic scales. The barriers are δ -functions of strength $0.3 \text{ eV} \times 5 \text{ nm}$ separated by 10 nm . The solid curve is $T(E)$ for the whole structure, the dashed curve shows the square of $T(E)$ for a single barrier and would apply to the double-barrier structure if there were no resonance, and the chain curve is the Lorentzian approximation to the lowest resonance.

$$T \approx \frac{T_{pk}}{1 + \left(\frac{\delta\phi}{\frac{1}{2}\phi_0}\right)^2} \quad \text{profil Lorentza}$$

$$\phi_0 = T_L + T_R$$

$$T_{pk} = \frac{T_L T_R}{(1 - \sqrt{R_L R_R})^2} \approx \frac{4T_L T_R}{(T_L + T_R)^2}$$

Quantized conductance



For metals $\mu_L = \mu + \frac{1}{2}eU$; $\mu_R = \mu - \frac{1}{2}eU$:

$$f(E, \mu_L) - f(E, \mu_R) \approx eU \frac{\partial f(E, \mu)}{\partial \mu} = -eU \frac{\partial f(E, \mu)}{\partial E}$$

$$I = \frac{2e^2 U}{h} \int_{E_L}^{\infty} \frac{\partial f(E, \mu)}{\partial E} T(E) dE$$

$$G = \frac{dI}{dU} = \frac{2e^2}{h} \int_{E_L}^{\infty} \frac{\partial f(E, \mu)}{\partial E} T(E) dE \approx \frac{2e^2}{h} T(\mu)$$

Resistance is finite even for the ideal conductor!

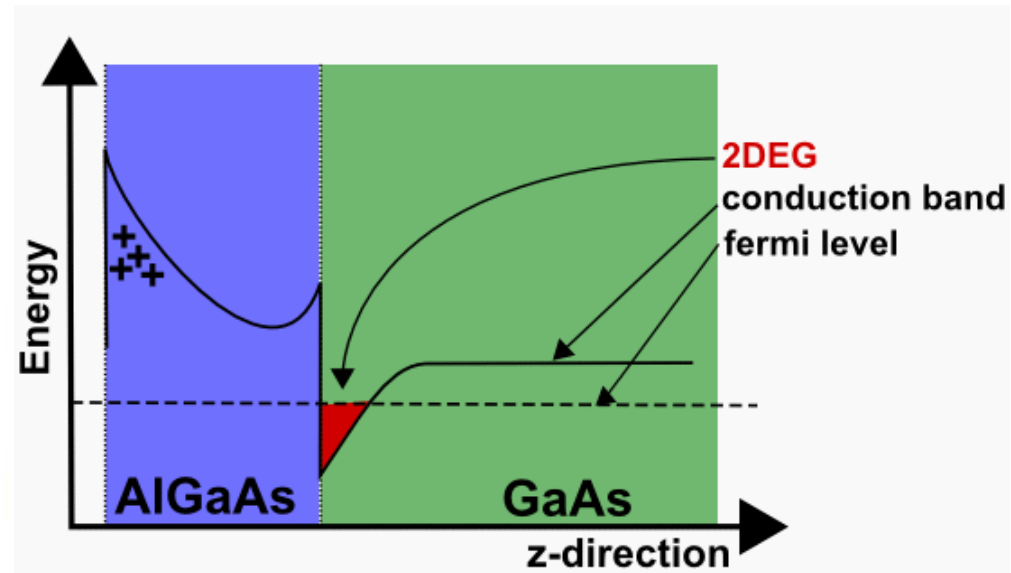
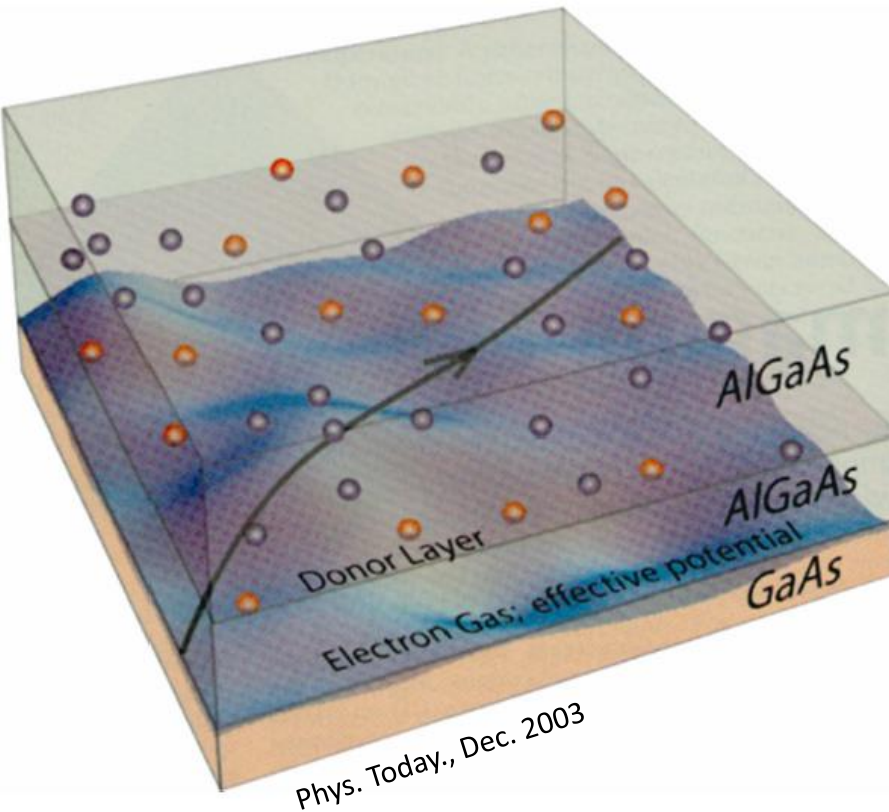
$$\frac{e^2}{h} = 38,7 \mu S$$

$$\frac{h}{e^2} = 25,8 k\Omega$$

Quantized conductance (S – Simens)

Triangular well

WKB approximation (Wentzel – Krammers – Brillouin) – for slowly varying potential



http://www.phys.unsw.edu.au/QED/research/2D_scattering.htm

$$E_n = \left[\frac{3}{2} \pi \left(n - \frac{1}{4} \right) \right]^{2/3} \left[\frac{(eF\hbar)^2}{2m} \right]^{1/3}$$

Quantized conductance

$$G = \frac{dI}{dU} = \frac{2e^2}{h} \int_{E_L}^{\infty} \frac{\partial f(E, \mu)}{\partial E} T(E) dE \approx \frac{2e^2}{h} T(\mu) = G_0 T(\mu)$$

$$\frac{e^2}{h} = 38,7 \mu S$$

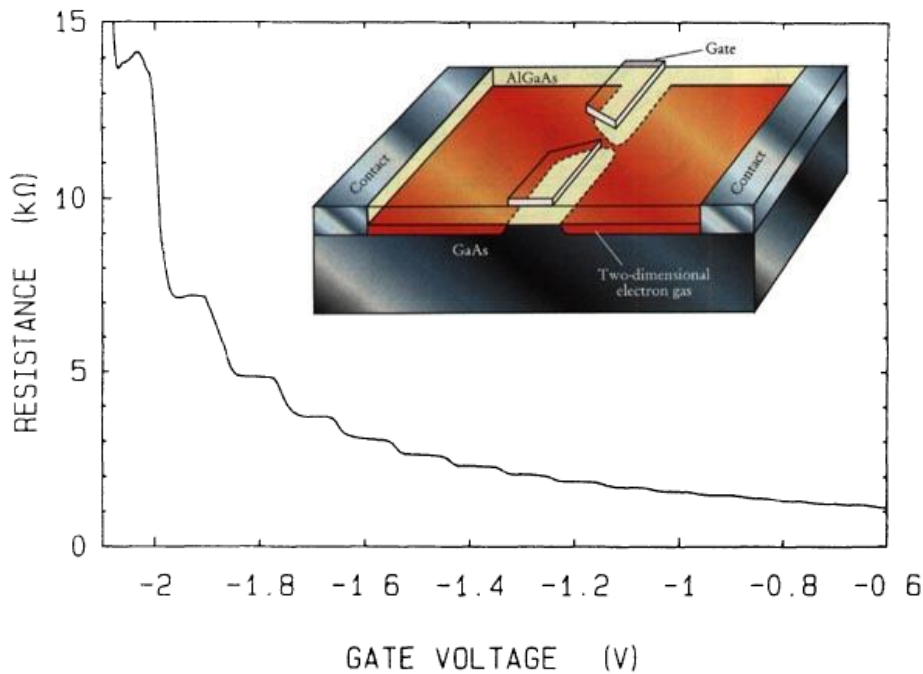


FIG. 1. Point-contact resistance as a function of gate voltage at 0.6 K. Inset: Point-contact layout.

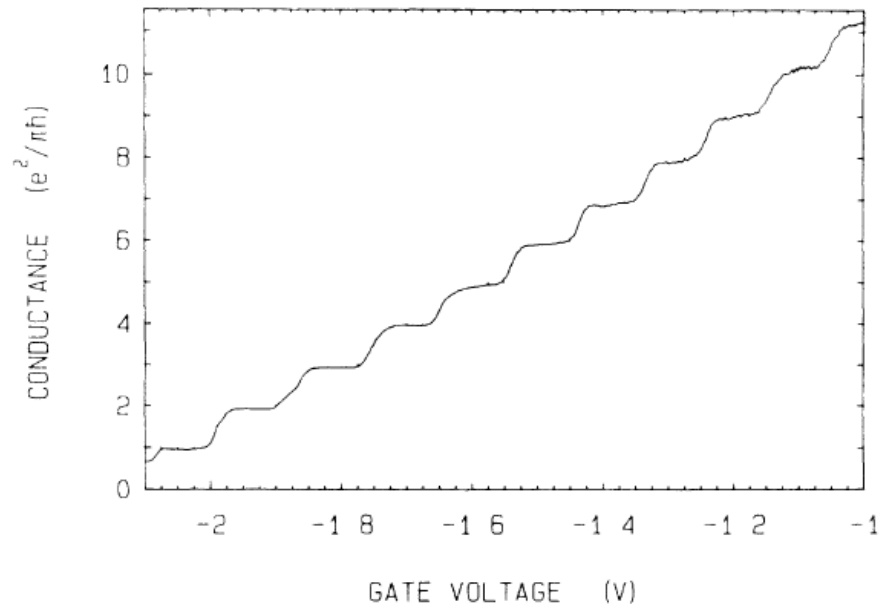
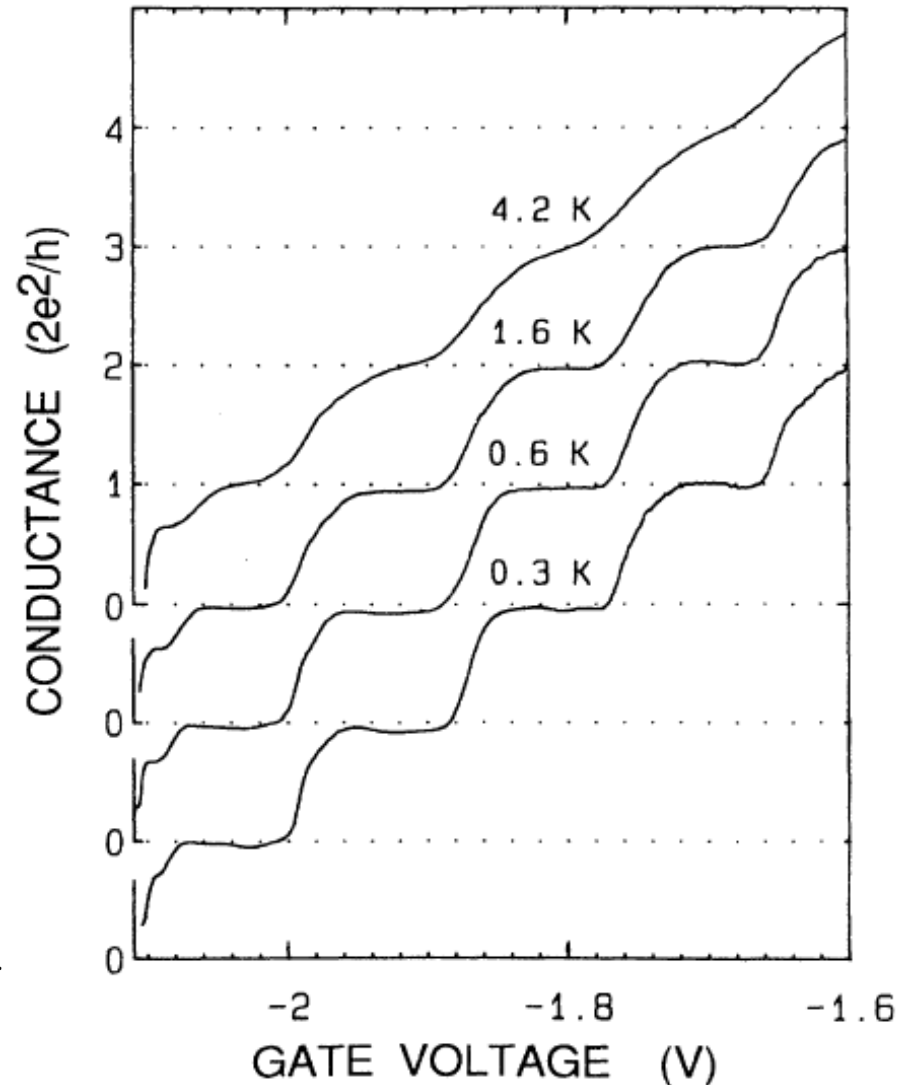


FIG. 2. Point-contact conductance as a function of gate voltage, obtained from the data of Fig. 1 after subtraction of the lead resistance. The conductance shows plateaus at multiples of $e^2/\pi h$.

B. J. van Wees et al. *Quantized conductance of point contacts in a two-dimensional electron gas*
 Phys. Rev. Lett. **60**, 848–850 (1988)

Quantized conductance

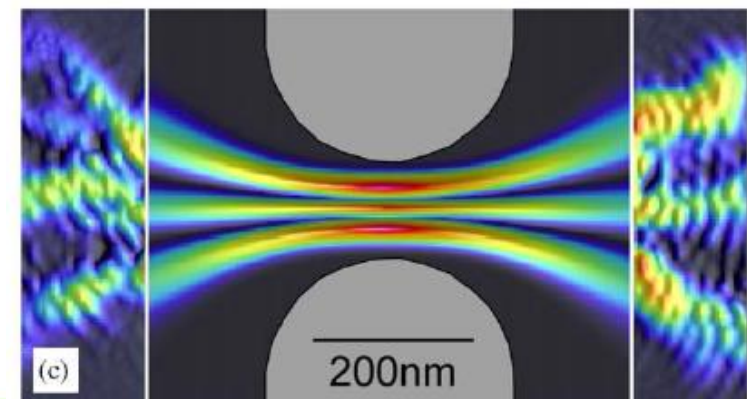
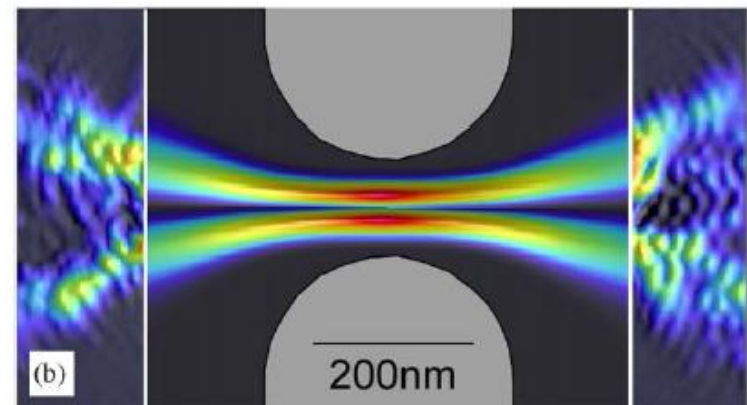
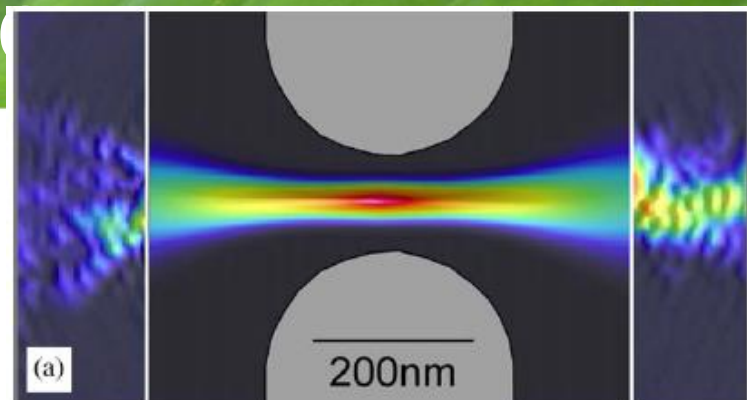
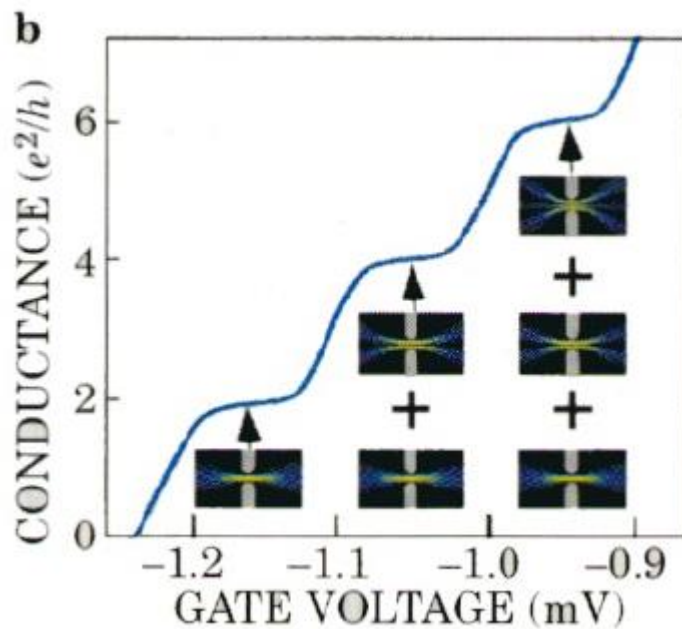
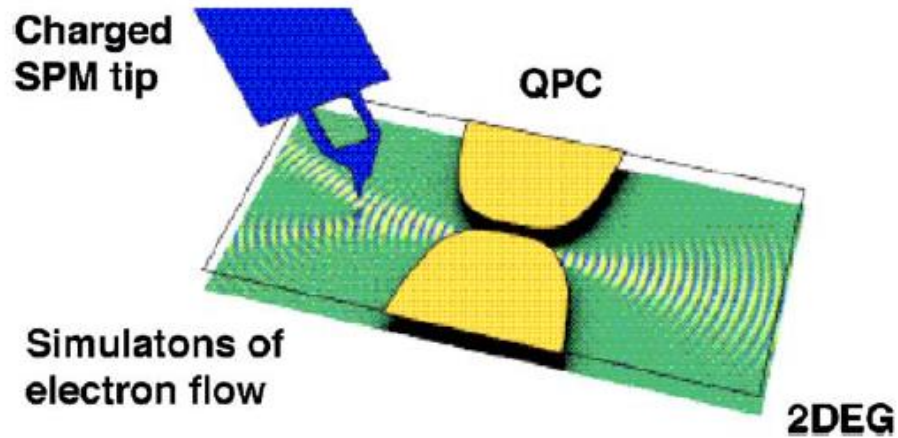
$$G = \frac{2e^2}{h} T(\mu) = G_0 T(\mu)$$



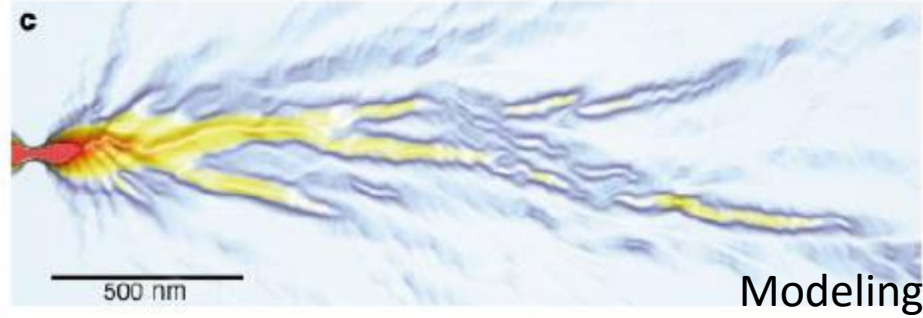
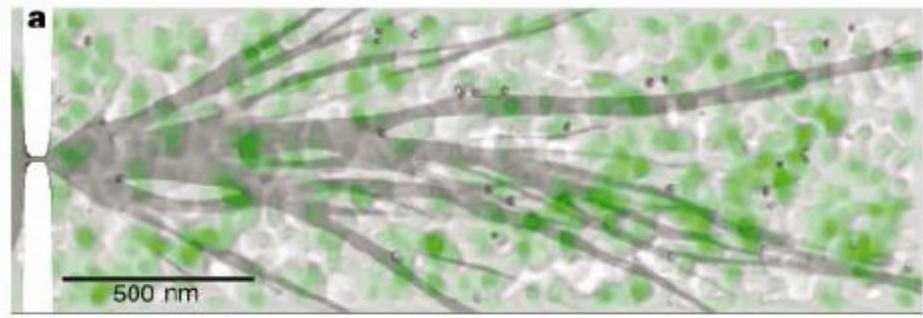
B. J. van Wees et al. *Quantum ballistic and adiabatic electron transport studied with quantum point contacts* Phys. Rev. B 43, 12431–12453 (1991)

FIG. 6. Breakdown of the conductance quantization due to temperature averaging. The curves have been offset for clarity.

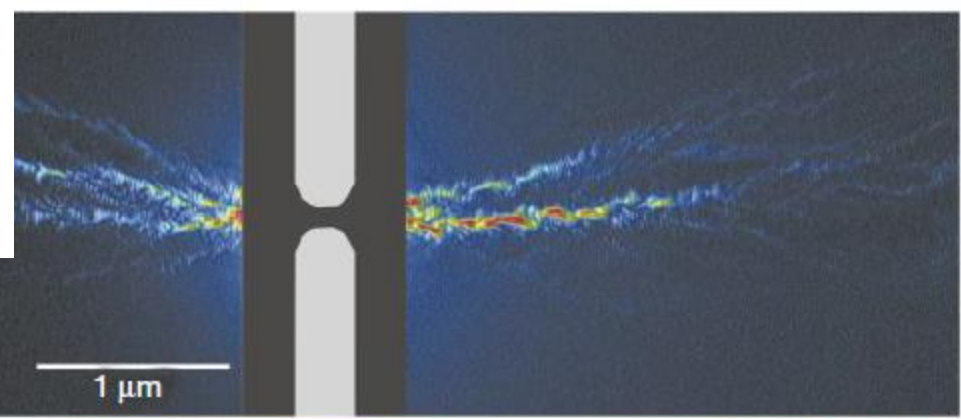
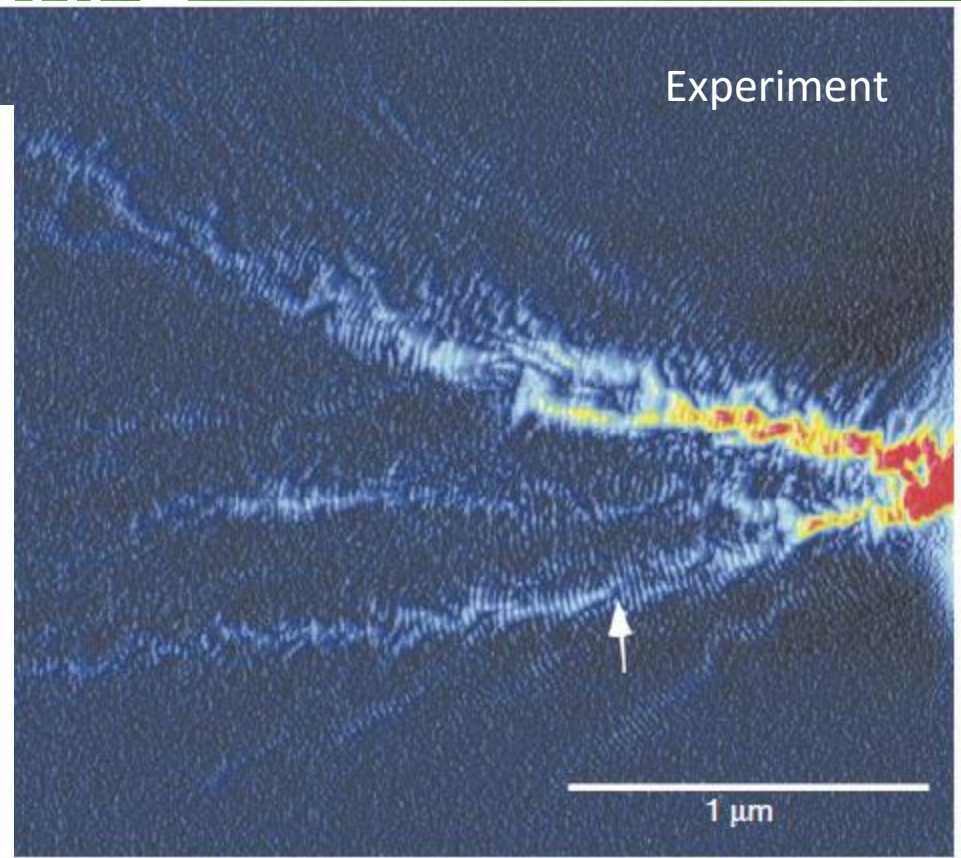
Quantized conductance



Quantized conductance



Modeling



M. A. Topinka et al.
Nature **410**, 183 (2001)

Coulomb blockade

Dot behaves like a small capacitor of energy $E_c \sim \frac{1}{2} \frac{e^2}{C}$

$$V_b = 0$$

$$V_g = 0$$

$$V_b = V_1$$

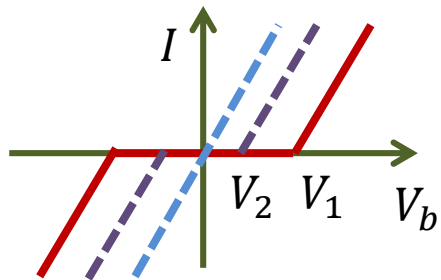
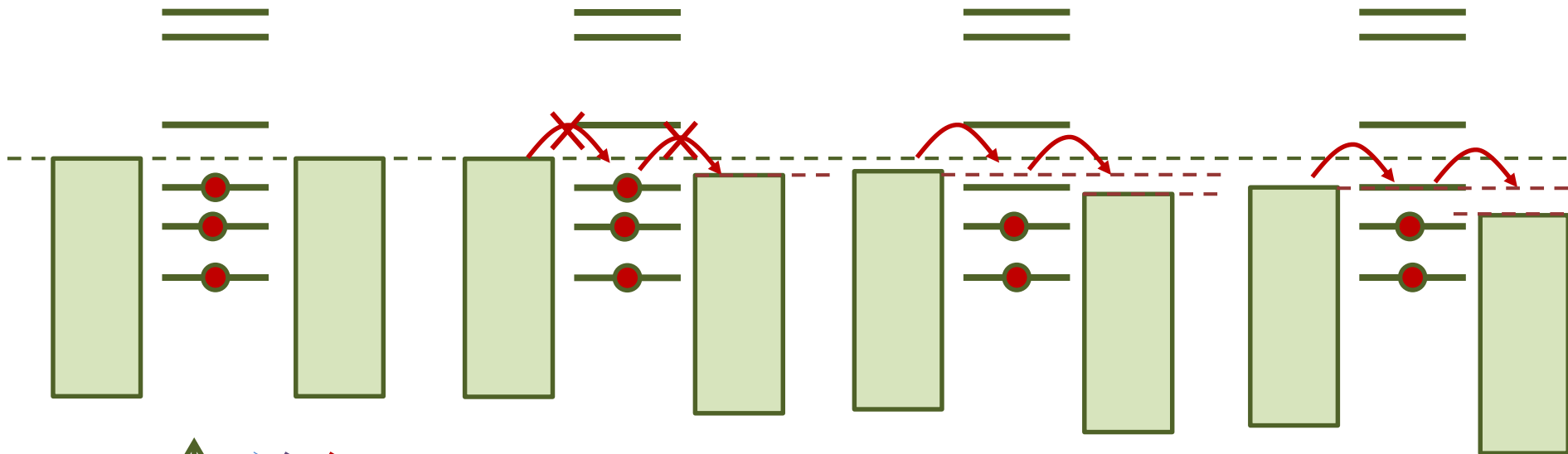
$$V_g = 0$$

$$V_b = V_2 < V_1$$

$$V_g \neq 0$$

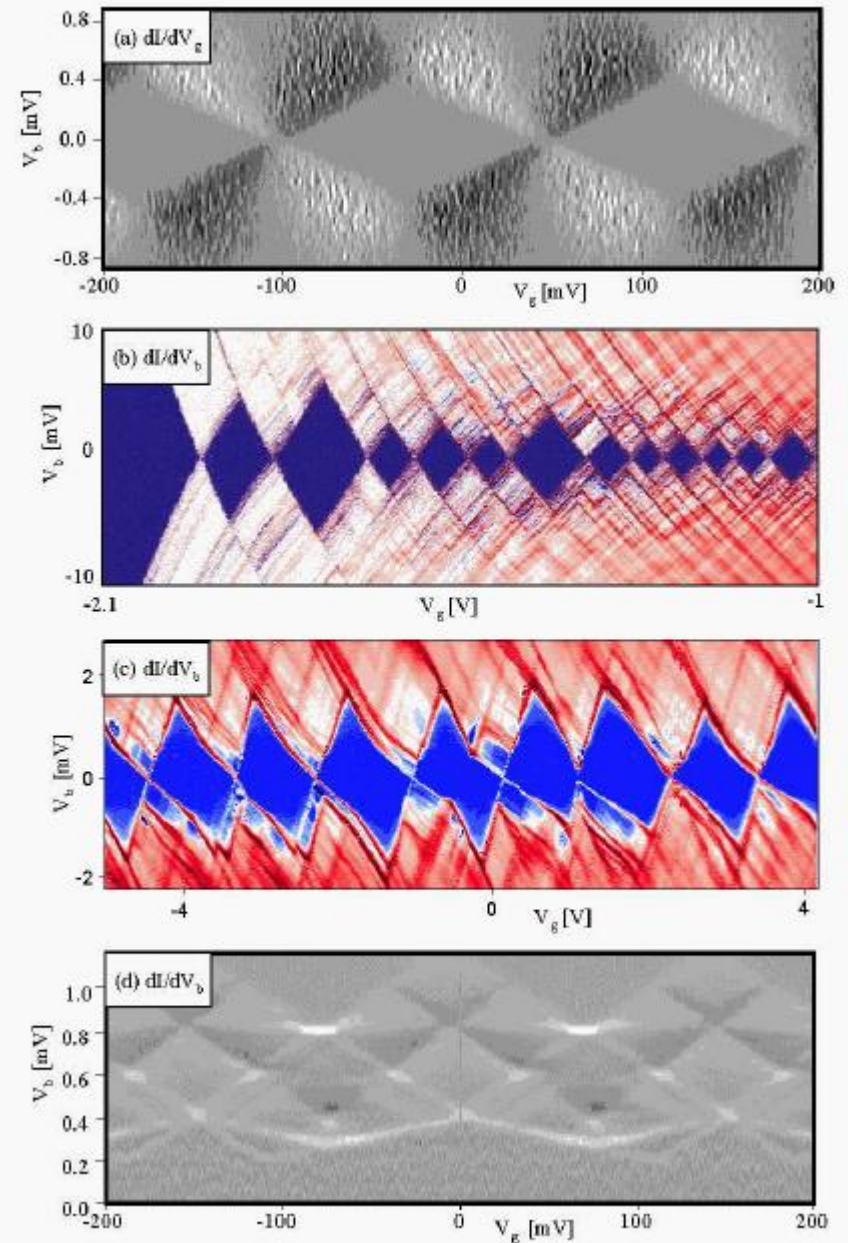
$$V_b = 0$$

$$V_g \neq 0$$



Coulomb blockade

Figure 6.7: The low temperature conductances of (a) a metal single-electron transistor (SET), (b) a semiconducting SET, (c) a carbon nanotube SET, and (d) a superconducting SET are plotted as a function of gate voltage and bias voltage. The diamond shaped regions along the zero bias voltage axis are regions of Coulomb blockade. The conductance is a periodic function of gate voltage for the metal SET and the superconducting SET where the confinement energy is negligible. The conductance is not a periodic function of gate voltage for the semiconductor SET and the carbon nanotube SET where the confinement energy is important. From: P. Hadley and J.E. Mooij, Delft University of Technology, <http://qt.tn.tudelft.nl/publi/2000/quantumdev/qdevices.html>



Clive Emary
Theory of Nanostructures nanoskript.pdf

Scalar and vector fields

Maxwell's equations in matter

$$\nabla \times \vec{E} = -\frac{\partial \vec{B}}{\partial t}$$

$$\nabla \times \vec{H} = \vec{j}_{sw} + \frac{\partial \vec{D}}{\partial t}$$

$$\nabla \cdot \vec{D} = \rho_{sw}$$

$$\nabla \cdot \vec{B} = 0$$

The equations written in the form of a scalar φ and vector A potentials:

$$\vec{B} = \nabla \times \vec{A}$$

$$\text{Then } \nabla \times \vec{E} = -\frac{\partial \vec{B}}{\partial t} = -\frac{\partial}{\partial t}(\nabla \times \vec{A}) \Rightarrow \nabla \times \vec{E} + \frac{\partial}{\partial t}(\nabla \times \vec{A}) = 0 \Rightarrow \nabla \times \left(\vec{E} + \frac{\partial \vec{A}}{\partial t} \right) = 0$$

$$\text{If the rotation of the gradient is zero, then: } -\nabla\varphi = \vec{E} + \frac{\partial \vec{A}}{\partial t} \text{ thus } \vec{E} = -\nabla\varphi - \frac{\partial \vec{A}}{\partial t}$$

Material equations (linear)

$$\vec{B} = \mu_0 \vec{H} + \vec{M} = \mu_0(1 + \chi_m) \vec{H} = \mu \vec{H} = \mu_r \mu_0 \vec{H}$$

$$\vec{D} = \epsilon_0 \vec{E} + \vec{P} = \epsilon_0(1 + \chi_e) \vec{E} = \epsilon \vec{E} = \epsilon_0 \epsilon_r \vec{E}$$

$$\vec{j}_{sw} = \hat{\sigma} \vec{E}$$

$$v^2 = \frac{1}{\mu_0 \epsilon_0} \frac{1}{\mu_r \epsilon_r} = \frac{c^2}{\mu_r \epsilon_r} = \frac{c^2}{n^2}$$

Scalar and vector fields

Maxwell's equations in matter

$$\vec{B} = \nabla \times \vec{A}$$

$$\vec{E} = -\nabla\varphi - \frac{\partial\vec{A}}{\partial t}$$

Example: $\varphi = -\vec{E}\vec{r} + C_\varphi$ $\vec{A} = -\vec{E}t + C_A$

Not only constants C_φ and C_A we can add for the scalar and vector potentials:

$$\varphi \rightarrow \varphi - \frac{d\chi}{dt} \quad \vec{A} \rightarrow \vec{A} + \nabla\chi \quad \text{eg.:} \quad \chi = \pm\vec{E}\vec{r}t$$

We call it **the gauge**

Landau gauge: field $\vec{B} = (0,0,B_z) \Rightarrow B_z = \frac{\partial A_y}{\partial x} - \frac{\partial A_x}{\partial y}$ $A_y = B_z x$ lub $A_x = -B_z y$
(unfortunately distinguishes direction)

Coulomb gauge: $\nabla\vec{A} = 0$ field $\vec{B} = (0,0,B_z) \Rightarrow \vec{A} = \frac{1}{2}B_z(-y, x, 0) = \frac{1}{2}\vec{B} \times \vec{r}$
(unfortunately complicates calculations)

Lorentz gauge: $\nabla\vec{A} + \frac{\partial\varphi}{\partial t} = 0$

Local density of states

The density of states (in general) can be defined as:

$$N^{3D}(E, z) \sim \frac{m}{\pi \hbar^3} \sqrt{2m\varepsilon_0} \int_{-\infty}^E Ai^2\left(\frac{eFz - \varepsilon}{\varepsilon_0}\right) d\varepsilon = \frac{m}{\pi \hbar^3} \sqrt{2m\varepsilon_0} \left[[Ai'(s)]^2 - s[Ai(s)]^2 \right]$$

Franz-Keldysh effect - in the electric field optical transitions occur at lower energies - the energy gap is „blurred”, the wavefunctions are „leaking” into the band gap:

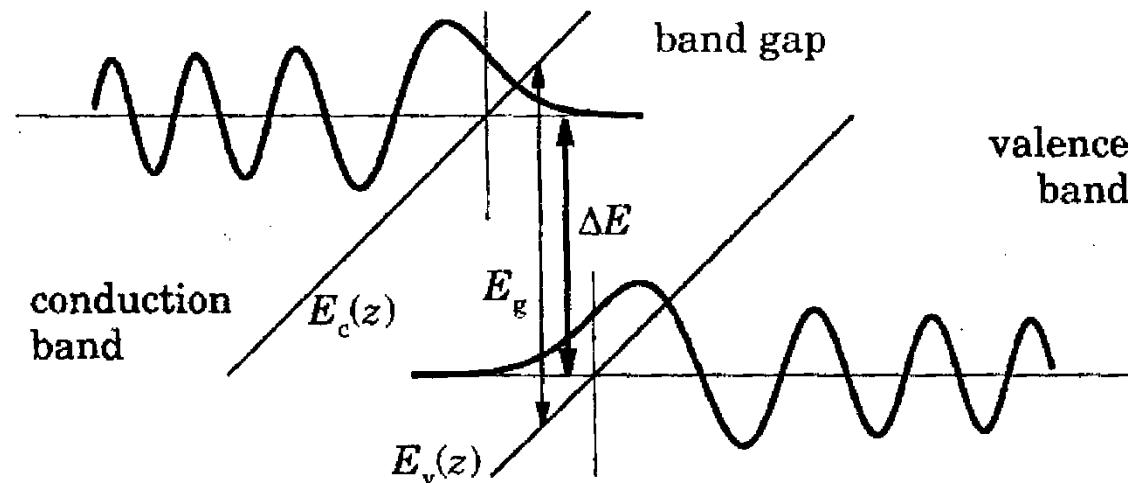


FIGURE 6.3. The Franz–Keldysh effect on interband absorption. The states shown in the valence and conduction bands are separated by $\Delta E < E_g$ but overlap because of the tail that tunnels into the band gap.

Homogenous magnetic field

$$\left[-\frac{\hbar^2}{2m} \nabla^2 - \frac{ie\hbar}{m} Bx \frac{\partial}{\partial y} + \frac{(eBx)^2}{2m} + U(z) \right] \psi(\vec{r}) = E\psi(\vec{r})$$

Vector potential does not depend on y , we can assume the function of the form:

$$\psi(\vec{r}) = w(z)u(x) \exp(ik_y y)$$

$$\left[-\frac{\hbar^2}{2m} \frac{d^2}{dx^2} + \frac{1}{2} m \omega_c^2 \left(x + \frac{\hbar k_y}{eB} \right)^2 \right] u(x) = \varepsilon u(x)$$

$$\omega_c = \left| \frac{eB}{m} \right|$$

$$R_c = \frac{v}{\omega_c} = \frac{\sqrt{2mE}}{|eB|}$$

Cyclotron frequency

Cyclotron radius (*gyroradius*)

k_y wave vector. What interesting in ε THERE IS NO k_y .

The parabolic potential of the form of $x_k = -\hbar k_y / eB$

Hall effect

The full conductivity tensor

$$\sigma = ne\mu \begin{pmatrix} \frac{1}{1+s^2} & \frac{-s}{1+s^2} & 0 \\ s & 1 & 0 \\ \frac{1}{1+s^2} & \frac{1}{1+s^2} & 0 \\ 0 & 0 & 1 \end{pmatrix}$$

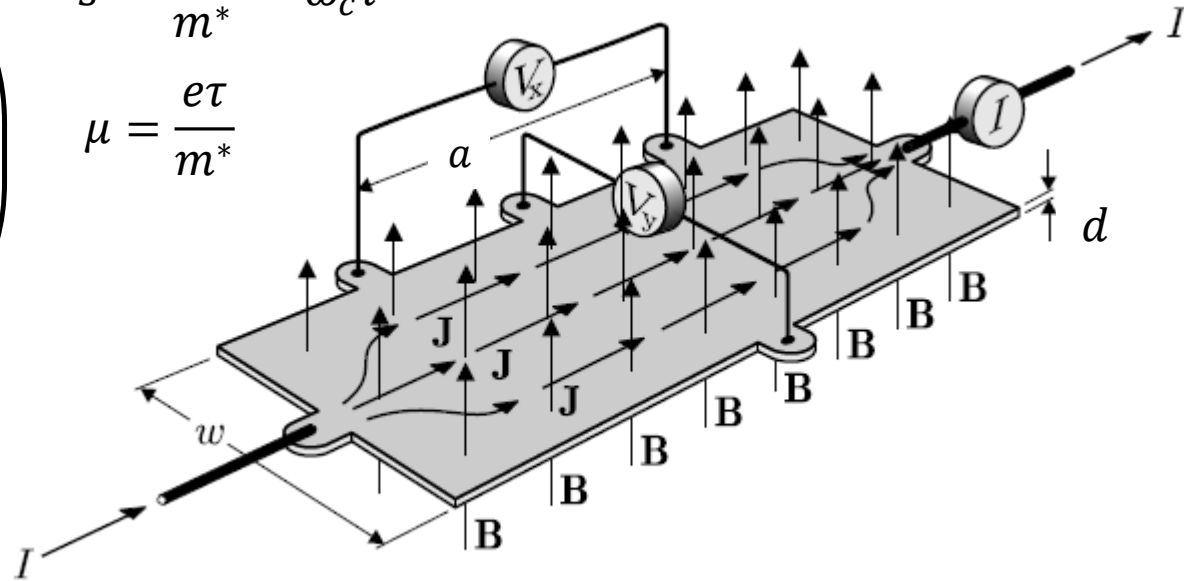
The full resistivity tensor

$$\rho = \sigma^{-1} = \frac{1}{ne\mu} \begin{pmatrix} 1 & s & 0 \\ -s & 1 & 0 \\ 0 & 0 & 1 \end{pmatrix}$$

$$\vec{E} = \rho \vec{j} = \begin{bmatrix} \frac{j_x}{ne\mu} \\ \frac{j_x B}{ne} \\ 0 \end{bmatrix}$$

$$s = \frac{eB\tau}{m^*} = \omega_c \tau$$

$$\mu = \frac{e\tau}{m^*}$$



$$U_{xy} = E_y w = \frac{I_x B}{wd ne} w = \frac{I_x}{dne} B = R_H \frac{I_x B}{d}$$

$$R_H = \frac{1}{ne} \quad \text{Hall constant}$$

Homogenous magnetic field

The Landau gauge solution

$$\left\{ \frac{1}{2m} [\hat{p} - q \vec{A}(\vec{r}, t)]^2 + q\varphi(\vec{r}, t) + U(\vec{r}, t) \right\} \psi(\vec{r}, t) = i\hbar \frac{d}{dt} \psi(\vec{r}, t)$$

Landau gauge: magnetic field $\vec{B} = (0, 0, B_z) \Rightarrow B_z = \frac{\partial A_y}{\partial x} - \frac{\partial A_x}{\partial y}$ (unfortunately distinguishes direction)

$$\vec{A} = [0, B_z x, 0] \text{ czyli } A_y = B_z x \stackrel{\text{def}}{=} Bx \quad q = -e$$

We assume that in a plane xy there is no other potential

$$\left\{ \frac{1}{2m} \left[-\hbar^2 \frac{\partial^2}{\partial x^2} + \left(-i\hbar \frac{\partial}{\partial y} + eBx \right)^2 - \hbar^2 \frac{\partial^2}{\partial z^2} \right] + U(z) \right\} \psi(\vec{r}) = E\psi(\vec{r})$$

Which gives:
$$\left[-\frac{\hbar^2}{2m} \nabla^2 - \frac{ie\hbar}{m} Bx \frac{\partial}{\partial y} + \frac{(eBx)^2}{2m} + U(z) \right] \psi(\vec{r}) = E\psi(\vec{r})$$

The evidence of the Lorentz force

Parabolic potential!

Homogenous magnetic field

The 2D case:

Solutions $\varepsilon_{nk} = \left(n - \frac{1}{2}\right) \hbar\omega_c + E_n$ (does not depend on k_y ; E_n - is any 2D energy).

$$\phi_{nk}(x, y) \propto H_{n-1}\left(\frac{x - x_k}{l_B}\right) \exp\left[-\frac{(x - x_k)^2}{2l_B^2}\right] \exp(ik_y y) \quad n = 1, 2, 3 \dots$$

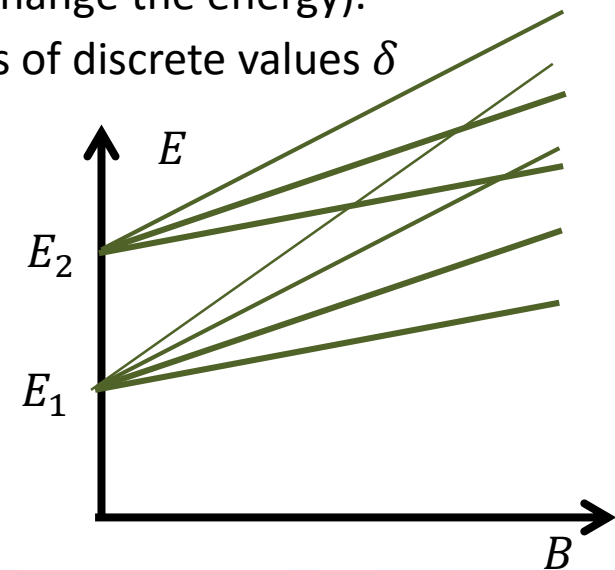
Wave functions are the functions of the oscillator (along x , of the order of $l_B/\sqrt{2}$) and travelling waves (along y) – weird, right? Why?

The energy does not depend on k vector – states of different k have the same energy, so they are degenerated (therefore any combination of them does not change the energy).

The density of states is reduced from the constant $\frac{m}{\pi\hbar^2}$ to a series of discrete values δ given by the equation of ε_{nk} - they are called **Landau levels**.

Full energy (including binding potential in z direction):

$$E = E_z + \varepsilon_{nk} = E_z + \left(n - \frac{1}{2}\right) \hbar\omega_c$$
$$n = 1, 2, 3 \dots$$

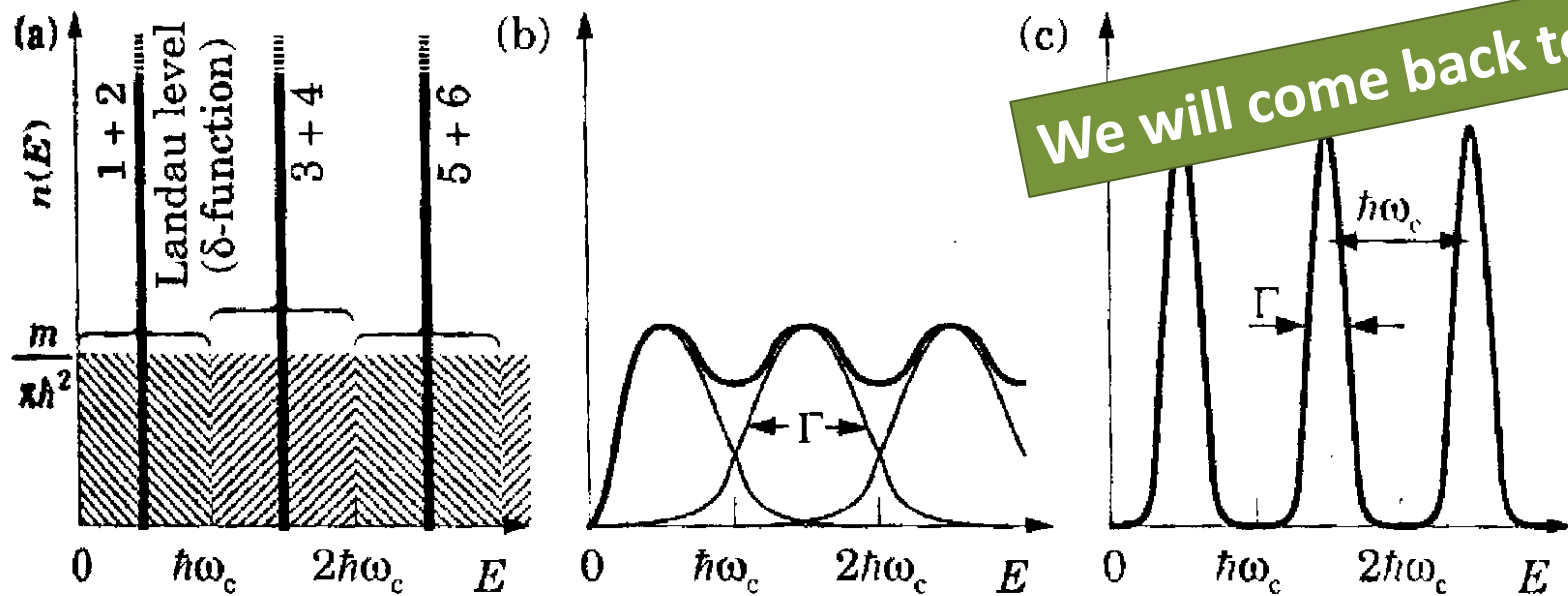


Homogenous magnetic field

The 2D case:

Solutions $\varepsilon_{nk} = \left(n - \frac{1}{2}\right) \hbar\omega_c + E_n$ (does not depend on k_y ; E_n - is any 2D energy).

$$\phi_{nk}(x, y) \propto H_{n-1} \left(\frac{x - x_k}{l_B} \right) \exp \left[-\frac{(x - x_k)^2}{2l_B^2} \right] \exp(ik_y y) \quad n = 1, 2, 3 \dots$$



We will come back to this

FIGURE 6.7. Density of states in a magnetic field, neglecting spin splitting. (a) The states in each range $\hbar\omega_c$ are squeezed into a δ -function Landau level. (b) Landau levels have a non-zero width Γ in a more realistic picture and overlap if $\hbar\omega_c < \Gamma$. (c) The levels become distinct when $\hbar\omega_c > \Gamma$.

Landau levels


The solution of the Schrödinger equation in a magnetic field gives a discrete spectrum.

What is the number of states per one level? The sample $S = L_x \times L_y$, in the Landau gauge for y coordinate we have plane wave condition $k = (2\pi/L_y)n_y$ (where n_y is an integer number).

For x coordinate the wavefunction is centered in $x_k = -\frac{\hbar k}{eB} = -(2\pi\hbar n_y/eBL_y)$.

The condition for x_k to be in the sample (rather than outside):

$$-L_x < \frac{2\pi\hbar n_y}{eBL_y} < 0 \quad \text{czyli} \quad 0 < n_y < \frac{eB}{h} L_x L_y = n_B S = \frac{e}{h} BS = \frac{\Phi}{\Phi_0}$$

flux $\Phi_0 = \frac{h}{e} = 4.135667516 \times 10^{-15} \text{ Wb} \quad [\text{Wb}] = [\text{T m}^2]$ 

The magnetic flux quantum (pol. *flukson*) (In a superconductor $h/2e$, so this is not a „quantum”)

$\Phi = BS$ the total magnetic flux in the sample $S = L_x \times L_y$

$$0 < n_y \Phi_0 < \Phi$$

The amount of allowed states is related to the amount of magnetic flux quanta passing through the sample!

Landau levels

The Fermi level lies **between** Landau levels - there is no DOS, change of E_F does not change DOS –incompressible states (*stany nieściśliwe*)

The Fermi level lies **inside** the Landau level – large DOS, change of E_F strongly affects the DOS – *compressible states* (*stany ściśliwe*)

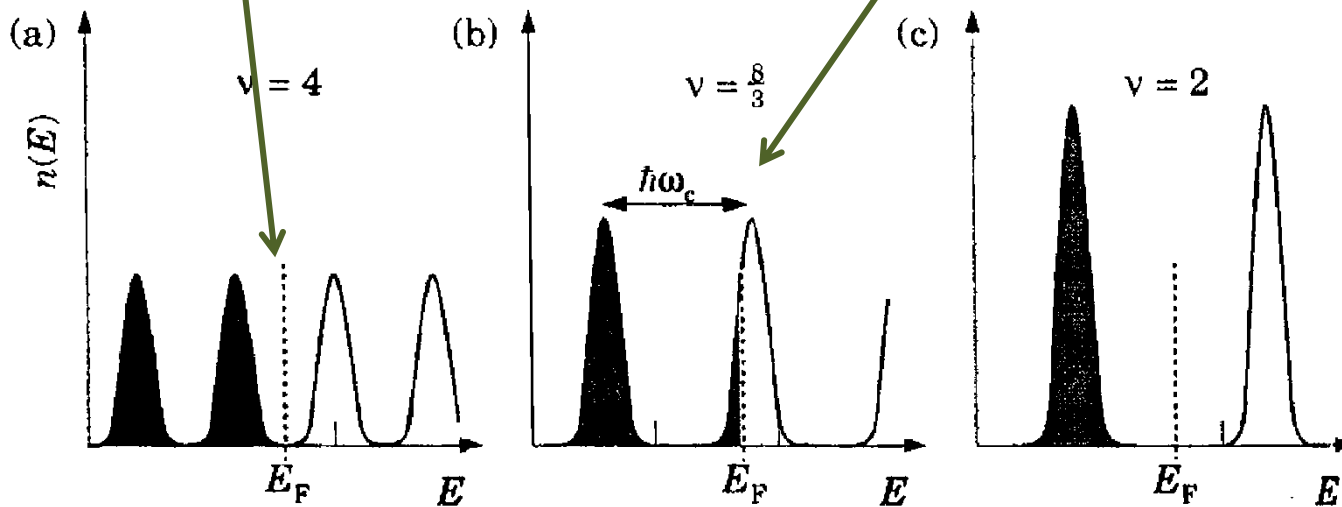


FIGURE 6.8. Occupation of Landau levels in a magnetic field neglecting the spin splitting, showing how the Fermi level moves to maintain a constant density of electrons. The fields are in the ratio 2 : 3 : 4 and give $\nu = 4$, $\frac{8}{3}$, and 2.

Landau levels

The Fermi level in the magnetic field:

$$\nu = \frac{n_{2D}}{n_B} = \frac{hn_{2D}}{eB} = \frac{\Phi_0 n_{2D}}{B} = 2\pi l_B^2 n_{2D}$$

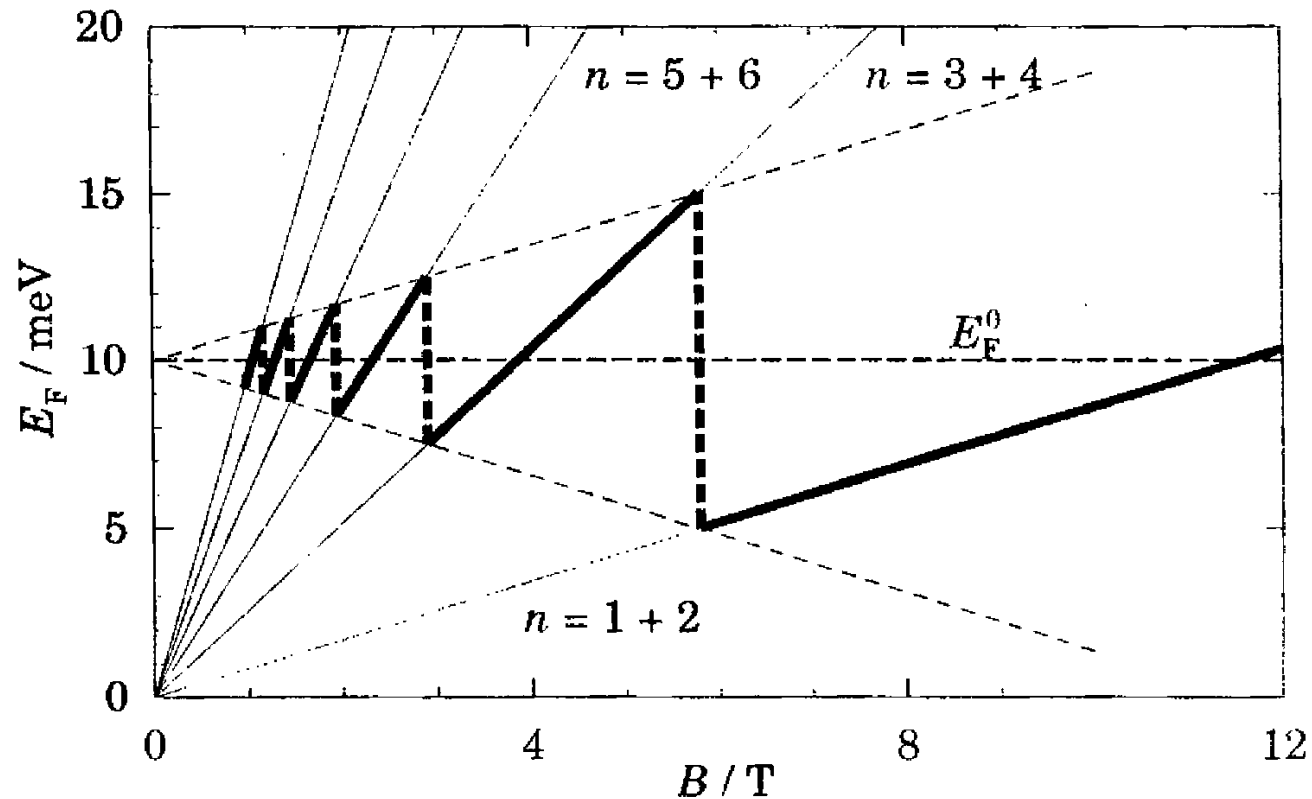


FIGURE 6.9. Variation of the Fermi level as a function of magnetic field for a two-dimensional electron gas in GaAs with $E_F^0 = 10$ meV before the field was applied. Spin splitting is neglected. The fan of thin lines shows the Landau levels, while the discontinuous thick line is E_F .

Shubnikov-de Haas effect

Shubnikov-de Haas effect

Density of states oscillates - falls to 0 for $\nu = n$ and is highest for $\nu \approx n + \frac{1}{2}$ - the easiest measurement is the magnetoresistance R_{xx} .

Oscillations depend on the ratio of the Fermi energy E_F to the cyclotron frequency $\hbar\omega_c = eB/m^*$. Oscillations are periodic in $1/B$.

$$\nu = \frac{n_{2D}}{n_B} = \frac{\hbar n_{2D}}{eB} = \frac{\Phi_0 n_{2D}}{B} = 2\pi l_B^2 n_{2D}$$

From SdH we can determine the effective mass m^* and quantum time τ_q . The amplitude of oscillation is given by

$$\Delta\rho_{SdH} = 4\rho_0\delta \cos(4\pi\nu) \frac{\xi(T)}{\sinh(\xi(T))} \exp\left(-\frac{\pi}{\omega_c\tau_q}\right)$$

$$\xi(T) = 2\pi^2 kT/\hbar\omega_c$$

Temperature dependence gives m^* , damping τ_q .

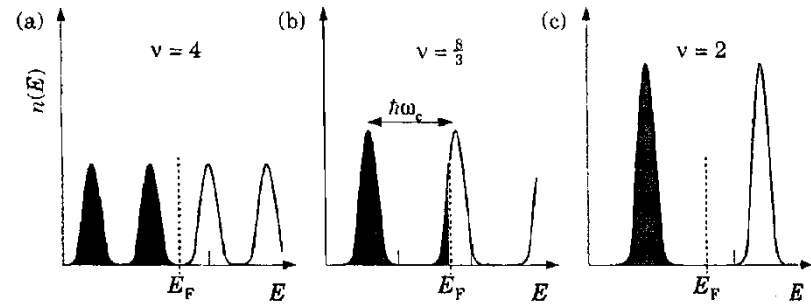
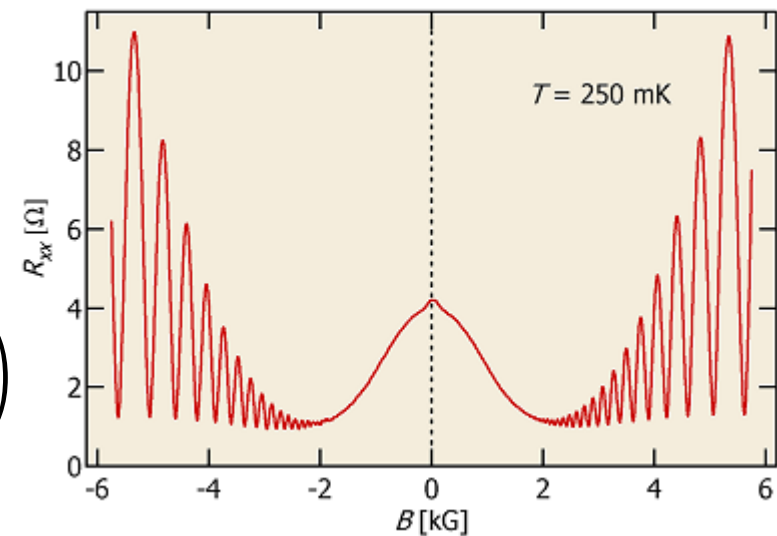


FIGURE 6.8. Occupation of Landau levels in a magnetic field neglecting the spin splitting, showing how the Fermi level moves to maintain a constant density of electrons. The fields are in the ratio 2 : 3 : 4 and give $\nu = 4, \frac{8}{3},$ and 2.



<http://groups.physics.umn.edu/zudovlab/content/sdho.htm>

Shubnikov-de Haas effect

Shubnikov-de Haas effect

Density of states oscillates - falls to 0 for $\nu = n$ and is highest for $\nu \approx n + \frac{1}{2}$ - the easiest measurement is the magnetoresistance R_{xx} .

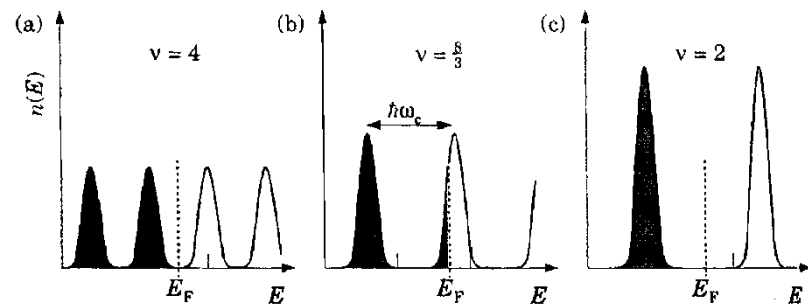


FIGURE 6.8. Occupation of Landau levels in a magnetic field neglecting the spin splitting, showing how the Fermi level moves to maintain a constant density of electrons. The fields are in the ratio

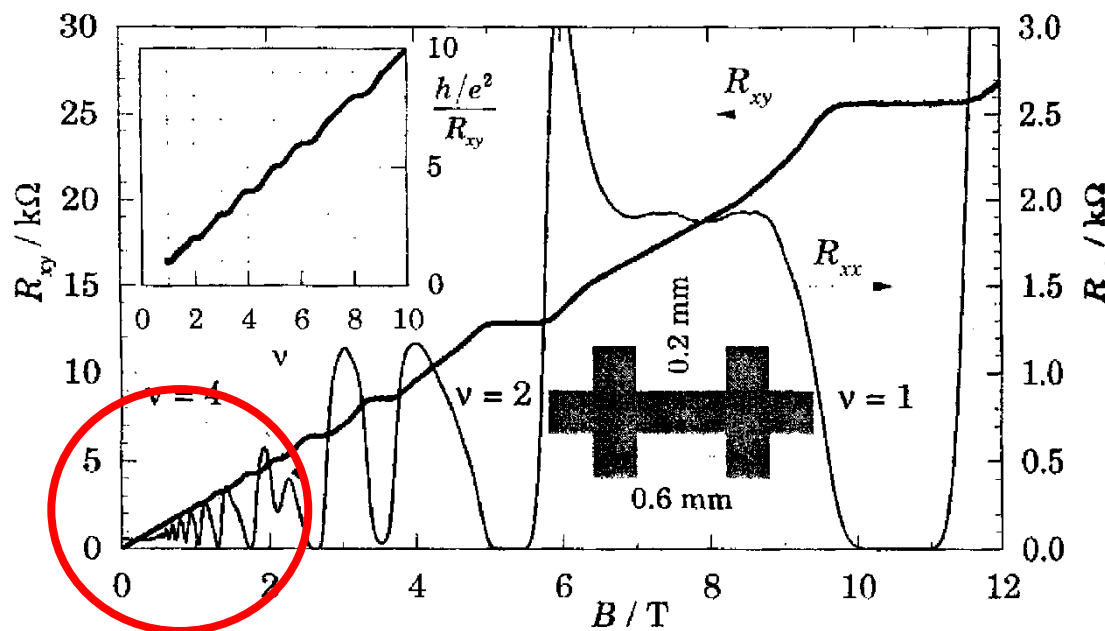


FIGURE 6.10. Longitudinal and transverse (Hall) resistivity, R_{xx} and R_{xy} , of a two-dimensional electron gas of density $n_{2D} = 2.6 \times 10^{15} \text{ nm}^{-2}$ as a function of magnetic field. The measurements were made at $T = 1.13 \text{ K}$. The inset shows $1/R_{xx}$ divided by the quantum unit of conductance e^2/h as a function of the filling factor ν . [Data kindly supplied by Dr A. R. Long, University of Glasgow.]

Integer Quantum Hall Effect (IQHE)

Integer Quantum Hall effect (IQHE) – for 2D gas: if the Fermi level is located in localized states the Hall resistance (*opór hallowski*) is quantized

$$R_H = \frac{1}{\nu} \frac{h}{e^2}$$

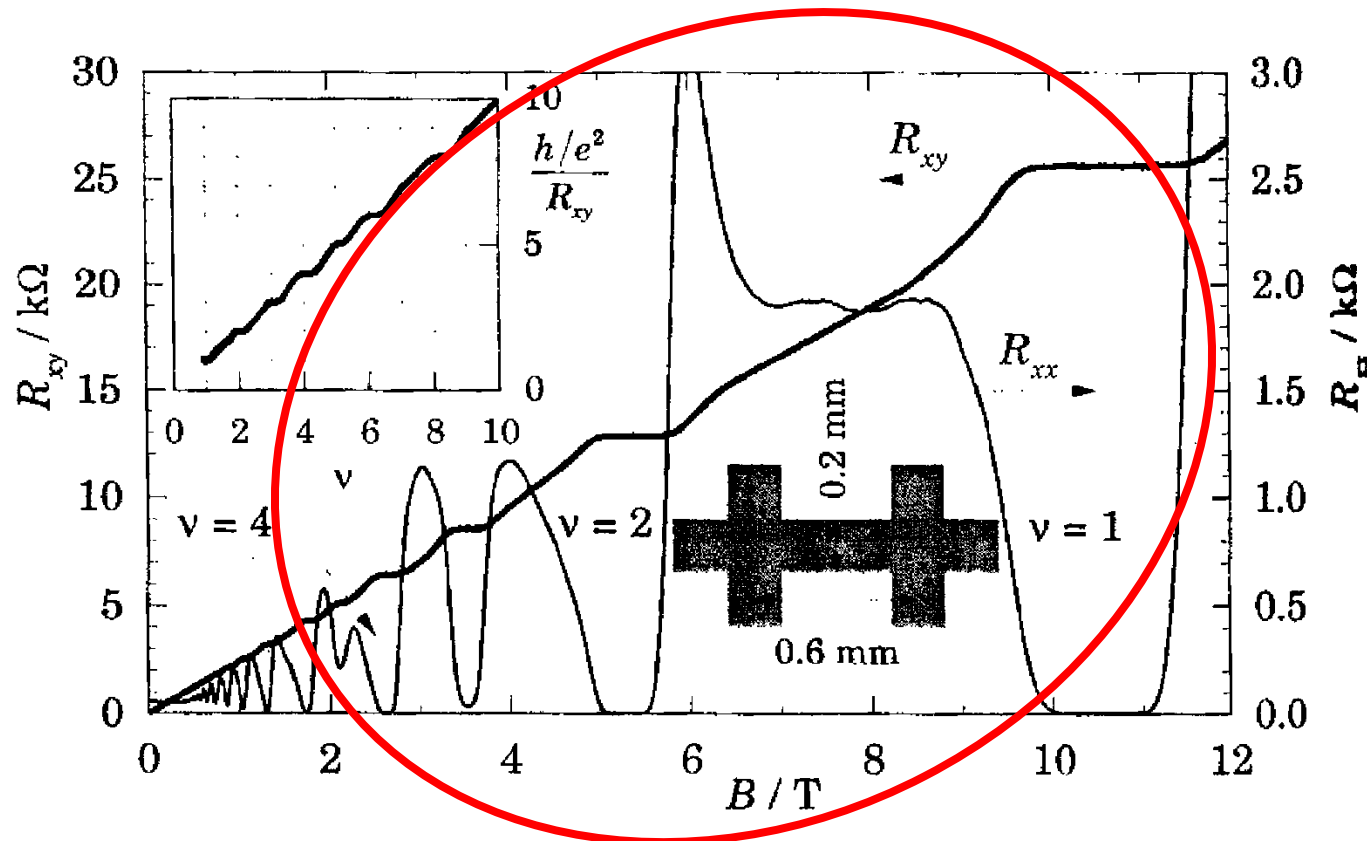


FIGURE 6.10. Longitudinal and transverse (Hall) resistivity, R_{xx} and R_{xy} , of a two-dimensional electron gas of density $n_{2D} = 2.6 \times 10^{15} \text{ nm}^{-2}$ as a function of magnetic field. The measurements were made at $T = 1.13 \text{ K}$. The inset shows $1/R_{xx}$ divided by the quantum unit of conductance e^2/h as a function of the filling factor ν . [Data kindly supplied by Dr A. R. Long, University of Glasgow.]

Quantum dots

$$E_{nl} = (2n + |l| - 1) \sqrt{(\hbar\omega_0)^2 + \left(\frac{1}{2}\hbar\omega_c\right)^2} + \left(\frac{1}{2}\hbar\omega_c\right) l$$
$$n = 1, 2, 3 \dots \quad l = 0, \pm 1, \pm 2, \pm 3 \dots$$

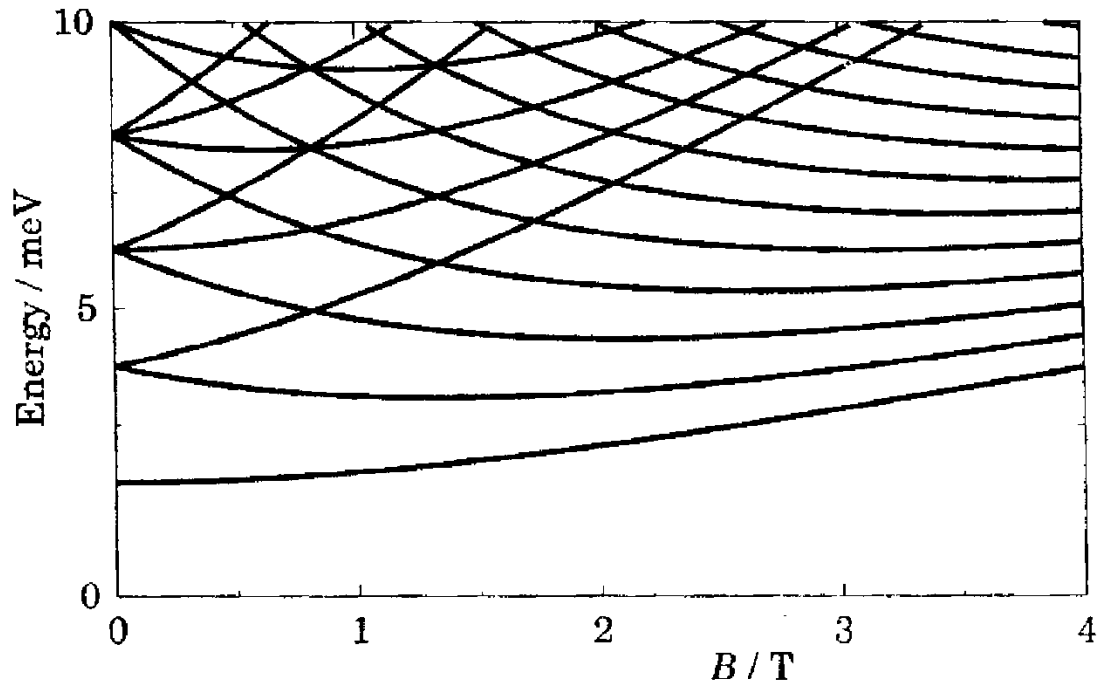
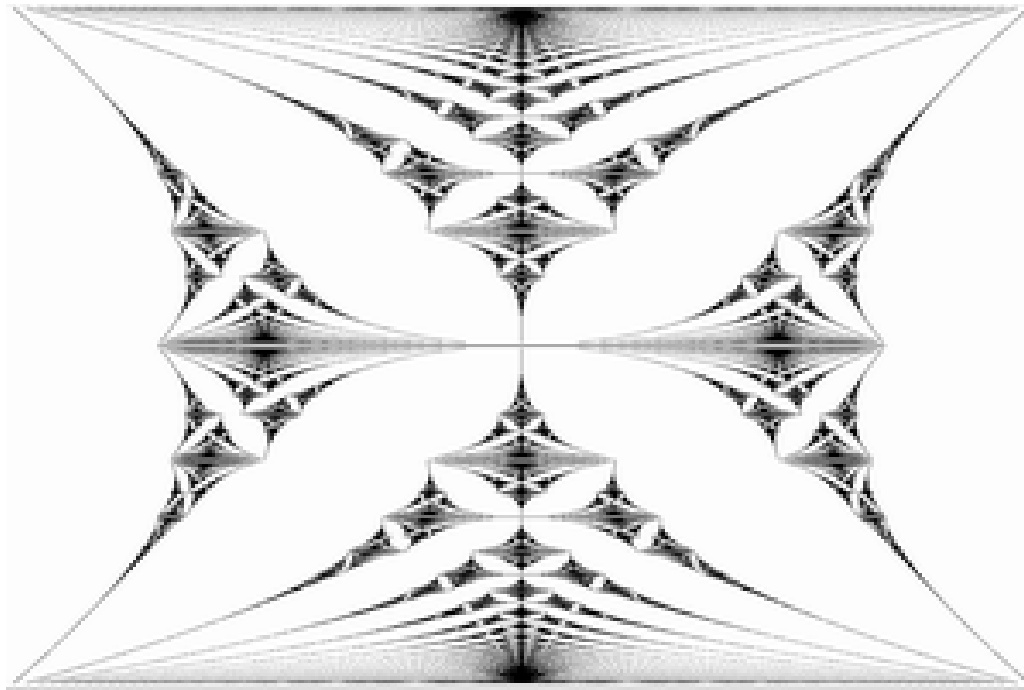


FIGURE 6.16. Energy levels in a magnetic field of a GaAs dot with a parabolic confining potential giving $\hbar\omega_0 = 2$ meV.

Hofstadter butterfly

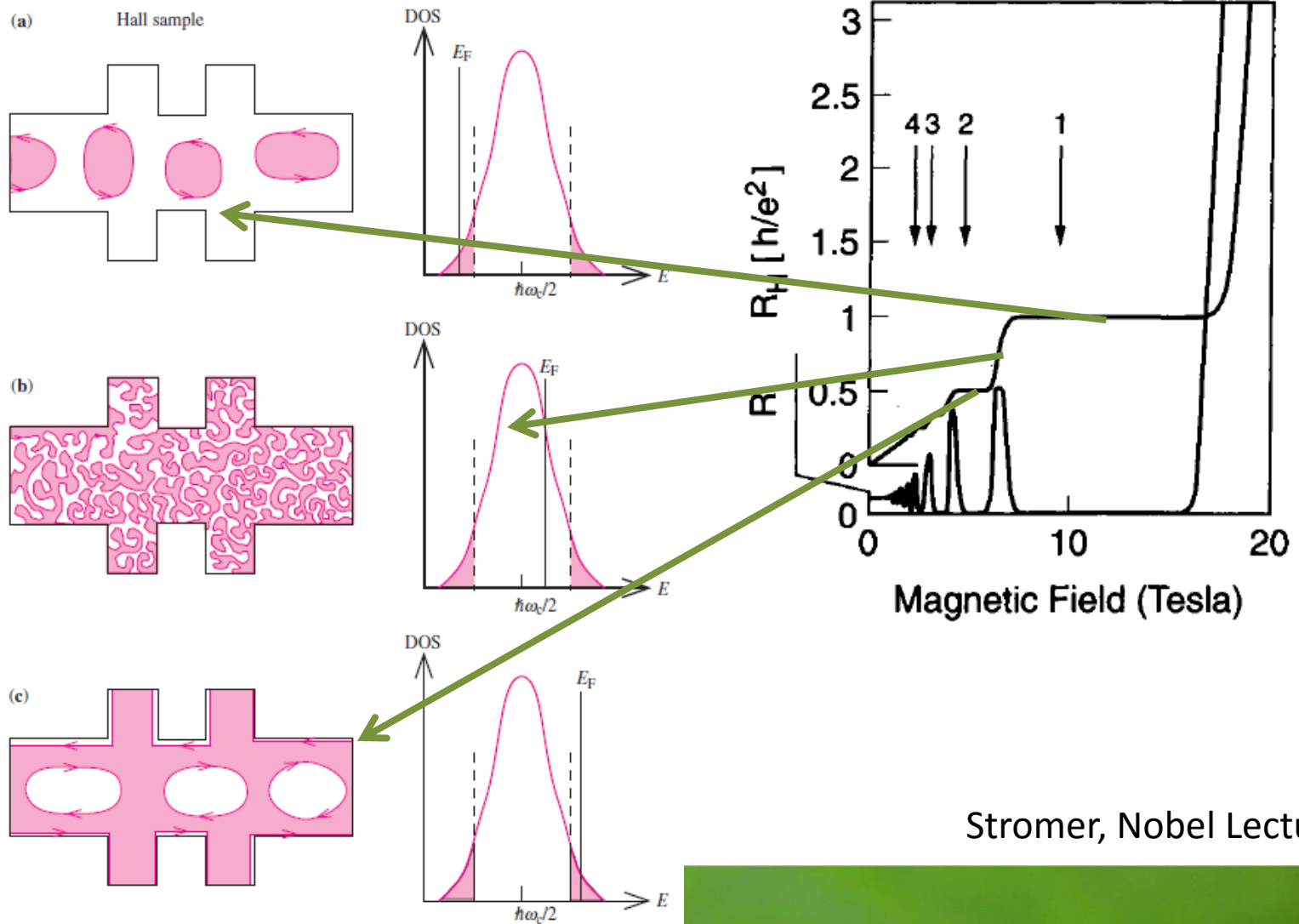


The Hofstadter butterfly is the energy spectrum of an electron, restricted to move in two-dimensional periodic potential under the influence of a perpendicular magnetic field. The horizontal axis is the energy and the vertical axis is the magnetic flux through the unit cell of the periodic potential. The flux is a dimensionless number when measured in quantum flux units (will call it α). It is an example of a fractal energy spectrum. When the flux parameter α is rational and equal to p/q with p and q relatively prime, the spectrum consists of q non-overlapping energy bands, and therefore $q+1$ energy gaps (gaps number 0 and q are the regions below and above the spectrum accordingly). When α is irrational, the spectrum is a cantor set.

Integer Quantum Hall Effect (IQHE)

Integer Quantum Hall effect (IQHE) – for 2D gas: if the Fermi level is located in localized states the Hall resistance (*opór hallowski*) is quantized

$$R_H = \frac{1}{\nu} \frac{h}{e^2}$$



Yu, Cardona

Stromer, Nobel Lecture

Fractional Quantum Hall Effect (FQHE)

Fractional Quantum Hall Effect (FQHE) – for 2D gas $\nu \leq 1$: if the Fermi level is located in localized states the Hall resistance (*opór hallowski*) is quantized

$$R_H = \frac{1}{\nu^*} \frac{h}{e^2}$$

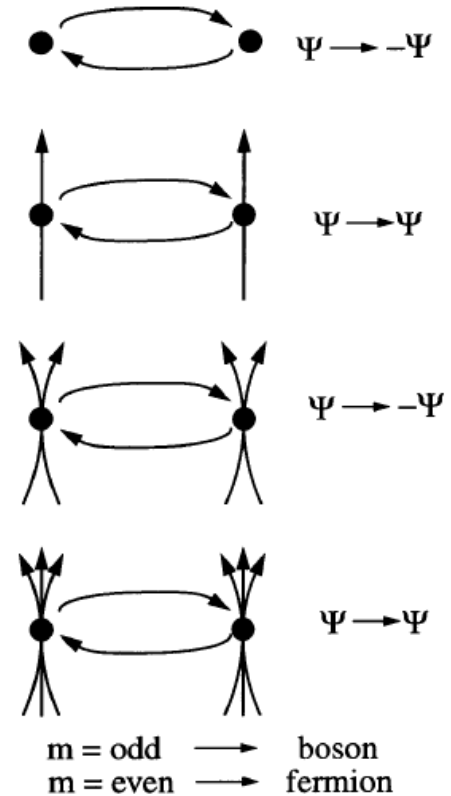
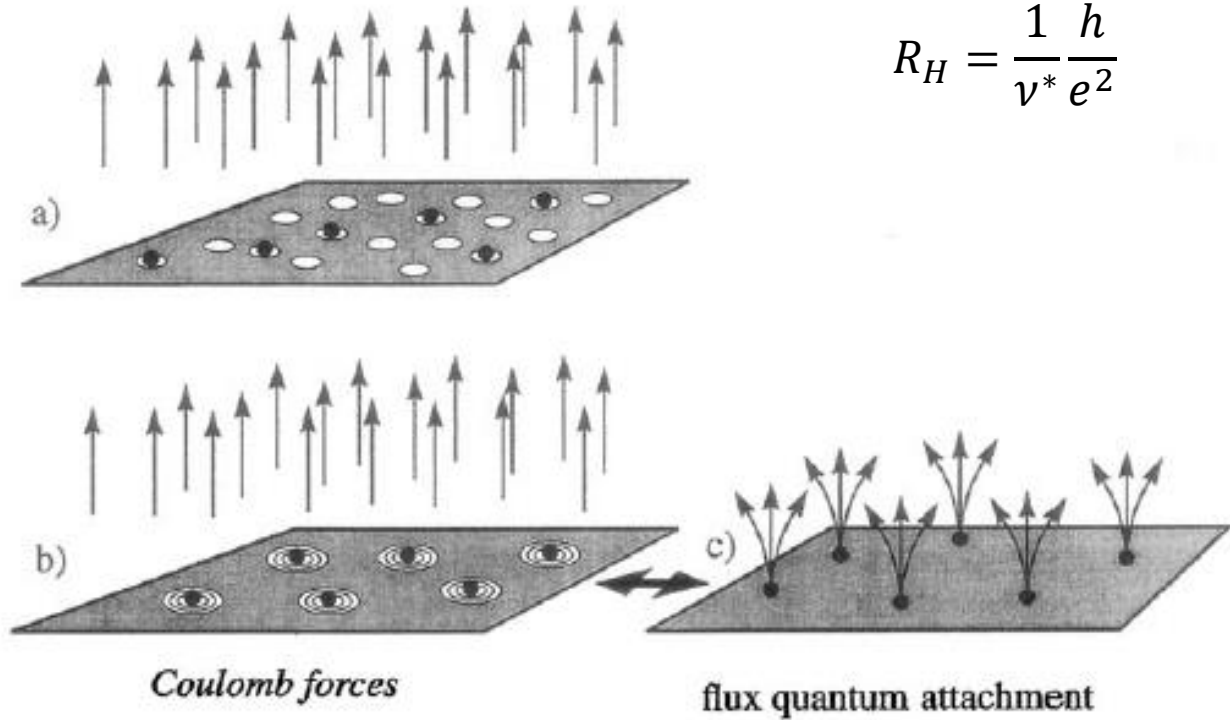


Figure 14. Schematic drawing of electron vortex attraction at fractional Landau level filling, $\nu=1/3$. Now there are three times as many vortices as there are electrons. The Pauli principle is satisfied by placing one vortex onto each electron (a). Placing three vortices onto each electron reduces electron-electron (Coulomb) repulsion (b). Vortex attachment can be viewed as the attachment of magnetic flux quanta to the electrons transforming them to composite particles (c).

of electrons and composite particles. Exchange of two particles affects the wavefunction Ψ which described the quantum-mechanical behavior of the system. For electrons, exchange is multiplied by -1 , identifying the particles as fermions. With the attachment of an odd number of flux quanta Ψ remains *unchanged* under exchange (multiplication by $+1$), identifying the particles as bosons. Attachment of an even number of flux quanta returns the particles to fermions.

Stromer, Nobel Lecture